

THESIS

GEOCHEMICAL MODELING-BASED PREDICTION OF WATER-ROCK INTERACTION DURING  
AQUIFER STORAGE AND RECOVERY UTILIZING SELECTED COLORADO FRONT RANGE  
AQUIFERS

Submitted by

Amanda Doherty

Department of Geosciences

In partial fulfillment of the requirements

For the Degree of Master of Science

Colorado State University

Fort Collins, Colorado

Summer 2023

Master's Committee:

Advisor: Sally Sutton

Thomas Sale  
Michael Ronayne

Copyright by Amanda Doherty 2023

All Rights Reserved

## ABSTRACT

# GEOCHEMICAL MODELING-BASED PREDICTION OF WATER-ROCK INTERACTION DURING AQUIFER STORAGE AND RECOVERY UTILIZING SELECTED COLORADO FRONT RANGE AQUIFERS

This study characterizes the Fountain Formation, Ingleside Formation, and sandstones of the Dakota Group and considers the potential of these three formations as hypothetical Aquifer Storage and Recovery (ASR) targets. Compositional data from surface rock samples, including major, minor and trace elements from bulk rock geochemical analysis and mineral identification from petrography are used to infer a generalized mineral suite to represent each of the formations of interest. Similarly, compositional analyses from domestic water well samples, including major anions and cations and selected metals, were used as generalized representations of native water from each formation of interest. Finally, compositional data from treated city water was obtained and used as a generalized representation of injection water.

The generalized rock data along with the generalized native water data represent a hypothetical injection environment while the treated water composition represents a hypothetical injection water. All water and rock data were used to populate a Single Pass Mixing equilibria Model that simulated an ASR system using the USGS geochemical modeling computer program PHREEQC (PH REdox EQuilibrium). Model results include mixed solution compositions, mineral saturation indices and estimates of mineral mass precipitation during simulated injection.

Results of modeling suggest there is limited geochemical water-rock interaction during ASR in the hypothetical environment in this study. Model results indicate that the mixed solution composition is controlled more by the injected solution than by reactions occurring between the injection fluid and aquifer host material. Specifically, as greater volumes of hypothetical injection water are introduced with

each model step, the compositions of the resulting mixed solutions increasingly resemble those of the injected water. The model predicted the precipitation of hematite, kaolinite and quartz during injection of the hypothetical injection water. Because aluminum was below detection in the water analyses and an arbitrary value less than the detection limit was used in the model, the prediction of kaolinite precipitation is not meaningful. Further, the model was constrained to not permit mineral dissolution, limiting the applicability of the model only to the consideration of mineral precipitation.

In addition, benchtop leaching experiments were performed on rock samples to provide additional information about potential water-rock interaction. Benchtop experiment results are presented, but the focus of the study is primarily on geochemical modeling results. Water analysis results presented here suggest that the formations of interest currently contain good quality water. Modeling results suggest that injection of treated water would likely not lead to volumetrically important precipitation of minerals in the formations.

## ACKNOWLEDGEMENTS

I would like to thank my thesis committee: Dr. Sally Sutton, Dr. Thomas Sale, and Dr. Michael Ronayne for their help throughout this process. Sally Sutton, for giving me this opportunity and sticking with me until the end. Thomas Sale, for all his guidance and for helping me collect water samples in the field. I would also like to thank the City of Fort Collins Water Treatment Facility for their help with water quality analyses. Kelly Donahue for showing me the ropes of PHREEQC. A special thanks to my dedicated field assistant Jacob Gehrz and editors Jordalyn Simpson and Alicia Speitz.

## TABLE OF CONTENTS

ABSTRACT .....	ii
ACKNOWLEDGEMENTS .....	iv
LIST OF TABLES .....	vii
LIST OF FIGURES .....	viii
Chapter 1 - Introduction.....	1
1.1 Overview .....	1
1.2 Project Objectives.....	2
1.3 ASR.....	3
Chapter 2 - Background.....	5
2.1 Previous Work.....	5
2.2 Study Area.....	7
2.3 Formations of Interest.....	7
2.3.1 Dakota Group (Lower Cretaceous) .....	7
2.3.2 Ingleside Formation (Lower Permian) .....	8
2.3.3 Fountain Formation (Pennsylvanian/Lower Permian) .....	10
Chapter 3 - Methods.....	12
3.1 Water Sample Collection, Preparation, and Analysis .....	12
3.2 Rock Sample Collection, Preparation, and Analysis .....	16
3.2.1 Sample Collection, Petrography, and Point Counting .....	16
3.2.2 Bulk Geochemical Analysis .....	17
3.2.3 Oxide Recalculation .....	19
3.3 Benchtop Leaching Experiments.....	21
3.3.1 Initial Experiment .....	21
3.3.2 Repeat Experiment.....	22
3.4 Geochemical Modeling .....	22
3.4.1 PHREEQC .....	22
3.4.2 Single Pass Mixing Model Explanation and Conceptual Model.....	23
3.4.3 Single Pass Mixing Model Input Overview.....	25
3.4.4 Mineral Phase Input .....	27
3.4.5 Initial Fluids, and Fluid Speciation .....	27
3.4.6 Mixing .....	29
3.4.7 Assumptions .....	30
Chapter 4 - Results .....	33

4.1 Water Chemistry Analysis .....	33
4.2 Rock Chemistry Analysis and Point Counting Results .....	36
4.2.1 Dakota Group Samples.....	36
4.2.2 Ingleside Formation Samples.....	37
4.2.3 Fountain Formation.....	40
4.2.4 Bulk Rock Geochemistry .....	45
4.2.5 Bulk Chemical Composition Approximated from Point Count Analyses Results.....	47
4.3 Leaching Experiments.....	50
4.4 Geochemical Modeling Results.....	53
4.4.1 Fluid Evolution Model .....	53
4.4.2 Mineral Precipitation.....	68
Chapter 5 - Discussion.....	76
5.1 Formation Aquifer Compositional Characterization.....	76
5.2 Bulk Chemical Composition Approximated from Point Count Analyses Results .....	76
5.3 Water Chemistry and Characterization .....	77
5.4 Leaching Experiments.....	77
5.4.1 Repeat Experiment Explanation.....	78
5.5 Interpretation of Geochemical Modeling Results .....	80
5.5.1 Implications of Model Input and Parameter Selection .....	80
5.5.2 Fluid Evolution, Mineral Solubility and Mineral Precipitation .....	83
5.5.3 Model Limitations.....	86
Chapter 6 - Conclusions and Recommendations.....	87
6.1 Conclusions .....	87
6.2 Future Recommendations.....	88
References Cited .....	89
Appendix .....	91
A.1 Injection Solution.....	92
A.2 Full Results of Water Chemistry Analysis for Experiment .....	92
A.2.1 First Leaching Experiment .....	93
A.2.2 Second Leaching Experiment .....	93
A.3 PHREEQC Model Input.....	97
A.3.1 Input parameters common to all three Single Pass Mixing Models .....	98
A.3.2 Dakota .....	100
A.3.3 Ingleside .....	101
A.3.4 Fountain.....	102

## LIST OF TABLES

Table 1 : Water Samples.....	15
Table 2: List of Analytes and Detection Limits .....	16
Table 3: Rock Samples and Analyses Performed .....	17
Table 4: Bulk Rock Geochemical Analysis Oxide Analytes .....	19
Table 5: Bulk Rock Geochemical Analysis Trace Element Analytes .....	20
Table 6: Leaching Experiment Samples.....	21
Table 7a - PHREEQC Model Input.....	31
Table 8: Results of Water Chemistry Analysis .....	35
Table 9: Results of Point Counting in Percent of Total Sample.....	44
Table 10: Results of Fusion ICP Analysis given in Percent Oxides.....	46
Table 11: Results of Fusion MS/ICP and INAA Analysis.....	48
Table 12: Comparison of Measured and Calculated Oxide Wt. % Values .....	49
Table 13: Results of Leaching Experiment (mg/L).....	51
Table 14 : Comparison Experiment Results (mg/L) .....	52
Table 15: Hypothetical Injection Water Pre-Mixing Solutions - All units mg/L.....	54
Table 16: Dakota Hypothetical Native Water Pre-Mixing Solutions - All units mg/L .....	55
Table 17: Ingleside Hypothetical Native Water Pre-Mixing Solutions - All units mg/L .....	56
Table 18: Fountain Hypothetical Native Water Pre-Mixing Solutions - All units mg/L.....	56
Table 19: Dakota Single Pass Mixing Model Results .....	59
Table 20: Ingleside Single Pass Mixing Model Results .....	61
Table 21: Fountain Single Pass Mixing Model Results.....	63
Table 22: Dakota SPMM Saturation Indices .....	70
Table 23: Ingleside SPMM Saturation Indices .....	72
Table 24: Fountain SPMM Saturation Indices .....	75
Table 25:WATQ4F Database Thermodynamic Data - Model Input.....	85

## LIST OF FIGURES

Figure 1: Cross section of a typical ASR well .....	6
Figure 2: Study area and location of rock (purple) and .....	9
Figure 3: Stratigraphic column of study area units .....	10
Figure 4: All rock and water sample locations.....	13
Figure 5: Water quality sampling procedure.....	14
Figure 6: Rock Sampling .....	18
Figure 7: ASR Conceptual Model.....	24
Figure 8: Single Pass Leaching Conceptual Model.....	25
Figure 9: Single Pass Mixing Conceptual Model.....	26
Figure 10: Piper Diagram .....	34
Figure 11: Photomicrograph of sample D1.....	37
Figure 12: Photomicrograph of sample D2.....	37
Figure 13: Photomicrograph of sample I1 .....	39
Figure 14: Photomicrograph of sample I3 .....	39
Figure 15: Photomicrograph of sample I4 .....	40
Figure 16: Photomicrograph of sample F1 .....	42
Figure 17: Photomicrograph of sample F2 .....	42
Figure 18: Photomicrograph of sample F3 .....	43
Figure 19: Classification of rock samples. Sandstone classification diagram after McBride (1963).....	43
Figure 20: Stiff diagrams representing the resulting fluids of the Dakota (A), Ingleside (B), and Fountain (C) formations, derived using a Single Pass Mixing Model .....	66
Figure 21: Piper diagram showing fluid composition results from each model step for all three formation Single Pass Mixing Models. Classification types based on (Sajil Kumar, 2013) .....	67
Figure 22: Tabulated results of the Dakota SPMM. Mineral precipitation is shown as bar graph. The concentration of aqueous species removed from the mixed fluids to form the minerals are plotted as points. A - kaolinite precipitation with $\text{Al}^{3+}$ and aqueous $\text{SiO}_2$ removal. B - quartz precipitation with aqueous $\text{SiO}_2$ removal.....	69
Figure 23: Tabulated results of the Ingleside SPMM. Mineral precipitation is shown as bar graph. The concentration of aqueous species removed from the mixed fluids to form the minerals are plotted as lines. A - hematite precipitation with $\text{Fe}^{2+}$ removal. B - kaolinite precipitation with $\text{Al}^{3+}$ and aqueous $\text{SiO}_2$ removal. C - quartz precipitation with aqueous $\text{SiO}_2$ removal.....	71
Figure 24: Tabulated results of the Fountain SPMM. Mineral precipitation is shown as bar graph. The concentration of aqueous species removed from the mixed fluids to form the minerals are plotted as lines. A - hematite precipitation with $\text{Fe}^{2+}$ removal. B - kaolinite precipitation with $\text{Al}^{3+}$ and aqueous $\text{SiO}_2$ removal. C - quartz precipitation with aqueous $\text{SiO}_2$ removal.....	74
Figure 25: Eh/pH Diagram after Garrels and Christ (1965) .....	81

## Chapter 1 - Introduction

### 1.1 Overview

Aquifer Storage and Recovery (ASR) is a process in which excess surface water is captured and sequestered underground for later use using dual-purpose injection and pumping water wells (Pyne, 2005). Excess water may come from a variety of sources including lakes, rivers, and reservoirs, as well as treated water (Pyne, 2005). Most ASR systems are used for potable water supply and long- or short-term storage of excess water to be used in emergencies. Water from ASR systems has been used for agricultural, industrial, and municipal purposes (Pyne, 2005). ASR systems have been implemented all over the world, including at least 136 in the U.S. as of 2016 (Ringleb et al., 2016). Cities with burgeoning populations seeking alternatives to traditional water storage, such as surface reservoirs, may benefit from ASR because of a lower capital cost, and reduced risk of contamination and evapotranspiration, as well as reduced land use issues (Pyne, 2005).

Fort Collins, Colorado is an example of a city that could benefit from additional water storage given its population growth. Several geologic formations along the northern Colorado Front Range have been identified as ASR target aquifers and studied for their hydrogeologic potential (Adam, 2017; Collazo, 2018). Hydrogeologic characterization based on well construction and drilling reports concluded that the Fountain Formation has the potential to store large volumes of water that would likely be naturally impeded from migration by impermeable layers within the formation acting as flow barriers (Collazo, 2018). A related study in Larimer County, Colorado by Adam (2017) considered all formations younger than the Fountain for ASR potential and identified sandstone members of the Pierre Shale, the Lytle Formation of the Dakota Group, and the Ingleside Formation as potential targets for ASR.

In addition to the volume of water storage, evaluating the geochemistry of these potential targets is critically important. During the ASR process, injection water may mix with native groundwater and interact with aquifer material, which can alter the geochemical state of the aquifer by changing redox conditions, pH, and chemical composition of the formation water. Potential effects of changing the hydrogeochemical environment within an aquifer by injection of surface water include mobilization of metals, changes to pore water composition, mineral precipitation and/or dissolution, and physical transport of particles. These processes are interdependent and happen at various rates, making it difficult to constrain the environment (Pyne, 2005; Ringleb et al., 2016). This study focuses on the potential of surface water injection to negatively impact water quality during injection, storage, and recovery of water, while also considering the role of mineral stability throughout this process.

## 1.2 Project Objectives

The purpose of this study is to use geochemical models to predict rock-water interaction during hypothetical ASR in three aquifers near Fort Collins, Colorado.

More specifically, the study will:

1. Determine the mineral and chemical composition of selected samples of the Fountain Formation, Ingleside Formation, and Dakota Group sandstones.
2. Characterize the quality of native groundwater in the above-mentioned potential host aquifers.
3. Comment on the feasibility of an ASR program that would utilize certain formations in the Front Range to store treated surface water for later recovery.

### 1.3 ASR

The success of an ASR system is measured by its recovery efficiency, which is defined as the volume of water stored compared with the useable volume of water extracted (Pyne, 2005). An ASR system needs to recover a specific volume of water meeting predetermined water quality standards. Geochemical investigation before the implementation of ASR provides a baseline understanding of the subsurface environment and is useful in avoiding three potential negative outcomes of ASR:

1. pore clogging due to mineral precipitation, activation of swelling clays, bioclogging, or particle dislodgment
2. aquifer damage by large scale dissolution of formation materials, specifically cements and soluble phases such as carbonates
3. degradation of water quality by mobilization of trace metals

Clogging of the aquifer pore throats caused by chemical precipitation or physical dislodgement of particles obstructs water flow, which in turn impedes recovery efficiency and can result in failure of the entire system (Pyne, 2005). Mineral precipitation can drastically reduce permeability within the pore spaces of the aquifer, and cause encrustation of the well screen. Commonly, carbonates (calcite) or iron and manganese oxyhydroxides encrust well screens. These mineral phases form due to changes in oxidation and reduction potential, pH, and temperature within the subsurface. Some metals exhibit biologically facilitated precipitation. Alternatively, a mechanical process called flocculation can produce clustering of solid or partially solid suspended particles ('flocs') that become caught in pore throats causing clogs. Physical dislodgement of particles, most often clays, can be a result of ion exchange reactions that affect their physical size, making particles easier to transport, by releasing them from attachment or anchoring points. Ion exchange reactions, such as  $\text{Na}^+$  for  $\text{Ca}^{2+}$ , are initiated by changes in composition of the solution, as well as changes in pH (Camprovin et al., 2017; Pyne, 2005; Rinck-Pfeiffer et al., 2000).

In addition to physically impeding recovery, dissolution of aquifer material has the potential to alter the pore water composition and degrade the quality of recovered water by releasing metals into solution. Common issues of water quality degradation arise from incorporation of metals such as As, Fe, Se, Pb, Ni, Cu, and Cr into the recovery water after they are leached from aquifer material. Iron-bearing minerals are particularly sensitive to fluctuations of redox conditions. In anoxic environments, iron in ferric oxyhydroxides can be reduced to form ferrous oxyhydroxides, whereas highly oxygenated environments cause liberation of elements from ferrous sulfides (pyrite) and production of acids (sulfuric acid). Both the oxidation and reduction of these iron species and minerals can lead to an increase of ferrous iron and any other metals sorbed to the iron phases going into solution (Hem, 1985). Iron carbonates and sedimentary organic material can be the source of metals leached into solution and are also highly susceptible to dissolution as a result of environmental changes in pH, temperature, and redox conditions (Azobu, 2013; Jones and Pichler, 2007; Mirecki et al., 2013; Ringleb et al., 2016). While pretreatment of injected and post treatment of recovered water can be implemented to impede or correct mobilization of trace metals, it is far more cost effective to avoid these issues before construction of an ASR system (Pyne, 2005).

## Chapter 2 - Background

### 2.1 Previous Work

Numerous studies on Aquifer Storage and Recovery have been conducted over the last 30 years, many of which were focused on geochemistry and water quality (Antoniou et al., 2014; Antoniou et al., 2013; Antoniou et al., 2012; Gaus et al., 2000; Gaus et al., 2002; Glynn and Plummer, 2005; Jones and Pichler, 2007). Central to these modelling studies is the concept of a recharge water bubble: a zone of injected fluid that extends 50 to 700 meters radially from the injection well (Fig. 1) (Pyne, 2005). A zone of a mixed solution develops on the periphery of the recharge bubble that effectively separates or buffers the injection water from the native groundwater (Fig. 1). While the chemistry of the water in the “buffer zone” may be highly variable in space and time, the composition of the injected water in the inner part of the injection bubble is often relatively unchanged from its initial concentration.

Antoniou and others (2013; 2012; 2015) published several papers assessing the effects of the injection bubble on recovery water quality and recovery efficiency. Geochemical modeling of data from functioning ASR wells, test wells, and column experiments retroactively characterized redox conditions and reactions that had caused poor recovery water quality and proposed solutions to mitigate mobilization of trace metals (Fe(II), Mn(II), As). A model simulated cells containing an initial solution that flowed radially outward from the well screen as one-dimensional linear flow lines that were recovered by simulating return flow along the same path after a holding period. The model was programmed to stop recovery simulation when concentrations of metals were about to exceed water quality standards. Model results suggest leaching of metals was caused by reductive dissolution of arsenic-bearing pyrite, manganese-bearing siderite, sedimentary organic material (SOM), and iron-(hydr)oxides. The model demonstrated the importance of the “injection bubble” and the separation that happens between relatively good quality injection water and poorer quality native water and demonstrated a way to maximize

recovery efficiency while minimizing post treatment costs. This study also illuminated the problem of bubble migration and showed that fluctuations in recovered water quality can happen after extended storage from displacement of injection water by natural groundwater flow and/or reducing conditions caused by anaerobic degradation of organic material.

Gaus et al. (2002) continued the conversation of the injection bubble hypothesis using geochemical modeling using the programs PHREEQC and SWIFT and including dual porosity variables. The study focused on an ASR system in a chalk aquifer where native groundwater had high concentrations of fluoride and was not potable. They hypothesized that creating an injection bubble with a large buffer zone might achieve separation of potable water from non-potable water. In this case, interaction between the solid aquifer material and the injected water was significant and the buffering zone was unable to achieve separation between the stored and native water compositions. In Gaus et al. (2002), the idea of the bubble is used to delineate zones of mixing with a predetermined ratio of native to injection water; however, results were not coupled with flow or transport modeling.

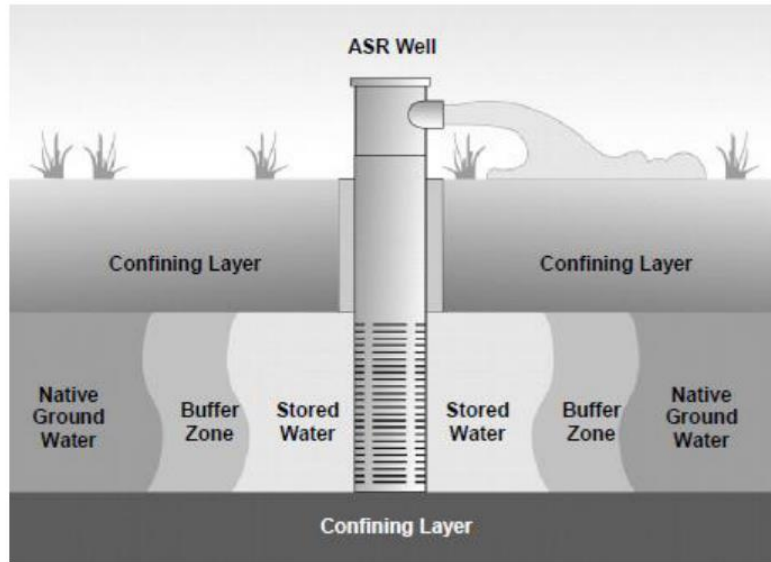


Figure 1: Cross section of a typical ASR well. The stored water and buffer zone labels are the bubble (from Pyne 2005).

Many geochemical ASR studies use bench top experiments where specific parameters such as grain size, water, and sediment composition are closely monitored. Ni et al. (2017) used a closed vessel to simulate the effects of changes in oxidation states on clay, fine sand, and sand sized particles to evaluate the behavior of arsenic in reduced and oxygenated environments. They looked at sediment maturity and degree of weathering for correlations to As behavior during successive cycles and found that grain size and composition of sediments affect As migration and fixation. Clay sized sediments released more As than sand sized particles, and As was more concentrated in sediments with high concentrations of Fe, Mn, P and TOC (Ni et al., 2017).

## 2.2 Study Area

The study site is a 35 by 16 km area along Colorado's Northern Front Range located in eastern Larimer County along the western margin of the Denver-Julesburg Basin (Fig. 2). The area was chosen because of outcrop exposure, availability of domestic well samples, and proximity to a possible Aquifer Storage Recovery (ASR) test well location. Possible aquifers for ASR studied in this thesis include the sandstones of the Lower Cretaceous Dakota Group, Permian Ingleside Formation, and Pennsylvanian/Permian Fountain Formation (Fig. 3).

## 2.3 Formations of Interest

### 2.3.1 Dakota Group (Lower Cretaceous)

The Dakota Group is exposed along the Front Range from the northern border of Larimer County and terminates to the south in Douglas county (Waagé, 1955). The Dakota Group was deposited as interbedded channels and delta deposits that formed during transgressive and regressive episodes of the Western Interior Seaway during the Early Cretaceous. It has been subdivided differently according to different authors due to its complex depositional history (Holbrook and Ethridge, 1996; Waagé, 1955). As

a result, sequences differ depending on location due to pinching out and interfingering of beds (Holbrook and Ethridge, 1996; Robson, 1987). Here I use the terminology of (Braddock et al., 1989) and subdivide the Dakota Group into the Lytle and the South Platte Formation.

The Lytle Formation paraconformably overlies a low stand erosional surface of the Morrison Formation. The depositional environment of the Lytle Formation varied from low sinuosity fluvial systems to braided streams and includes a variety of lithologies from coarse grained conglomeratic sandstones to medium to fine grained sandstones (Holbrook and Ethridge, 1996).

The South Platte Formation is composed of a lower sandstone member, middle shale member, and the upper Plainview sandstone member. The middle shale member is carbonaceous shale, dark grey in color with thin siltstone and sandstone beds, while the Plainview sandstone member is carbonaceous sandstone, tan to grey in color, fine grained and bedded thinly (Braddock et al., 1989). The first sandstone member overlies the middle shale and Plainview members and is a well sorted, grey to tan, fine to medium grained sandstone (Braddock et al., 1989). Its depositional environment was interpreted as a transgression of an intracratonic seaway (Holbrook and Ethridge, 1996).

### 2.3.2 Ingleside Formation (Lower Permian)

The lower Permian Ingleside Formation directly overlies the Fountain Formation in the Northern Front Range and pinches out to the south. The Ingleside is a reddish-pink, fine-grained quartz sandstone with thick crossbedding, usually well cemented with quartz or calcite (Braddock et al., 1989). The source material for the fine to medium-grained sandstones came from erosion of the Fountain Formation during the Late Pennsylvanian by a transgressive sea. The Ingleside Formation also contains limestone beds that were deposited when the area was inundated by the ancient seaway (Nair, 2018).

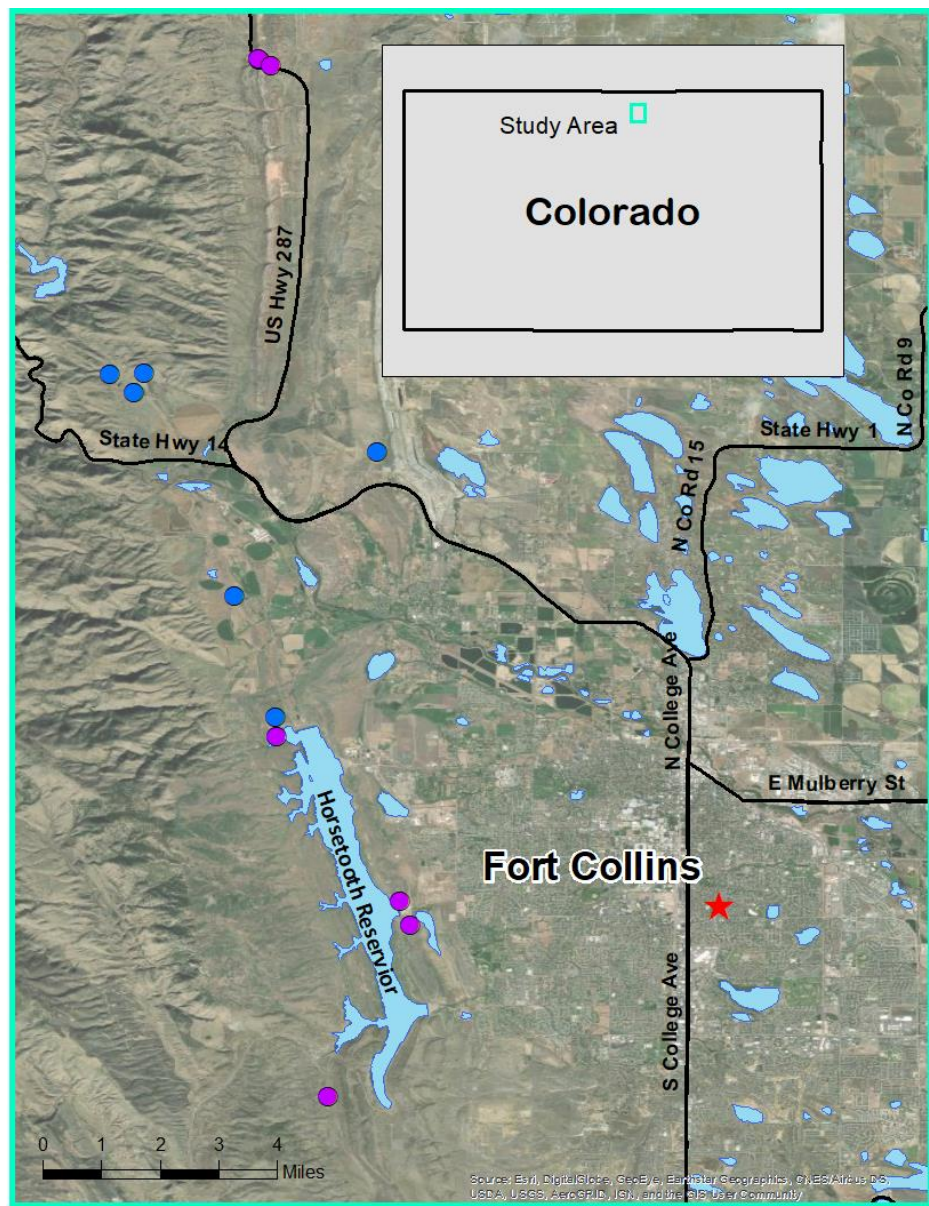


Figure 2: Study area and location of rock (purple) and water (blue) sample locations

ERA	PER.	FORMATION	THICKNESS (m)
CEN.	QUAT.	Undiff.	0-120
	TERT.	Undiff.	0-420
	Laramie		0-30
	Fox Hills Ss.		0-45
	Pierre Sh.		300-2500
MESOZOIC	Niobrara		6-112
	Codell SS.		0-6
	Carlile Sh.		12-30
	Greenhorn Ls.		60-85
	Graneros/ Mowry Sh.		50-65
	Dakota Gp.		60-150
	Morrison		27-75
	Entrada		0-40
	Jelm		0-40
	Lykins		150-200
	Lyons		6-40
	Satanka/ Owl Canyon		30-75
	Ingleside		30-100
PALEOZOIC	PERM.		
	PENN.	Fountain Fm.	30-365
		PRECAMBRIAN	

Figure 3: Stratigraphic column of study area units (Sutton et al., 2004)

### 2.3.3 Fountain Formation (Pennsylvanian/Lower Permian)

The Pennsylvanian-Permian Fountain Formation outcrops along the eastern Front Range of the Rocky Mountains and typically contains both low and high permeability lithologies (Hogan and Sutton, 2014). The thickness of the Fountain ranges from 500 to 4500 ft; however, within the study area it is reported to be 800 to 900 ft (Braddock, 1988; Braddock et al., 1989). The lithology of the Fountain Formation varies from a reddish-brown to purplish-grey arkosic conglomerate to a medium to coarse grained feldspathic sandstone with red-brown siltstones and shales (Braddock et al., 1989). The

depositional environment for the Fountain was likely alluvial fans and braided streams which sourced sediment from formations created by the uplift of the Ancestral Rocky Mountains (Blakey, 2008).

## Chapter 3 - Methods

### 3.1 Water Sample Collection, Preparation, and Analysis

Seven water samples were collected along the Front Range from domestic water supply wells including outdoor spigots or garden hose attachments (Figs. 4 & 5) (Table 1). Information about the wells, including drilling permits, was obtained from the Colorado Department of Natural Resources, Colorado's Decision Support System (CDSS) Mapviewer portal (DNR, 2018). Driller's logs from the domestic sample sites provided some information about the aquifer material; however, reports were not available for all wells. Table 1 shows what information was available.

For each sample, two five-gallon buckets of water were filled from the well prior to sample collection to purge stagnant water. Field parameters, including pH, temperature, conductivity, and dissolved oxygen, were recorded with a YSI water quality probe (Fig. 5). The instrument was calibrated at the beginning of each field day. During sampling, the instrument was given 2-3 minutes to stabilize and then measurements were recorded. Samples from the tap were collected in 500mL sample bottles when possible and otherwise from water collected in the 5-gallon bucket. Bottles were filled to the top and head space was minimized. Samples were kept cool in an ice filled cooler during collection in the field (roughly 7-8 hours) and then by refrigeration in the lab at Colorado State University's Engineering Research Center for a maximum of 24 hours prior to the delivery to the Fort Collins Water Treatment Facility. Samples were then analyzed for major cations and anions and selected metals (Table 2) by the City of Fort Collins Water Treatment Facility Water Quality Lab.

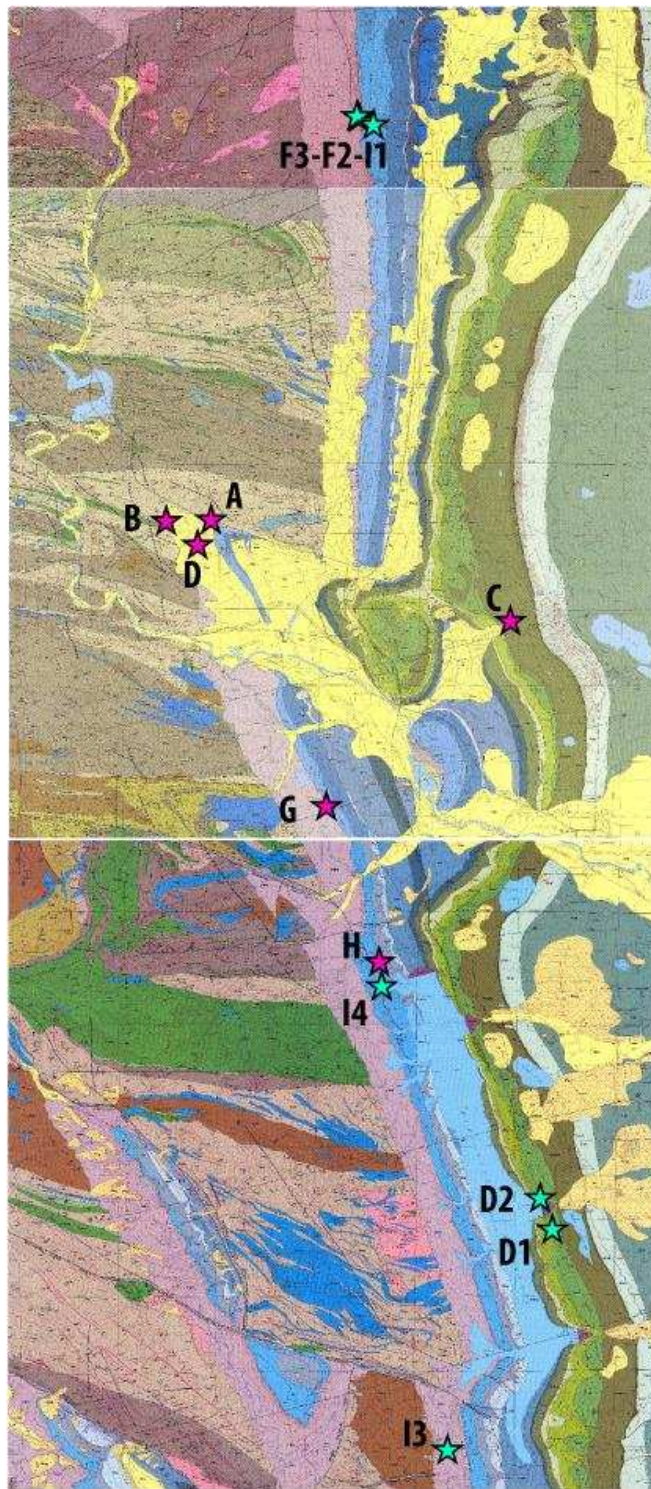


Figure 4: All rock and water sample locations. Water samples B, D, G, H = Fountain; samples A and F= Ingleside and sample C= Dakota. Initial associated with rock samples denotes formation (ex: I3 = Ingleside).



Figure 5: Water quality sampling procedure.

Table 1 : Water Samples

Sample	A	B	C	D	G	H	F
Formation	Ingleside	Fountain	Dakota	Fountain	Fountain	Fountain	Ingleside
Collection Date	5/31/2017	5/31/2017	5/31/2017	6/1/2017	6/1/2017	6/1/2017	6/1/2017
Collection Time	9:14am	10:05am	11:01am	9:37am	3:24pm	4:03pm	11:12am
Use	domestic	domestic	domestic	domestic	domestic	domestic	domestic
Bottles filled from permit number	tap 79953	tap 82877-A	bucket 205932	tap 297041	tap 140795	tap 161546-A	tap n/a
Easting	482375.32 2	481628.597	486875	481999	486838.9	484264.4	n/a
Northing	4503799.3 4	4503963.48	4501862	4503453	4501798.3	4494153.8	n/a
date constructed	1/3/1976	10/27/1995	8/12/1998	3/20/2015	8/13/1985	9/13/2000	n/a
Depth (ft)	540	295	300	1000	200	750	n/a
Yield (gpm)	1	7	9	20	2	4	n/a
testing method	Air	Blow test	Air Pumping	Air Lift	Air	Blow Test	n/a
static level (ft)	125	18	50	100	32	90	n/a
pumping level (ft)	500	295	298	1000		750	n/a
test length (hrs)	2	1	3	2	2	1	n/a
screen slot size	n/a	0.028	0.25	0.032	n/a	0.028	n/a
filter pack	n/a	silica sand	n/a	n/a	n/a	n/a	n/a
drilling method	air rotary	air percussion	air percussion	air percussion	n/a	air percussion	n/a
grouting intervals	cement 0-21ft	cement 3-20 ft	cement 0-20 ft	n/a 0-61	cement 0-20 ft	cement n/a	n/a n/a
method	hand pour	hand pour	hand pour	mixed	dumped	pumped	n/a
disinfection type	n/a	HTH	n/a	dry HTH	n/a	HTH	n/a
amount used	n/a	10 gal	n/a	6 cups	n/a	10 gal	n/a

Table 2: List of Analytes and Detection Limits

<b>Parameter</b>	<b>formula</b>	<b>DL (mg/L)</b>
chloride	Cl <sup>-</sup>	1
sulfate	SO <sub>4</sub> <sup>2-</sup>	5
total phosphorous	PO <sub>4</sub> <sup>-</sup>	0.01
fluoride	F <sup>-</sup>	0.04
calcium	Ca <sup>2+</sup>	0.2
potassium	K <sup>+</sup>	0.1
sodium	Na <sup>+</sup>	0.2
magnesium	Mg <sup>2+</sup>	0.1
iron	Fe <sup>2+</sup>	0.01
aluminum	Al <sup>3+</sup>	0.01
manganese	Mn <sup>2+</sup>	0.001
copper	Cu <sup>+</sup>	0.001
arsenic	As	0.001
selenium	SeO <sub>4</sub> <sup>2-</sup>	0.005
ammonia	NH <sub>3</sub> <sup>+</sup>	0.01
-	Alkalinity	2
total dissolved solids	TDS	10
total suspended solids	TSS	1
total organic carbon	TOC	0.5

### 3.2 Rock Sample Collection, Preparation, and Analysis

#### 3.2.1 Sample Collection, Petrography, and Point Counting

A total of eight rock samples were collected from the Fountain Formation, Ingleside Formation, and Dakota Group (Table 3) (Fig. 4). All samples were collected from outcrop walls by removing weathered surfaces with rock hammers and extracting a less weathered interior section; however, all samples exhibit evidence of modern weathering (Fig. 6). Thin section billets from each sample were prepared at the CSU Department of Geosciences and sent to Spectrum Petrographics for standard thin section preparation (27 x 46mm dimensions polished to 30-micron thickness). Half of each thin section was stained with alizarin red to enable detection of various carbonate minerals including calcite, ferroan calcite, and aragonite (pink-orange); ferroan dolomite and cerussite (mauve), and witherite (red). Petrographic analysis was performed on a standard petrographic microscope and point counts (300-600 points per sample) were conducted to determine mineral abundances.

Table 3: Rock Samples and Analyses Performed

Sample	Formation	Bulk Rock Chemical Analysis			Bench Top Experiment	Petrographic Analysis
ID		FUS-ICP	FUS-MS	INAA		
F1	Fountain	x	x		x	x
F2	Fountain	x	x		x	x
F3	Fountain	x	x		x	x
I1	Ingleside	x	x	x	x	x
I3	Ingleside	x	x	x	x	x
I4	Ingleside	x	x	x	x	x
D1	Dakota	x	x	x	x	x
D2	Dakota	x	x		x	x

### 3.2.2 Bulk Geochemical Analysis

Rock samples collected were sent to Actlabs, in Ancaster, Ontario, Canada, for bulk geochemical analysis. Tables 4 and 5 list major oxide and trace element analytes and their detection limits. The analysis methods include Lithium Metaborate/Tetraborate Fusion - ICP (Inductively coupled plasma) for major and minor element analysis and ICP-MS (Inductively coupled plasma mass spectrometry) for trace element analysis. Instrumental neutron activation analysis (INAA) was performed on four of the rock samples (Table 3) for detection of As, Br, Cr, and Se, which can fall below detection limits of the other methods.



Figure 6: Rock Sampling - I3 - Ingleside Formation - Blue Sky Trail near Horsetooth Reservoir; D2 -Dakota Sandstone - Dixon Canyon near Horsetooth reservoir; I1 - Ingleside Formation - Owl Canyon, north of Fort Collins, near highway 287; D1 - Dakota Formation - Dixon Canyon near the Aggie A.

Table 4: Bulk Rock Geochemical Analysis Oxide Analytes

<u>Analyte</u>	<u>Detection Limit (%)</u>
SiO <sub>2</sub>	0.01
Al <sub>2</sub> O <sub>3</sub>	0.01
Fe <sub>2</sub> O <sub>3</sub> (total Fe)	0.01
MnO	0.001
MgO	0.01
CaO	0.01
Na <sub>2</sub> O	0.01
TiO <sub>2</sub>	0.001
P <sub>2</sub> O <sub>5</sub>	0.01

### 3.2.3 Oxide Recalculation

As a verification measure, petrographic data on modal abundances was compared to bulk rock chemical data. Minerals with larger than 1% of the total sample composition were identified as representative for the sample and used in the model. Weight percent oxide values for a theoretical end-member mineral composition determined from a mineral database were multiplied by the modal percent of the mineral, resulting in a data set of approximate oxide abundances that represented the compositional contributions of each mineral found from point counting. A goal in this recalculation is to compare the oxides calculated from the petrographic data to the oxides determined from whole rock geochemical analyses and then to use the comparison to determine whether the minerals utilized in geochemical modeling accurately represent the whole rock.

Table 5: Bulk Rock Geochemical Analysis Trace Element Analytes

Analysis Method: FUS-MS		Analysis Method: FUS-ICP		
Analyte Symbol	Detection Limit (ppm)	Analyte Symbol	Detection Limit (ppm)	
As	5	Sc	1	
Ga	1	Be	1	
Ge	1	V	5	
Rb	2	Sr	2	
Nb	1	Y	1	
Mo	2	Zr	2	
Ag	0.5	Ba	2	
Bi	0.4	Analysis Method: INAA		
Pb	5	Analyte Symbol	Detection Limit	unit
Cr	20	Au	2	ppb
Co	1	As	0.5	ppm
Pr	0.05	Br	0.5	ppm
Nd	0.1	Cr	5	ppm
Ni	20	Ir	5	ppb
In	0.2	Sb	0.2	ppm
Sn	1	Sc	0.1	ppm
Sb	0.5	Se	3	ppm
Cs	0.5			
La	0.1			
Cu	10			
Zn	30			
Th	0.1			
Lu	0.01			
Ce	0.1			
Sm	0.1			
U	0.1			
Hf	0.2			
Eu	0.05			
Gd	0.1			
Tb	0.1			
Dy	0.1			
Ho	0.1			
Er	0.1			
Tm	0.05			
Yb	0.1			
Ta	0.1			
W	1			
Tl	0.1			

### 3.3 Benchtop Leaching Experiments

#### 3.3.1 Initial Experiment

Benchtop leaching experiments were conducted using collected rock samples. The experiments were meant to be compared to the model results and serve as model validation. All eight rock samples were cut with a rock saw, then crushed by rock hammer into 0.5-1 cm sized pieces. Samples were portioned into ~150g sample sizes, placed into individual 500ml glass Erlenmeyer flasks, filled with 300 ml of tap water, and sealed with a rubber stopper (Table 6). Additionally, there was 1 control sample of only tap water. Temperature and pH of the tap water used in the experiment were measured immediately. The samples then underwent a holding period of six months in a lighted room with manual agitation 2-3 times. No additional heating or vibration was performed on the samples. After incubation, the water from each sample was vacuum filtered through a 0.45 micron Express Pluss® (glass fiber) Membrane at the CSU Plant Sciences Lab and then analyzed by the City of Fort Collins Water Treatment Center Water Quality Lab for major anions and cations and select metals (detection limits are listed in Table 2).

Table 6: Leaching Experiment Samples

Sample ID	mass (g)
F1	143.69
F2	150.72
F3	150.39
I1	150.07
I3	150.63
I4	150.46
D1	150.46
D2	150.53

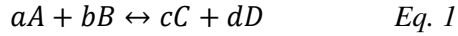
### 3.3.2 Repeat Experiment

The rock leaching experiment was repeated with sample I3 because of an anomalous arsenic result of 3.4 mg/L from the first experiment. Contamination of the sample by the rock saw used to cut it or the hammer or plate used to break the sample into smaller pieces is suspected as the cause of the high concentration. Another sub-sample of I3 was crushed to the same general size as in the previous experiment. This time the rock saw was not used, and a towel was placed between the metal plate, the rock, and the rock hammer to create a barrier. The sample was held for one month instead of six months because time was not available to recreate the first experiment completely. Water quality analysis of a repeat experiment was done by ACZ Labs located in Steamboat Springs; analytes and detection limits are listed in Table 2.

## 3.4 Geochemical Modeling

### 3.4.1 PHREEQC

The geochemical modeling in this study was done using the USGS program PHREEQC- (pH-REdox-EQuilibria-C++) version 3 (Parkhurst and Appelo, 2013). PHREEQC is a widely used computer-modeling program capable of simulating a multitude of aqueous geochemical processes. The code is commonly used to model equilibrium and kinetic reactions, batch reactions, surface exchange, speciation calculations, advective and reactive transport, and inverse modeling (Parkhurst and Appelo, 2013). PHREEQC operates by referencing thermodynamic databases, either provided by the program or specified by the user. The thermodynamic databases are modifiable to fit any system. Chemical reactions modeled in this study do not consider kinetics, they are thermodynamically reversible, independent of time, and calculated using the mass-action law of thermodynamics (Eq. 1 and 2) (Merkel and Planer-Friedrich, 2002).



$$K = \frac{\{C\}^c \cdot \{D\}^d}{\{A\}^a \cdot \{B\}^b} \quad Eq. 2$$

With a, b, c, d = number of moles of the reactants A, B, and the products C, D, respectively for the given reaction, (1);  
 K = thermodynamic equilibrium or dissociation constant (general name)

The program utilizes either the ion-association theory or the ion-interaction theory to calculate species concentrations in a solution, depending on the concentration of dissolved species. The ion-association theory requires a known ionic strength of a given solution and uses the Debye-Hückel limiting-law to calculate activity coefficients (correction factors) for individual ions. The ion-interaction theory is used for more concentrated solutions using the semi-empirical PITZER model based on the Debye- Hückel limiting-law, which employs viral equations that consider intermolecular forces. PHREEQC uses both models and a solver to compute nonlinear sets of equations to calculate species distribution. This requires a presupposition of thermodynamic equilibrium and mass balance where Gibbs free energy and equilibrium constants are known from a database (Merkel and Planer-Friedrich, 2002). PHREEQC was used in this study to analyze fluid mixing, fluid/rock interaction at equilibrium and mineral stability with respect to fluids.

### 3.4.2 Single Pass Mixing Model Explanation and Conceptual Model

The overall goal of the study was to simulate mineral precipitation reactions that might occur during Aquifer Storage Recovery. Figure 7 shows an idealized cross section of an ASR injection process and the concept of an injection bubble (Pyne, 2005). A Single Pass Mixing Model (SPMM) simulates injection of treated surface water into the subsurface. The Single Pass Mixing Model created for this

study is conceptually similar to a bench top experiment mixing two fluids in varying ratios and passing them through a series of seven beakers containing identical, nonreactive rock material (Fig. 8).

An initial step mixes two fluids; one, a hypothetical injection fluid and the other, a hypothetical native groundwater fluid. All consecutive steps introduce an additional increment of hypothetical native fluid. Conceptually, each “beaker” is a cell, each cell is a closed system and each iteration of mixing is a model step. As the mixed solution passes from one cell to the next, aqueous species can increase or decrease in concentration depending on the mixing proportions of injected and native water and on whether any minerals precipitate, removing some species from solution. During the progression of a generalized mixing model in a reactive rock matrix, dissolution of rock material could potentially increase the concentration of some species in the solution. However, the SPMM created here does not allow dissolution of minerals, only precipitation. Therefore, the only mechanisms modifying fluid mixture is the change in proportions of the injected and native water and the removal of aqueous species by mineral precipitation.

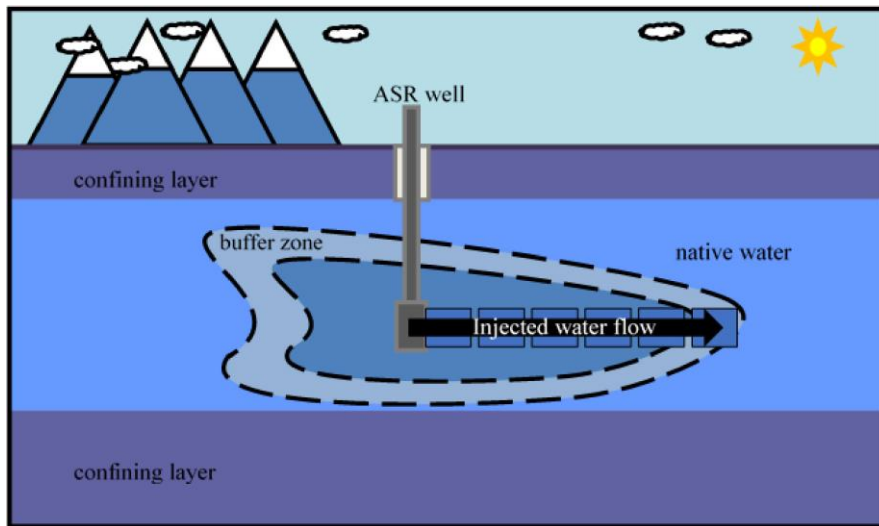


Figure 7: ASR Conceptual Model = Idealized cross section of an ASR injection well with injection bubble after Pyne (2005).

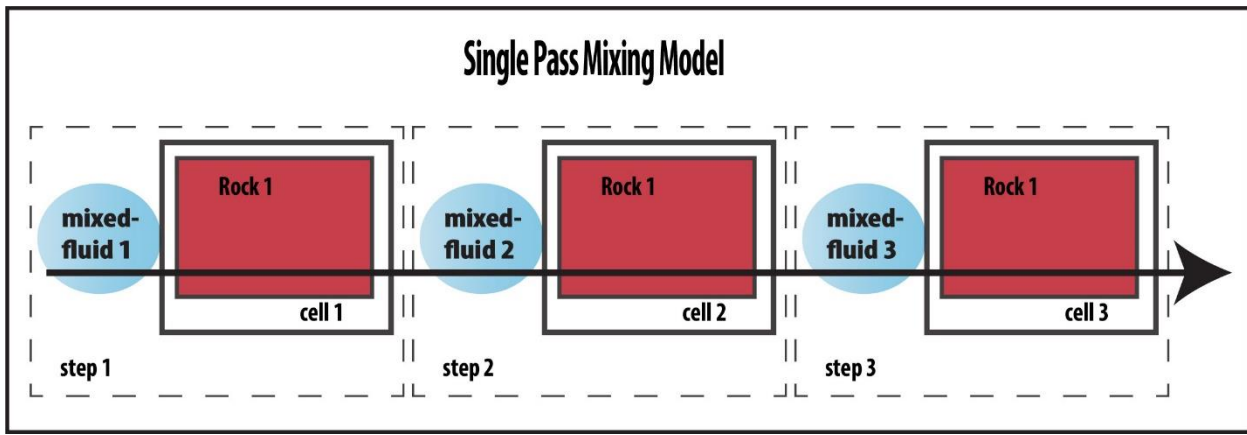


Figure 8: Single Pass Leaching Conceptual Model - Dashed squares are model steps. Squares represent the cellblocks. Red squares represent rock material, which is assumed non-reactive in the model used here. Ovals are fluid mixtures. Black arrow represents the flow fluid as it passes through the cellblocks evolving each time.

### 3.4.3 Single Pass Mixing Model Input Overview

One SPMM was written and then applied to three datasets, each corresponding to the three formations of interest described previously. A full example of a PHREEQC input file is included in Appendix A.3. Each model uses three initial input datasets consisting of two initial fluids and one generalized mineral suite. In this case, *mineral suite* refers to a group of minerals that can precipitate if the fluid in question becomes supersaturated with respect to them. First of the two initial fluid input datasets, is a *Hypothetical Injection Water* and is referred to as HIW from here forward. The HIW is the composition of treated municipal water and comes from the water chemistry analysis provided by the City of Fort Collins Water Treatment facility. The initial HIW composition is used for all three formation models. Second of the two initial fluid input datasets is a *Hypothetical Native Water* and is referred to as HNW from now on. The HNW is the native groundwater water composition derived from an analysis of one or several domestic well samples taken from the three formations of interest. Lastly, the third and final input dataset is the generalized mineral suites provided from whole rock chemical and petrographic

analyses of the Dakota, Ingleside and Fountain formations. The generalized mineral suites inform the model of which minerals to precipitate and only minerals specified in this list are able to precipitate.

The SPMM has seven conceptualized rock chambers, and each cell is a closed system. Each model step first calculates mixing between the HIW and HNW fluids and produces a new intermediate fluid composition. The intermediate fluid is then charge balanced and equilibrated with the generalized mineral assemblage and precipitation will take place if the system allows; this produces another new fluid that will become the input solution for the next cycle (Fig. 9). The final fluid composition from each step is recorded and given as output and presented here as the step results. The step results show the evolution of the aqueous fluid as it progresses within the model (Fig. 9).

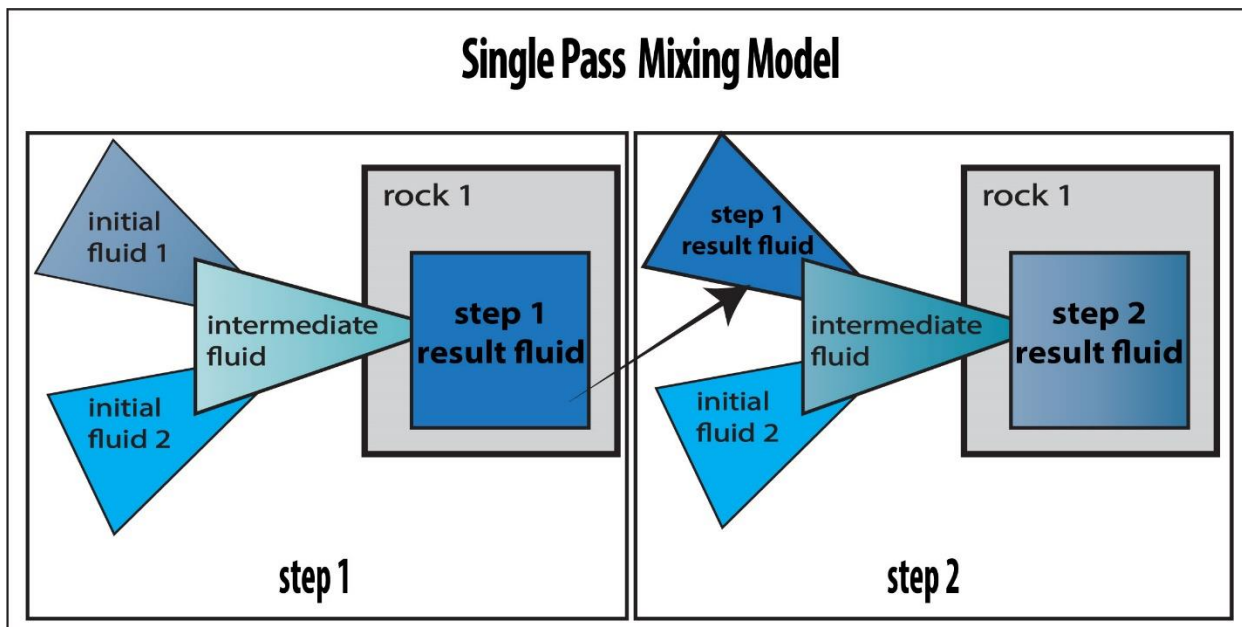


Figure 9: Single Pass Mixing Conceptual Model - Initial fluid 1 = Hypothetical Injection Solution, Initial fluid 2 = Hypothetical Native Solution, Intermediate fluid = mixture of HIW and HNW in step 1 and mixture of step 1 result fluid and HNW in step 2, Step 1 result fluid = fluid composition after reacting with rock material

#### 3.4.4 Mineral Phase Input

The mineral dataset for each formation, which the model uses to constrain minerals permitted to precipitate, is extremely simplified, since it is impossible to generalize an entire formation from a small list of minerals. However, the suite is based on the minerals found in the formation and was informed by whole rock geochemical analysis and petrographic analysis methods described previously. Minerals not observed in the formations are not considered in the model. In each model, minerals are assigned target saturation index values and amounts in mass units. A target saturation index is a value that the model will try to achieve while maintaining chemical equilibrium. A target saturation index of 0.0 indicates the mineral is in equilibrium with the fluid and deviations from 0.0 inform the program to dissolve or precipitate a given mineral while maintaining equilibrium with respect to the solution. The mass assigned to each mineral indicates how much the mineral can dissolve. Indicating an amount of 0.0 mole/kg means that the minerals within the model can precipitate if supersaturated, however, there is no mineral initially available to dissolve. For this study, each mineral is assigned a target saturation index of 0.0 and an initial amount of 0.0 mole/kg. Given the assignment of 0.0 mole/kg, the models described here only consider the possibility of mineral precipitation, not dissolution.

#### 3.4.5 Initial Fluids, and Fluid Speciation

HNW fluid compositions come from domestic well water samples representing specifically:

1. Dakota Group water sample C
2. an averaged Fountain formation composition from water samples B, D, G, H
3. an average of Ingleside water samples A and F

Analytes included in the fluid input datasets are provided in Table 7a. When a fluid is initially input into PHREEQC the composition is defined in terms of total elemental concentrations. Using the ion-association theory the program performs a speciation calculation to distribute elemental totals among

aqueous species. The results of the speciation calculation are activities of aqueous species. A speciation calculation also adjusts pH, pe and temperature to calculate equilibrium for the solution. Furthermore, the speciation calculation can be useful if the initial input fluid analysis is incomplete or does not specify redox couples that may exist. For example, a chemical analysis that reports total iron does not give any information about the amount of  $\text{Fe}^{2+}$  vs  $\text{Fe}^{3+}$  that make up the total iron amount.

During the initial speciation calculations and after each mixing calculation PHREEQC will modify the resulting fluids to ensure it is electrically balanced and in equilibrium and then calculate the equilibrium of mineral phases with respect to the resulting solution by the following process. The charge balanced fluids are then used as the input of the subsequent mixing calculations (Appelo and Postma, 2005). The code uses ion-association (IA) theory with the Debye-Hückel equation and ideal gases, which is appropriate for dilute solutions such as the ones modeled in this study. The activity coefficient  $\gamma$  for ion  $i$  is found from the Debye-Hückel equation (Eq. 3) for dilute solutions where  $I$  or ionic strength is less than 0.1,  $A$  and  $B$  are temperature dependent constants,  $z$  is the charge of an ion, and  $\bar{a}_i$  is an ion size parameter (Appelo and Postma, 2005).

$$\log \gamma_i = - \left( \frac{Az_i^2 \sqrt{I}}{1 + B\bar{a}_i \sqrt{I}} \right) \quad Eq. \ 3$$

The program determines a Saturation Index to assess which minerals may be thermodynamically stable in the various fluids modeled. A Saturation Index (Eq. 4) is the log of a ratio given by dividing the *Ion Activity Product* (IAP) (calculated from the activities or effective concentration in an aqueous solution) by the equilibrium constant of a mineral (calculated at equilibrium by molar concentrations).

$$SI = \log \left( \frac{IAP}{K} \right) \quad Eq. \ 4$$

The Saturation Index of a mineral within an aqueous solution indicates the potential for a mineral to dissolve or precipitate where an index  $< 0$  indicates the aqueous solution is undersaturated with respect to

the mineral (has a potential to dissolve), an index > 0 has a potential to precipitate and an index at 0 indicates equilibrium. In nature, many factors such as time and availability of nucleation sites control the actual dissolution or precipitation; however, modeling kinetic reactions is beyond the scope of this study.

Models described here attempted to replicate a system where a HIW fluid originated above the ground surface and a HNW fluid originated below the ground surface. To achieve this, the HIW is introduced to carbon dioxide and oxygen gases before mixing occurred and the HNW is introduced to carbon dioxide before mixing. Oxygen and carbon dioxide are defined by log partial pressures and a molar amount. Within PHREEQC, the log partial pressure is to a gas phase as a target saturation index is to a mineral phase. Log partial pressures used in the input model for carbon dioxide ( $p\text{CO}_2$ ) and oxygen ( $p\text{O}_2$ ) are the atmospheric values,  $10^{-3.4}$  and  $10^{-0.67}$  atm, respectively. The amount of carbon dioxide and oxygen in the injection solution are both set to 10 moles/kg because the injection solution is theoretically a surface water reservoir that has constant exposure to the atmosphere.

### 3.4.6 Mixing

Each model step first calculates mixing between the HIW and HNW fluids and produces a new intermediate fluid composition. The first cell of the simulation is a mixture of 95% HIW and 5% HNW with a total of 1 kilogram of water. The last cell block, or the last model step, has a calculated ratio of 5% HNW mixed with 95% of the intermediate fluid composition from the previous cell (model step 6). Mixing simulations in PHREEQC are done by batch-reaction calculations that calculate chemical equilibrium between aqueous phases defined by the user (Parkhurst and Appelo, 2013). Each initial input fluid is assigned a value that is a fraction of the total of 1 kilogram of water. Species within the fluid are multiplied by the user-defined fraction and totals are summed. For example, mixing between hypothetical fluids x and y with a 1:1 ratio would contain 50% of each fluid, respectively. Thus, the molar amount of each constituent in both hypothetical fluids is multiplied by 0.5.

Ex:  $(Ca_x * 0.5) + (Ca_y * 0.5) = Ca_{total}$  for the mixture

### 3.4.7 Assumptions

Results of the water chemistry analyses include several analytes reported below the limit of detection. This is not unusual for water chemistry analyses, however, for geochemical modeling it is preferable to have input datasets that are as complete as possible (Pyne, 2005). Therefore, analytes reported below the limit of detection were included in the initial input datasets but given values equal to half of the detection limit. For example, the analytical detection limit of aluminum is 0.01 mg/L, so if the result was <0.01 mg/L the model input was 0.005 mg/L. This assumption was made in order to account for the potential existence of a chemical species that was not picked up by the analysis but may be, in fact, present. While a conservative assumption, an advantage of overestimating the existence of species like arsenic or aluminum identifies a “worst case” scenario in terms of poor water quality or significant mineral precipitation. In addition, because PHREEQC can only utilize the elements and species given as input, either as aqueous species or mineral components, it is better for the model to account for the presence of even a small amount of an aqueous species than to exclude it completely. However, a disadvantage of assuming the presence and concentrations of species that may not be there or may be there in smaller concentrations than assumed is potentially predicting the precipitation of a mineral that would not actually have the ingredients necessary to form in a real system. Additionally, the assumption of a species in a solution was only made if there was a result below the detection limit, meaning that not every possible element was included in the solution. For instance, the hypothetical injection water (Fort Collins treated city water) had values for copper and nitrite and the other analyses lacked these results, so they were not included. In addition, an approximate charge balance was calculated by allowing the concentration of sulfate to be modified. Sulfate was chosen as the charge balancing species because it was an abundant cation (Eq. 5 from Zhu and Anderson (2002)).

$$charge\ balance = \frac{\sum cation - \sum anions}{(\sum |cation| + \sum |anions|)} \quad Eq. 5$$

Another assumption made in the model was the redox potential of the input solutions. Due to insufficient measurement of ORP (oxidation-reduction potential) and DO (dissolved oxygen) caused by malfunction or operator error, it was difficult to constrain a redox environment. Parameters commonly used to specify a redox state of a solution are Eh in volts or pe, a unitless value of electron potential related to activity of a hydrated electron and which is the negative log of the activity of an electron (Eq. 6) (Zhu and Anderson, 2002).

$$pe = -\log a_e \quad Eq. 6$$

Specifying a redox state is important when defining a system that contains species that can exist in more than one valence state, such as Fe<sup>2+</sup>/Fe<sup>3+</sup>, As<sup>3+</sup>/As<sup>5+</sup> or S<sup>2-</sup>/S<sup>6+</sup>. For species like iron, a ratio of activities for its oxidation pair and a total concentration is needed to identify a redox state. The HIW analysis specified concentrations of both nitrite and nitrate (NO<sup>2-</sup>/NO<sup>3-</sup>) which can be used to estimate a pe value; however, the other input water solutions did not have redox couples. Therefore, an input pe value of 10 was arbitrarily selected for the HIW and pe 4 for the HNW input solutions.

Table 7a - PHREEQC Model Input

Aqueous Solution Parameter	Species	Phreeqc notation
Temperature		temp
pH		pH
pe		pe
Aluminum	Al <sup>+3</sup>	Al
Alkalinity	HCO <sub>3</sub> <sup>-</sup>	Alkalinity
Arsenic	H <sub>3</sub> AsO <sub>4</sub>	As

Calcium	$\text{Ca}^{+2}$	Ca
Chloride	$\text{Cl}^{-}$	Cl
Fluoride	$\text{F}^{-}$	F
Iron	$\text{Fe}^{+2}$	Fe
Potassium	$\text{K}^{+}$	K
Magnesium	$\text{Mg}^{+2}$	Mg
Manganese	$\text{Mn}^{+2}$	Mn
Nitrite	$\text{NO}^{2-}$	N(3)
Sodium	$\text{Na}^{+}$	Na
Phosphorous	$\text{PO}_4^{-3}$	P
Sulfate*	$\text{SO}_4^{-2}$	S(6)
Selenium	$\text{SeO}_4^{-2}$	Se
Silicon	$\text{SiO}_2$	Si
* - charge balancing species		

Table 7b - PHREEQC Model Input - Mineral Phases

Equilibrium Phase	Mineral formula from PHREEQC
Albite	$\text{NaAlSi}_3\text{O}_8$
Anhydrite	$\text{CaSO}_4$
Calcite	$\text{CaCO}_3$
Dolomite (disordered)	$\text{CaMg}(\text{CO}_3)_2$
Hematite	$\text{Fe}_2\text{O}_3$
Illite	$\text{K}_{0.6}\text{Mg}_{0.2}\text{Al}_{2.3}\text{Si}_{3.5}\text{O}_{10}(\text{OH})_2$
Kaolinite	$\text{Al}_2\text{Si}_2\text{O}_5(\text{OH})_4$
Adularia (K-feldspar)	$\text{KAlSi}_3\text{O}_8$
K-mica (muscovite)	$\text{KAl}_3\text{Si}_3\text{O}_{10}(\text{OH})_2$
Quartz	$\text{SiO}_2$
full list of mineral reaction, equilibrium constants and enthalpies for the reactions can be found in the appendix	

## Chapter 4 - Results

### 4.1 Water Chemistry Analysis

Water quality analysis results for formation water samples and treated water provided by the City Fort Collins are tabulated and compared to EPA regulations to determine if the water is potable (Table 8, Appendix A.3) as well as plotted on a piper diagram (Fig. 10). All samples, aside from Dakota sample (C) and Fountain sample D, are calcium - bicarbonate type waters. Dakota sample (C) is a calcium-sulfate type water and Fountain sample D is a sodium-bicarbonate type water. All water samples were reported below the EPA standard limits for acceptable drinking water except Dakota sample (C) which showed an exceedance in secondary maximum contaminant level for sulfate and total dissolved solids (Table 8).

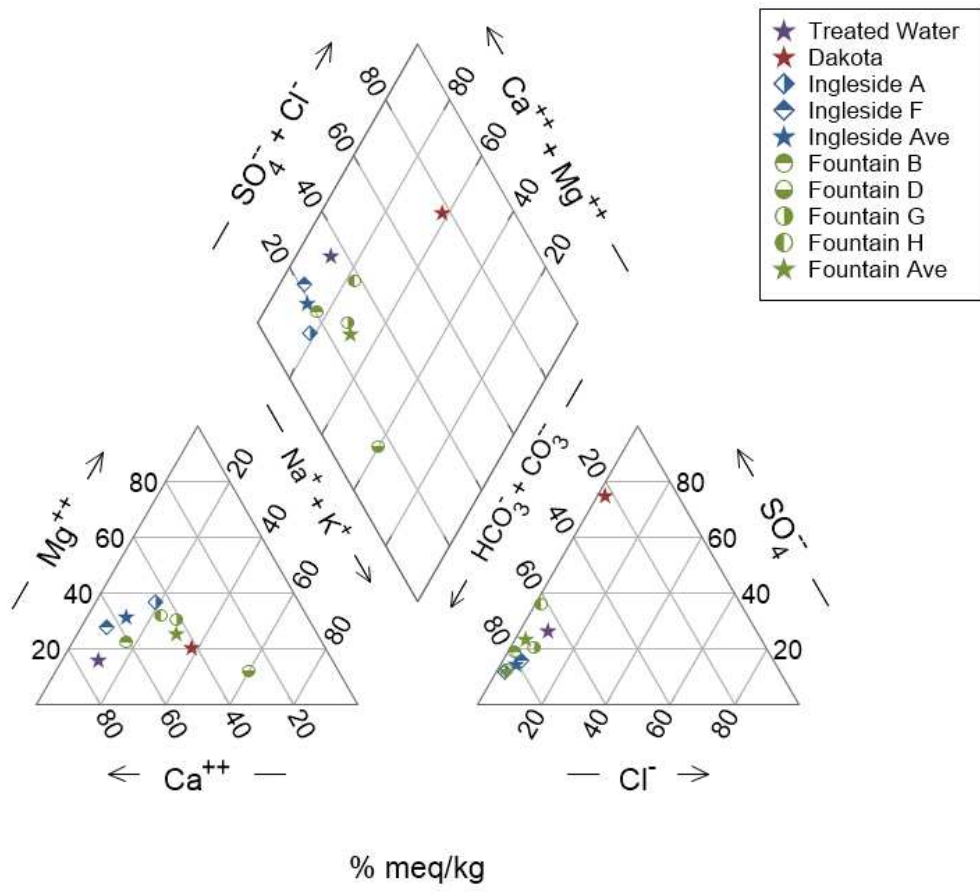


Figure 10: Piper Diagram - Water analysis results and water types of sampled and treated water compositions. Units = meq/L

Table 8: Results of Water Chemistry Analysis

Parameter (mg/L)	Primary DWS	Secondary MCL	Detection Limit	Treated Water	Dakota C	Ingleside			Fountain				
						A	F	Average Ingleside	B	D	G	H	Average Fountain
Alkalinity*	-	-	2	*46.6	195.8	146	217.6	181.8	194	183.4	224	204	201
Ammonia	-	-	0.01	<0.02	0.61	0.011	0.012	0.012	0.011	0.013	0.013	0.012	0.012
ortho-P	-	-	0.005	0.005	<0.005	0.027	0.009	0.018	0.036	0.021	0.014	0.008	0.020
Silica**	-	-	2	5.1	14.3	17.8	13.2	15.5	18.8	14.8	15.8	11.6	15.3
Chloride	-	250	1	3.72	14.1	3.2	9.91	6.6	3.37	3.97	14.4	3.69	6.4
Fluoride	4	2	0.04	0.6	0.78	0.562	0.54	0.55	0.53	0.95	0.46	0.27	0.55
Nitrate	10	-	0.04	0.02	<0.04	2.13	5.13	3.63	2.77	1.5	4.3	2	3
Nitrite	-	-	-	0.07	-	-	-	-	-	-	-	-	-
Sulfate	-	250	5	14.9	508	15.5	33.9	24.7	35.7	21.1	49.9	92.3	49.8
Aluminum	-	0.2	0.01	0.0299	<.01	<.01	<.01	<.01	<.01	<.01	<.01	<.01	<.01
Arsenic	0.01	-	0.001	<.001	<.001	.002	.002	.002	<.001	.002	.002	.002	.002
Calcium	-	-	0.2	16.9	133	34.8	76	55	55.2	25.9	53.8	56	48
Copper	1.3	1.3	-	0.0004	-	-	-	-	-	-	-	-	-
Iron	-	0.3	0.01	0.0109	.018	<.01	.013	.013	.01	<.01	<.01	<.01	.01
Potassium	-	-	0.1	3.7	4.75	2.58	1.02	1.80	2.19	2.74	2.61	1.32	2.22
Magnesium	-	-	0.1	2.2	39.6	17.2	19.8	18.5	12.2	6.43	23.6	24.1	16.6
Manganese	-	-	0.001	0.0012	.131	.001	<.001	.001	<.001	<.001	<.001	<.001	<.001
Sodium	-	-	0.2	0.9	138	15.3	10.7	13	16.6	63	41.4	32.4	38
Selenium	0.05	-	0.005	<.005	<.005	<.005	<.005	<.005	<.005	.007	<.005	<.005	.007
Total-P	-	-	0.01	<0.01	<0.01	0.037	0.02	0.03	0.02	0.3	0.02	0.018	0.1
TDS	-	500	10	84	1005	233	357	295	275	289	385	354	326
TOC	-	-	0.5	1.78	1.74	0.73	0.6	0.7	0.91	0.52	1.25	0.73	0.9
temperature			°C	15	14.95	12.29	12.89	12.59	13.18	14.2	13.54	16.26	14.3
pH			units	7.91	7.13	7.54	7.32	7.43	7	7.62	7.56	7.62	7
conductivity			(µS/cm)	126	1165	281	453	367	358	360	495	516	432

\*calculated from Alkalinity as CaCO<sub>3</sub> by multiplying by 1.22, \*\*silica - SiO<sub>2</sub>, DWS = Drinking Water Standard, MCL = Maximum Contaminant Level

## 4.2 Rock Chemistry Analysis and Point Counting Results

### 4.2.1 Dakota Group Samples

#### *Sample D1 hand sample description*

This sample was collected from Dixon Canyon west of Fort Collins. It is a well-rounded, well-sorted, fine grained quartz arenite (Fig. 19) with an average grain size of 0.22 mm (Fig. 11). There are silica overgrowths on almost all the quartz grains and many of the grains have abundant fluid inclusions. There are chert rock fragments present, as well as trace amounts of zircon. The principal cement is quartz overgrowths.

#### *Sample D2 hand sample description*

This sample was collected from Dixon Canyon west of Fort Collins. It is a rounded to sub-rounded, well-sorted, fine-grained quartz arenite sandstone (Fig. 19) with an average grain size of 0.22 mm (Fig. 12). Many of the quartz grains have cement overgrowths but the overgrowths are not usually euhedral. The quartz grains have abundant fluid inclusions, and some have deformation lamellae. Many of the quartz grains are fractured.

#### *Samples D1 and D2 point counting results*

Point count results (including points counted as pore space) showed samples D1 and D2 to have the highest total quartz percentage of all the samples at ~88 and ~76% respectively. Total quartz is defined here as points identified as mono- or poly-crystalline quartz grains as well as quartzite, chert rock fragments, chalcedony and silica cement. Points identified exclusively as mono- or poly-crystalline quartz grains comprised ~72 and ~67% of samples D1 and D2 respectively. Both samples also had high percentages of pore space at ~10% for D1 and ~13% for D2 (Table 9). The Dakota Group samples were both the most compositionally mature of the samples.

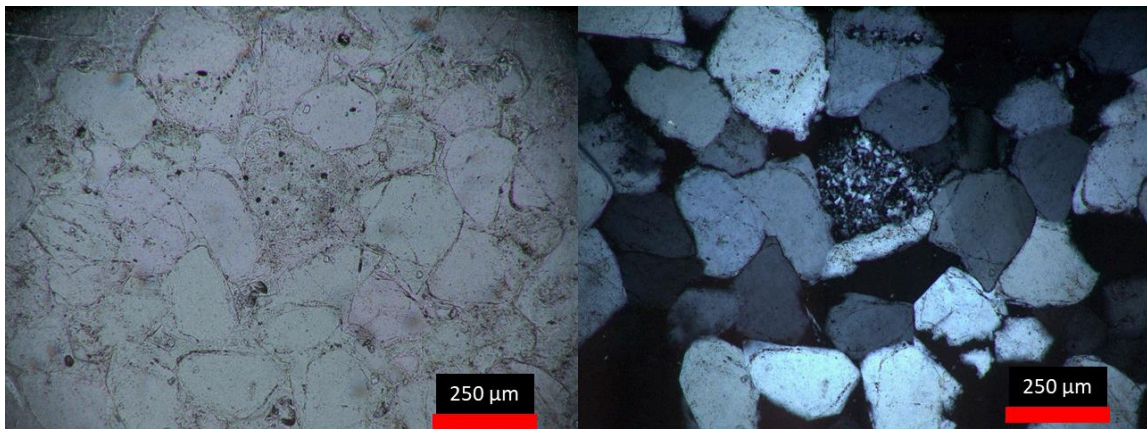


Figure 11: Photomicrograph of sample D1 - PPL (left) and XPL (right), showing quartz grains, and one chert fragment in the center. Note original grain rims and silica cement on the perimeter of the grains.

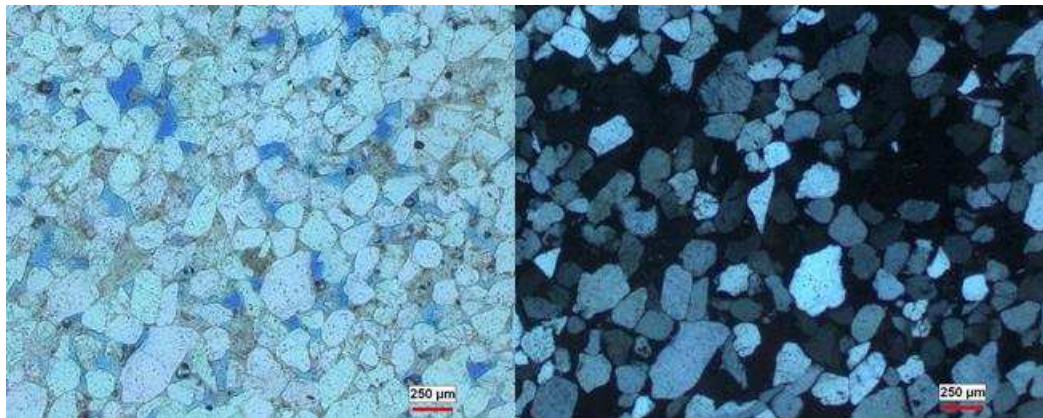


Figure 12: Photomicrograph of sample D2 - PPL (left) and XPL (right), showing mostly quartz grains with silica cement.

#### 4.2.2 Ingleside Formation Samples

##### *Sample I1 hand sample description*

This sample was collected from Owl Canyon north of Fort Collins. This sample is a sub-angular to sub-rounded, moderately sorted, fine-grained, sub-arkose (Fig. 19) with an average grain size of

0.14mm (Fig. 13). The rock is texturally immature and cemented by amorphous silica overgrowths, dolomite, calcite, and iron oxide.

#### *Sample I3 hand sample description*

This sample was collected from the Blue Sky Trail near Horsetooth Reservoir in Fort Collins. It is a sub-rounded, moderately-sorted, very fine-grained, sub-arkose sandstone (Fig. 19) with an average grain size of 0.10mm (Fig. 14). The rock is heavily cemented with poikilotopic dolomite cement. There is quartz overgrowth cement present on some of the quartz grains, but where present it is commonly abraded. Iron oxide cement is present as both rim cement around grains and pore filling cement in some areas of the section.

#### *Sample: I4 hand sample description*

This sample was collected from the Satanka Cove in the northern area of Horsetooth Reservoir west of Fort Collins. It is a rounded, well-sorted, very fine sandstone (Fig. 19). The cements include quartz overgrowths, dolomite, calcite, and hematite. Ferroan dolomite and calcite are identified by alizarin red staining (Fig. 15). The iron oxide cement is mostly in the form of a rim cement around the framework grains.

#### *Samples II, I3 and I4 point counting results*

Ingleside samples are the most heterogeneous, are the least compositionally mature and contain far more matrix compared to the other formation samples. Where material was too fine-grained to determine a specific mineral points were counted as matrix. Ingleside samples had relatively low porosity with I1 at 3.3%, I3 at 2.9% and I4 1.5% (Table 9). Ingleside samples showed a range for percentage of total quartz (points identified as mono- or poly-crystalline quartz grains as well as quartzite, chert rock

fragments, chalcedony and silica cement) at ~59 and ~44 and ~77% for samples I1, I3 and I4 respectively excluding pore space (Table 9).

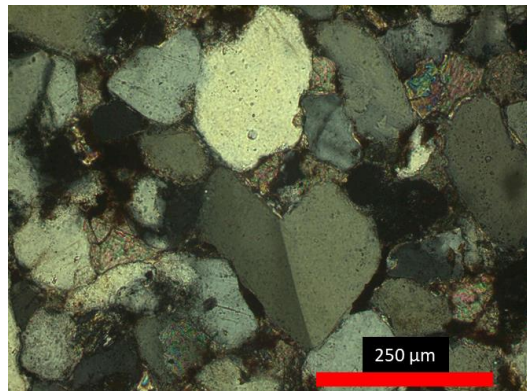


Figure 13: Photomicrograph of sample I1 - XPL, showing quartz, feldspar (sanidine) and anhydrite cement.

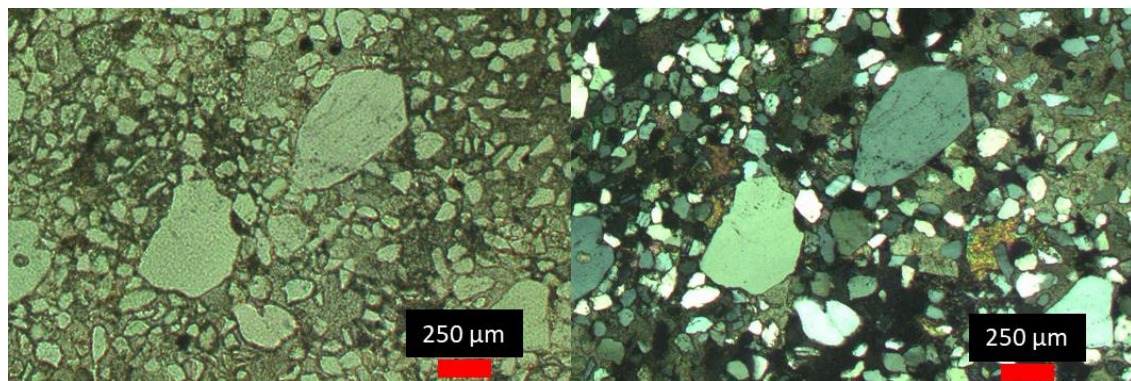


Figure 14: Photomicrograph of sample I3 - PPL (left) and XPL (right). The sample is moderately sorted and the silt to sand sized grains are cemented by a dominantly dolomite cement.

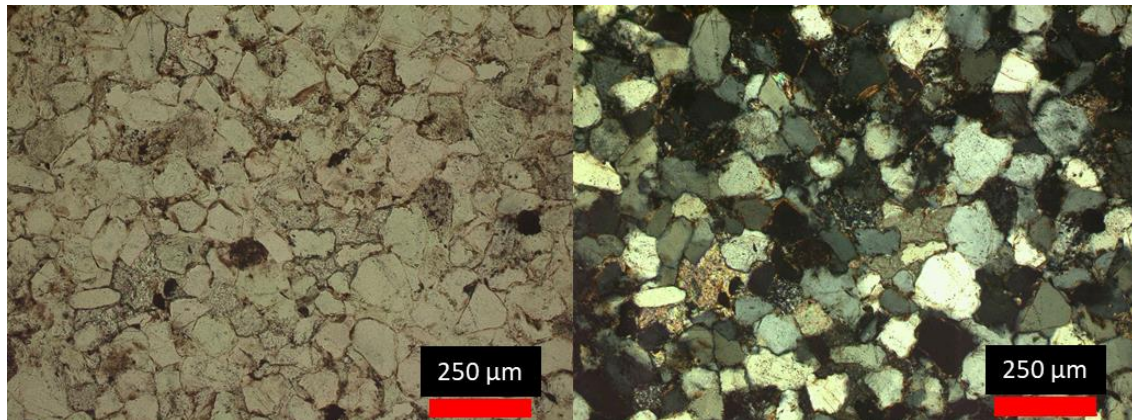


Figure 15: Photomicrograph of sample I4 - PPL (left) and XPL (right), showing silt sized quartz and feldspar grains and carbonate cement.

#### 4.2.3 Fountain Formation

##### *Sample F1 hand sample description*

This sample was collected from Owl Canyon north of Fort Collins. This sample is sub-angular to sub-rounded, well-sorted, very fine-grained sub-arkose sandstone (Fig. 19) with an average grain size of 0.09 mm. The rock is grain supported. Primary cement types are silica, dolomite, and calcite. Calcite cement is often rimming framework grains. The thin section has an uneven distribution of the calcite and dolomite cement in concentrated patches (Fig. 16). Grains of biotite and muscovite are abundant throughout the section and show a preferred orientation parallel to bedding. Partial dissolution of feldspar is common. Abundant secondary pore space is very small and commonly resulting from the dissolution of feldspars, calcite and/or other grains. Some small unidentified opaque minerals are present throughout the section as well as trace amounts of organic matter. Heavy mineral inclusions are common within framework grains and among the matrix and cement. There is evidence of compaction from bent mica grains and convex/concave relationships between quartz grains as well as quartz overgrowths.

### *Sample F2 hand sample description*

This sample was collected from Owl Canyon north of Fort Collins. This sample is a sub-rounded, moderately-sorted, very fine-grained sub-arkose sandstone (Fig. 19) with an average grain size of 0.10mm (Fig. 17). This sample is grain supported, but heavily cemented by calcite. The principal minerals are quartz (mono- and polycrystalline), feldspar (microcline), and abundant rock fragments (chert, siltstone, limestone, quartzite). Accessory minerals are muscovite and anhydrite. Some sericitized feldspar grains are present.

### *Sample F3 hand sample description*

This sample was collected from Owl Canyon north of Fort Collins. This sample is a sub-rounded, moderately well-sorted, medium-grained, sub-arkose sandstone (Fig. 19) with an average grain size of 0.37mm (Fig. 18). Feldspar grain skeletons and partially dissolved feldspars are common and some completely sericitized feldspars are present. Micas that are present are slightly bent around framework grains (quartz and feldspar). Most quartz grains have syntaxial overgrowths. Squashed siltstone rock fragments are present containing muscovite, biotite, iron-oxide, clay, and matrix.

### *Sample F1, F2 and F3 point counting results*

Fountain Formation samples vary in composition, but the dominant minerals are quartz and feldspar. F1, F2 and F3 had the most microcline, albite and untwinned feldspar of the three formations at ~17, ~13 and ~5% respectively including pore space. In contrast, none of the Dakota or Ingleside samples had greater than 10% total feldspar (Table 9). Sample F2 was heavily cemented with calcite and it was the second most abundant mineral from the analysis for that sample. Similar to the Ingleside sample set, Fountain samples show a range for percentage of total quartz (points identified as mono- or polycrystalline quartz grains as well as quartzite, chert rock fragments, chalcedony and silica cement) at ~62

and ~42 and ~72% for samples F1, F2 and F3 respectively excluding pore space (Table 9). F3 had the highest porosity of all eight samples at 14.8%, while samples F1 and F2 had 2.7 and 1.2% porosity respectively.

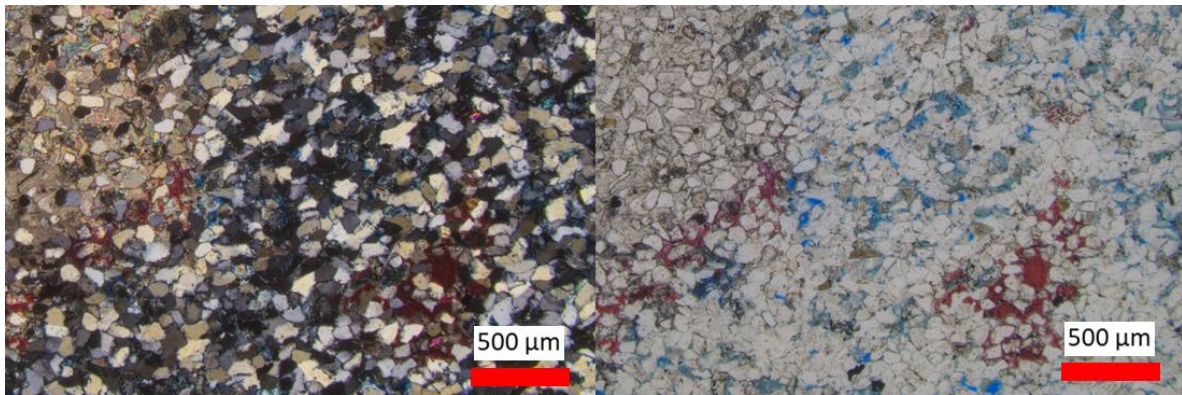


Figure 16: Photomicrograph of sample F1 - PPL (right) and XPL (left), showing red stained carbonate cement that is not continuous throughout the section.

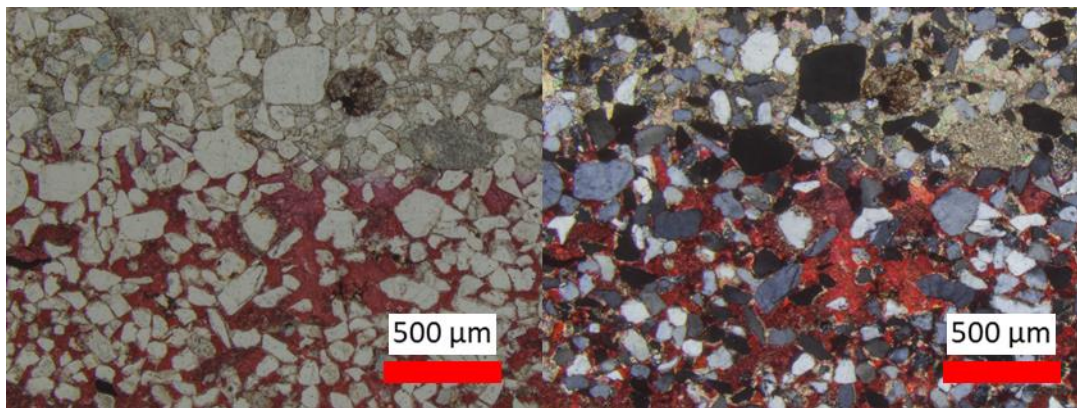


Figure 17: Photomicrograph of sample F2 - PPL (left) and XPL (right), showing abundant carbonate cement (red staining).

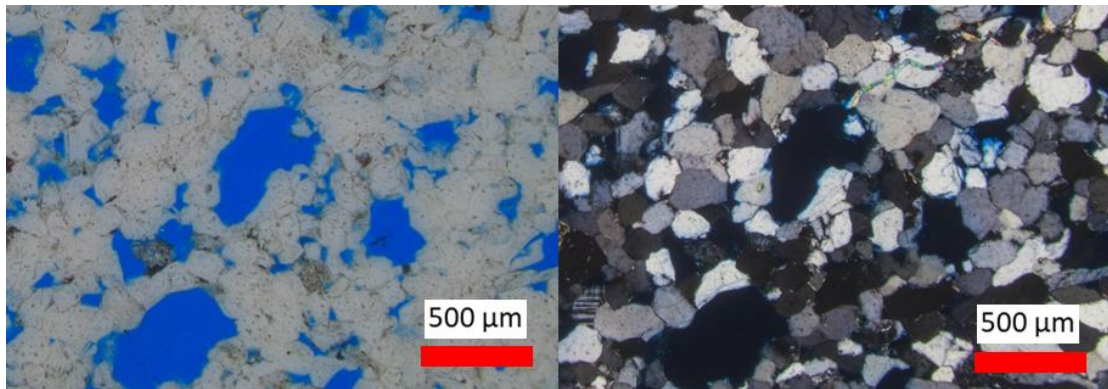


Figure 18: Photomicrograph of sample F3 - PPL (left) and XPL (right), showing abundant pore space (blue epoxy).

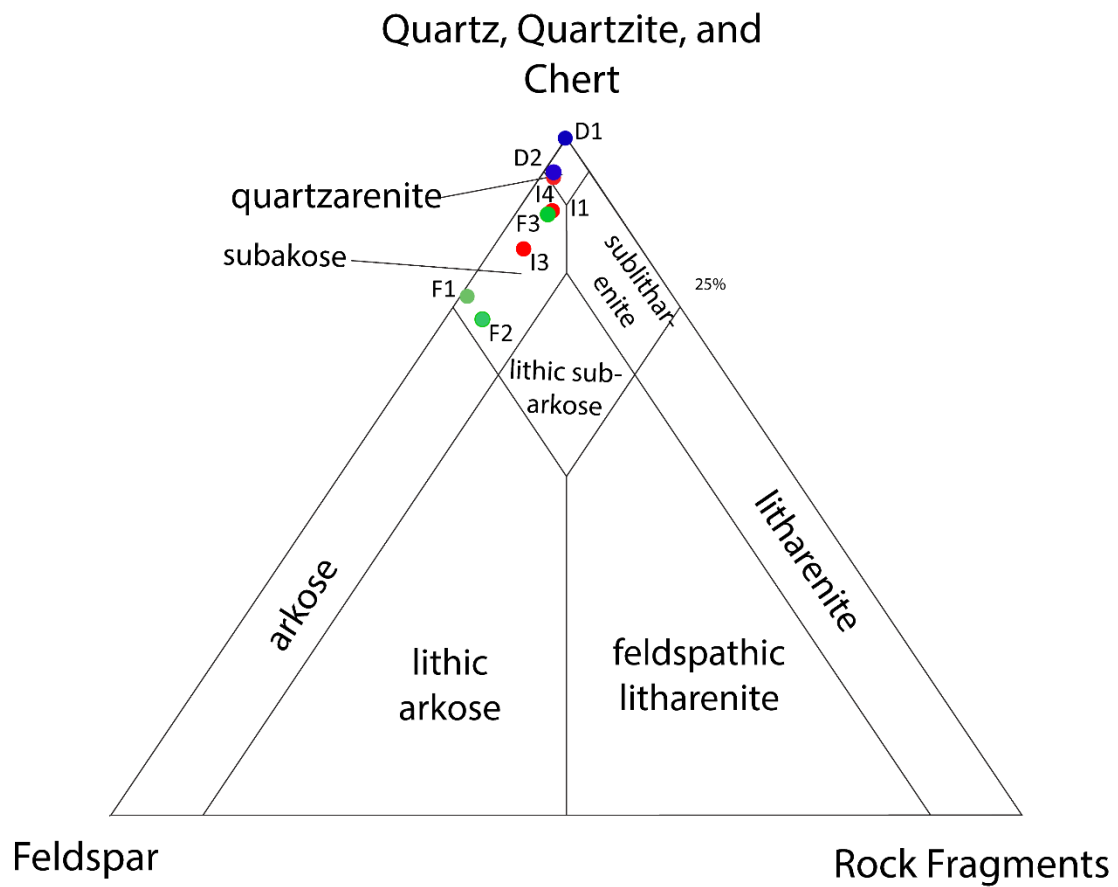


Figure 19: Classification of rock samples. Sandstone classification diagram after McBride (1963)

Table 9: Results of Point Counting in Percent of Total Sample

		D1	D2	I1	I3	I4	F1	F2	F3
	pore space	10.0	13.1	3.3	2.9	1.5	2.7	1.2	14.8
Quartz	mono-crystalline	72.0	66.9	52.6	40.0	66.2	56.3	38.2	62.6
	poly-crystalline	-	-	-	0.0	0.9	0.7	2.1	-
	quartzite	-	0.9	-	0.6	2.6	1.7	0.6	-
	chert RF	-	0.9	0.7	0.6	1.2	0.3	1.2	0.3
	chalcedony	-	0.6	-	2.6	-	-	-	-
	silica cement	15.5	7.1	5.6	-	5.9	3.0	-	9.0
Feldspar	microcline	0.1	-	1.2	0.6	-	1.0	1.2	0.6
	albite	-	-	0.3	3.4	1.2	6.0	5.9	1.6
	untwinned feldspar	-	2.9	2.6	2.3	2.1	10.3	5.6	3.2
Accessory	muscovite	-	0.3	0.2	-	0.3	3.7	-	1.0
	biotite	-	-	0.3	-	-	2.0	-	0.3
	zircon	-	0.3	0.2	0.3	-	-	-	-
	opaque	-	-	1.3	-	0.6	2.7	-	-
Cement	calcite	-	0.9	0.5	0.6	0.3	1.7	39.4	0.3
	dolomite	-	-	10.4	30.6	4.7	3.0	3.2	-
	anhydrite	-	-	2.0	6.9	0.3	0.7	-	-
	illite clay	-	-	-	2.3	-	1.7	-	1.9
	kaolinite	2.4	-	-	-	-	-	-	-
	matrix	-	6.3	15.3	3.1	10.6	2.0	-	1.0
	iron oxide	-	-	2.0	2.3	1.8	0.3	0.3	1.0
Rock Fragments	claystone RF	-	-	-	-	-	-	1.2	-
	siltstone RF	-	-	1.3	0.9	-	-	-	2.3
	mudstone RF	-	-	-	-	-	0.3	-	-
	igneous RF	-	-	-	0.3	-	-	-	-
	metamorphic RF	-	-	0.3	-	-	-	-	-

#### 4.2.4 Bulk Rock Geochemistry

All rock samples were analyzed for major elements as well as trace elements (Tables 10 and 11). In terms of relative abundances of oxides, all samples were highest in SiO<sub>2</sub>. Two rounds of bulk rock geochemical analyses were run, the second of which included a more sensitive INAA analysis. Only the Ingleside samples and one Dakota Group sample, D1, were included in the second analysis due to lack of material.

##### *Dakota Group*

Dakota Group samples were most abundant in SiO<sub>2</sub> with an average of 95 wt. %, a minimum of 92.63 wt. %, and maximum of 97.37 wt. % in samples D1 and D2, respectively. Of the 45 trace elements analyzed by FUS-MS and FUS-ICP, results for sample D2 returned 14 values below detection limit and sample D1 returned 28. Analysis of sample D2 resulted in values for Cu, Pb, and U of 180, 6, and 1 ppm, respectively, and sample D1 resulted in a value of 0.3 ppm U. Sample D1 was also analyzed for trace elements As, Cr, Sb, and Sc using INAA and all were below detection limits except for Cr and Sc which had values of 12 and 0.2 ppm, respectively.

##### *Ingleside Formation*

Ingleside Formation samples had an average weight percent SiO<sub>2</sub> of ~77% with a minimum of 62.8% and maximum of 86.37% in samples I3 and I4, respectively. All Ingleside samples measured below detection limits in Be, Ge, In, Ni, and Zn. Trace elements As, Cr, Sb and Sc were analyzed with both FUS-MS or FUS-ICP, and INAA because the later method has lower limits of detection. For example, Arsenic was recorded below limit of detection (5 ppm) for samples I1 and I3 using FUS-MS while I4 had a value of 8 ppm. However, only I3 was recorded below the detection limit of 0.5 ppm for the INAA technique and the rest of samples recorded values above detection at 0.6, 1.5, and 6.3 for

samples I1, I3, and I4, respectively. All four Ingleside samples were reported below the detection limit of 20 ppm for FUS-MS for Cr except I3 which had a recorded value of 30 ppm. However, while I1, I3, and I4 showed values smaller than 20 ppm using the INAA technique, which had a limit of detection of 5 ppm, sample I3 was recorded as 19 ppm. Sample I3 recorded values of Cu, and Pb at 10, and 7 ppm, respectively.

### *Fountain Formation*

Fountain Formation samples had an average SiO<sub>2</sub> value of ~68 wt. percent. As, Be, Bi, Ge, In, Mo, Ni, Sn and Zn all reported at or below the detection limits for Fountain Formation samples.

Table 10: Results of Fusion ICP Analysis given in Percent Oxides

oxide	Detection Limit	D1	D2	F1	F2	F3	I1	I3	I4
SiO <sub>2</sub>	0.01	97.37	92.63	83.83	60.49	59.4	81.07	62.8	86.37
Al <sub>2</sub> O <sub>3</sub>	0.01	0.63	3.84	4.91	3.08	2.93	2.53	2.49	3.66
Fe <sub>2</sub> O <sub>3</sub> (T)	0.01	0.56	0.38	0.96	0.56	0.53	0.8	0.73	1.04
MnO	0.001	0.007	0.006	0.021	0.017	0.018	0.02	0.09	0.027
MgO	0.01	0.05	0.08	0.76	0.31	0.29	2.47	6.2	1.26
CaO	0.01	0.13	0.15	2.58	17.81	19.85	4.34	10.23	2.43
Na <sub>2</sub> O	0.01	< 0.01	0.01	1.06	0.1	0.08	0.05	0.06	0.06
K <sub>2</sub> O	0.01	< 0.01	0.05	1.62	1.54	1.45	1.07	1.2	1.65
TiO <sub>2</sub>	0.001	0.016	0.093	0.187	0.117	0.103	0.125	0.148	0.132
P <sub>2</sub> O <sub>5</sub>	0.01	< 0.01	0.02	0.03	0.01	0.02	0.02	0.02	0.05
LOI		0.37	1.89	3.38	14.82	15.89	6.66	15.16	3.78
Total		99.15	99.14	99.33	98.85	100.6	99.16	99.12	100.5
LOI - Loss On Ignition									

#### 4.2.5 Bulk Chemical Composition Approximated from Point Count Analyses Results

The mineral recalculation of the bulk rock chemical analysis served as an additional check, but the results of the recalculation did not match the point counted modal abundances well in many cases. Results from the oxide abundance calculations were meant to compare the accuracy in characterizing the composition of each sample by point counting. Table 12 shows discrepancies between the analyzed elemental composition of the samples and the point counted results.

Discrepancies between the measured and calculated values are largest for SiO<sub>2</sub>, CaO and LOI (Loss on Ignition). For instance, SiO<sub>2</sub> is underestimated in sample I3 by 12 wt. % and by 7.7 and 8.9 wt. % in samples I1 and F2 respectively. However, the most significant difference in SiO<sub>2</sub> is actually the over estimation in sample F3 by 31 wt. %. The overestimation in sample F3 is accompanied by large underestimations of both calcium oxide and the cumulative Loss on Ignition measurement.

Table 11: Results of Fusion MS/ICP and INAA Analysis

Element	unit	Detection Limit	Analysis	D1	D2	I1	I3	I4	F1	F2	F3
Ag	ppm	0.5	FUS-MS	< 0.5	< 0.5	0.7	0.9	2.4	0.7	< 0.5	< 0.5
As	ppm	0.5	INAA	< 0.5	-	0.6	< 0.5	6.3	-	-	-
Ba	ppm	2	FUS-ICP	17	15	172	190	269	261	235	230
Br	ppm	0.5	INAA	< 0.5	-	< 0.5	< 0.5	< 0.5	-	-	-
Ce	ppm	0.1	FUS-MS	5.6	11.2	10.5	11.4	13.7	25.2	14.8	13.9
Co	ppm	1	FUS-MS	< 1	1	1	1	3	3	< 1	< 1
Cr	ppm	5	INAA	12	-	18	19	15	-	-	-
Cr	ppm	20	FUS-MS	< 20	< 20	< 20	30	< 20	30	< 20	< 20
Cs	ppm	0.5	FUS-MS	< 0.5	< 0.5	0.6	0.5	1	1.2	0.8	0.8
<b>Cu</b>	ppm	10	FUS-MS	< 10	180	< 10	10	30	260	110	180
Dy	ppm	0.1	FUS-MS	0.2	0.6	0.7	1	0.9	1.5	0.9	0.9
Er	ppm	0.1	FUS-MS	0.1	0.3	0.4	0.6	0.6	0.9	0.5	0.5
Ga	ppm	1	FUS-MS	< 1	4	3	3	4	4	3	3
Gd	ppm	0.1	FUS-MS	0.2	0.5	0.7	1.1	1.2	1.7	1.1	1.1
Hf	ppm	0.2	FUS-MS	0.6	1.1	3.6	4.6	1.9	2.2	2.3	1.6
Ho	ppm	0.1	FUS-MS	< 0.1	0.1	0.1	0.2	0.2	0.3	0.2	0.2
La	ppm	0.1	FUS-MS	3.2	6.8	5.3	8.1	7.1	10.8	8.2	7.9
Lu	ppm	0.01	FUS-MS	< 0.01	0.05	0.09	0.1	0.1	0.14	0.09	0.08
Mo	ppm	2	FUS-MS	< 2	< 2	< 2	7	< 2	< 2	< 2	< 2
Nb	ppm	1	FUS-MS	< 1	4	1	1	2	2	2	2
Nd	ppm	0.1	FUS-MS	2.1	3.9	4.7	6.1	6.3	11.1	6.9	6.8
Pb	ppm	5	FUS-MS	< 5	6	< 5	7	59	9	10	7
Pr	ppm	0.05	FUS-MS	0.61	1.21	1.21	1.66	1.69	2.91	1.81	1.77
Rb	ppm	2	FUS-MS	< 2	< 2	24	26	38	40	32	30
Sb	ppm	0.2	INAA	< 0.2	-	0.3	0.3	9	-	-	-
Sb	ppm	0.5	FUS-MS	< 0.5	0.7	< 0.5	< 0.5	7.3	0.6	0.7	0.8
Sc	ppm	0.1	INAA	0.2	-	1.2	1.1	1.6	-	-	-
Sc	ppm	1	FUS-ICP	< 1	< 1	2	1	2	4	2	2
Sm	ppm	0.1	FUS-MS	0.4	0.7	0.9	1.2	1.2	2.2	1.4	1.3
Sn	ppm	1	FUS-MS	< 1	2	< 1	< 1	5	1	< 1	1
Sr	ppm	2	FUS-ICP	6	37	51	76	55	45	115	121
Ta	ppm	0.1	FUS-MS	< 0.1	0.5	0.1	0.2	0.1	0.4	0.2	0.2
Tb	ppm	0.1	FUS-MS	< 0.1	0.1	0.1	0.2	0.2	0.3	0.2	0.2
Th	ppm	0.1	FUS-MS	0.5	2.4	1.5	1.5	2	2.6	1.4	1.4
U	ppm	0.1	FUS-MS	0.3	1	1.1	1.1	0.7	0.8	0.9	0.7
V	ppm	5	FUS-ICP	< 5	14	18	13	13	15	14	14
V	ppm	5	FUS-ICP	< 5	14	18	13	13	15	14	14
Y	ppm	1	FUS-ICP	2	4	7	7	6	8	5	4
Zr	ppm	2	FUS-ICP	28	41	177	228	92	103	108	76

Table 12: Comparison of Measured and Calculated Oxide Wt. % Values

		SiO <sub>2</sub>	Al <sub>2</sub> O <sub>3</sub>	MnO	MgO	CaO	Na <sub>2</sub> O	K <sub>2</sub> O	TiO <sub>2</sub>	P <sub>2</sub> O <sub>5</sub>	Fe <sub>2</sub> O <sub>3</sub> (T)	LOI	Total
D1	measured	97.4	0.6	-	0.1	0.1	< 0.01	< 0.01	-	< 0.01	0.6	0.4	99.2
	calculated	98.5	1.1	-	-	-	-	-	-	-	-	0.4	100
	diff. abs.	1.1	0.5	-	0.1	0.1	-	-	-	-	0.6	-	0.8
D2	measured	92.6	3.8	-	0.1	0.2		0.1	0.1	-	0.4	1.9	99.1
	calculated	94.3	2	-	0.2	0.6	-	1.1	-	-	0.1	1.3	99.7
	diff. abs.	1.7	1.8	-	0.1	0.4	-	1	0.1	-	0.3	0.6	0.6
I1	measured	81.1	2.5	-	2.5	4.3	0.1	1.1	0.1	-	0.8	6.7	99.2
	calculated	73.4	3.7	-	2.9	4.4	-	2	-	-	2.4	8.5	97.4
	diff. abs.	7.7	1.2	-	0.4	0.1	0.1	0.9	0.1	-	1.6	1.8	1.8
I3	measured	62.8	2.5	0.1	6.2	10.2	0.1	1.2	0.1	-	0.7	15.2	99.1
	calculated	50.8	1.8	-	7	12.8	0.4	0.8	-	-	2.4	19.7	95.9
	diff. abs.	12	0.7	0.1	0.8	2.6	0.3	0.4	0.1	-	1.7	4.5	3.2
I4	measured	86.4	3.7	-	1.3	2.4	0.1	1.7	0.1	0.1	1	3.8	100.5
	calculated	85.1	4.9	-	1	1.8	0.1	1	0.3	-	2.1	3.6	100
	diff. abs.	1.3	1.2	-	0.3	0.6	-	0.7	0.2	0.1	1.1	0.2	0.5
F1	measured	83.8	4.9	-	0.8	2.6	1.1	1.6	0.2	-	1	3.4	99.3
	calculated	79.8	6.2	-	1.2	2.2	0.7	2.8	1.4	-	2	3.3	99.7
	diff. abs.	4	1.3	-	0.4	0.4	0.4	1.2	1.2	-	1	0.1	0.4
F2	measured	60.5	3.1	-	0.3	17.8	0.1	1.5	0.1	-	0.6	14.8	98.9
	calculated	51.6	2.9	-	0.7	23.4	0.7	1.2	-	-	0.3	19.3	100
	diff. abs.	8.9	0.2	-	0.4	5.6	0.6	0.3	0.1	-	0.3	4.5	1.1
F3	measured	59.4	2.9	-	0.3	19.9	0.1	1.5	0.1	-	0.5	15.9	100.6
	calculated	90.4	2.7	0.2	0.2	0.4	0.4	1.1	0.2	-	1.5	1	97.9
	diff. abs.	31	0.2	0.2	0.1	19.5	0.3	0.4	0.1	-	1	14.9	2.7

#### 4.3 Leaching Experiments

The leaching experiment resulted in nine aqueous solutions, one each for the 8 rock samples and one control (Table 13). The resulting leachate solutions are referred to by their original rock sample ID plus the letter E to indicate they are from the experiment. Leachate solutions E-F2 and E-D2 had high levels of nitrate which were all well above the EPA primary drinking water standard of 10 mg/L. In addition, sample E-F1 showed an arsenic concentration of 0.02 mg/L, while sample E-I3 showed an extremely high concentration of arsenic of 3.4 mg/L compared to the EPA primary drinking water standard of 0.01 mg/L. Additionally, secondary exceedances in manganese and TDS were reported in samples E-D2, and E-F2. Because of the anomalously high value of arsenic returned for sample E-I3 additional sample material from rock sample I3 was used to repeat the experiment. Results from the second analysis are called E-I3.2 and show an arsenic value below the detection limit of 0.04 mg/L (Table 14). However, values for TDS, sulfate, and nitrate were much higher in the second experiment run than the first, with values of 1620, 454, and 118 mg/L, respectively and far exceeded the primary drinking water standard of 10 mg/L. TDS and sulfate exceed the secondary maximum contaminant levels as stated by the EPA

Table 13: Results of Leaching Experiment (mg/L)

Parameter (mg/L)	Primary DWS	Secondary MCL	DL	E-F1	E-F2	E-F3	E-I1	E-I3	E-I4	E-D1	E-D2	T.W.C.
Alkalinity	-	-	2	80	172	86.2	79.6	82	76.4	43.2	68	37.6
Ammonia	-	-	0.01	0.03	2.28	1.1	0.05	0.09	0.1	0.82	3.13	0.03
ortho-P	-	-	0.005	0.032	0.027	0.046	0.016	0.358	0.011	0.065	0.098	<0.005
Silica	-	-	2	11	17.5	9.9	10.6	10.1	11	9.8	19.8	5.5
Chloride	-	250	1	5.1	135.2	36	26.7	5	4.2	4.2	37.4	3.9
Fluoride	4	2	0.04	0.45	0.48	0.68	0.69	0.58	0.43	0.6	0.57	0.63
Nitrate	10	-	0.04	1.81	<b>34.3</b>	3.19	2.13	0.13	0.14	0.63	<b>173</b>	0.06
Sulfate	-	250	5	14.1	244.6	14.6	17.5	14.3	13.2	14.2	104	12.9
Aluminum	-	0.2	0.01	<0.01	<0.01	0.038	0.012	0.012	<0.01	0.011	<0.01	<0.01
Arsenic	0.01	-	0.001	<b>0.022</b>	0.008	0.008	0.006	<b>3.39</b>	0.002	0.004	0.006	<0.001
Calcium	-	-	0.2	34.2	187.8	34.4	34	13.5	23	18.5	154	17
Copper	1.3	1	0.001	0.075	0.089	0.099	0.042	0.07	0.035	0.057	0.251	0.17
Iron	-	0.3	0.01	<0.01	<0.01	<0.01	<0.01	<0.01	<0.01	<0.01	<0.01	<0.01
Potassium	-	-	0.1	3.8	8.7	4.1	2.3	3.4	3.8	1.4	90	0.8
Magnesium	-	-	0.1	1.7	37.8	8	5.6	14.8	7.2	2.4	76.2	2
Manganese	-	0.05	0.001	<0.001	0.003	0.002	<0.001	0.006	<0.001	0.003	0.051	<0.001
Sodium	-	-	0.2	3.9	58.7	18.1	16.7	4.6	3.7	4.5	13.6	3.9
Selenium	0.05	-	0.005	<0.005	<0.005	<0.005	<0.005	<0.005	<0.005	<0.005	0.022	<0.005
Total Phos.	-	-	0.01	0.04	0.04	0.05	0.02	0.5	<0.01	0.08	0.13	<0.01
TOC	-	-	0.5	4.3	24.3	3.59	4.74	3.22	2.44	3.6	52	1.84
TDS	-	500	10	104	<b>1042</b>	158	144	102	98	86	<b>1432</b>	38
DWS - Drinking Water Standards, MCL - Maximum Contaminant Level, T. W. C. - tap water control, DL- Detection Limit, values in bold exceed EPA drinking water standards												

Table 14 : Comparison Experiment Results (mg/L)

I3 - 1st analysis			I3 - 2nd analysis		
Parameter	DL	Experiment 1 - I3	Experiment 2 - I3	DLimit	Parameter
Aluminum	0.01	0.012	<0.03	0.03	Aluminum, dissolved
Selenium	0.005	<0.005	<0.05	0.05	Selenium, dissolved
Total Phos	0.01	0.50	<1	1	Phosphorus, total
Iron	0.01	<0.01	<0.02	0.02	Iron, dissolved
Copper	0.001	0.07	0.02	0.01	Copper, dissolved
Manganese	0.001	0.006	0.009	0.005	Manganese, dissolved
Fluoride	0.04	0.58	0.3	0.1	Fluoride
Sodium	0.2	4.6	11.3	0.2	Sodium, dissolved
Silica	2	10.1	16.7	0.2	Silica, dissolved
Ammonia	0.01	0.09	5.36	0.05	Nitrogen, ammonia
Arsenic	0.001	<b>3.39</b>	<0.04	0.04	Arsenic, dissolved
Alkalinity	2	82	206	2	Total Alkalinity
Potassium	0.1	3.4	21.2	0.2	Potassium, dissolved
Chloride	1	5.0	31	0.5	Chloride
TOC	0.5	3.22	32.7	5	Carbon, total organic (TOC)
Magnesium	0.1	14.8	74.7	0.2	Magnesium, dissolved
Nitrate	0.04	0.13	<b>118</b>	2	Nitrate as N, dissolved
Calcium	0.2	13.5	330	0.1	Calcium, dissolved
Sulfate	5	14.3	<b>454</b>	30	Sulfate
TDS	10	102	<b>1620</b>		TDS (calculated)
values in bold exceed EPA drinking water standards					
Analyses were done by two different labs with differing detection limits					
DL- Detection Limit					

## 4.4 Geochemical Modeling Results

### 4.4.1 Fluid Evolution Model

#### *Hypothetical Injection Water Pre-Mixing Solutions*

Tables 15-18 show a progression of water chemistry data used in this study, transitioning from raw to the form used as input for the SPMMs. These data include: 1. raw data from lab analysis, 2. data manually entered as input to PHREEQC, 3. the result of an initial speciation calculation, and 4. the data after equilibrium with carbon dioxide and oxygen gases. The only differences between the raw data and the data manually input into PHREEQC were the substitution of  $\frac{1}{2}$  the indicated detection limit value in cases where analytes were reported below detection. Technically the first processing done by PHREEQC is the solution speciation calculation. The resulting fluid after speciation minimally differed from the initial PHREEQC input, with deviations  $< 1 \text{ mg/L}$  except for sulfate and bicarbonate (Tables 15-18). During initial speciation of raw data, bicarbonate decreased in every fluid;  $\sim 0.5 \text{ mg/L}$  loss in the HIW,  $\sim 7 \text{ mg/L}$  in Dakota HNW,  $5 \text{ mg/L}$  in Ingleside and  $4 \text{ mg/L}$  in Fountain. Sulfate concentration increased in the Dakota ( $53 \text{ mg/L}$ ), Ingleside ( $46 \text{ mg/L}$ ) and Fountain ( $\sim 0.4 \text{ mg/L}$ ) HNWs but decreased by  $\sim 3 \text{ mg/L}$  in HIW during speciation of raw data. During the next premixing step when speciated fluid equilibrated with  $O_2$  or  $CO_2$ , only dissolved concentrations of bicarbonate and nitrate were modified. Bicarbonate concentrations decreased during the equilibration step in the Dakota HNW by  $1 \text{ mg/L}$ , the Fountain by  $\sim 0.6 \text{ mg/L}$  and in the HIW by  $\sim 0.7 \text{ mg/L}$  (Tables 15-18). Very small decreases in nitrate were observed in the Dakota ( $\sim 1.0 \mu\text{g/L}$ ), Ingleside ( $\sim 0.3 \mu\text{g/L}$ ) and Fountain ( $\sim 1.0 \mu\text{g/L}$ ) HNW fluids. Bicarbonate and nitrate concentration changes here are less than the analytical limit of detection and are therefore not statistically significant. However, in all models the  $p_e$  increased during the mineral precipitation process: HIW (+3.5), Dakota HNW (+8.3), Ingleside HNW (+ 8.8) and Fountain HNW (+8.8).

Table 15: Hypothetical Injection Water Pre-Mixing Solutions - All units mg/L

	raw	PHREEQC	speciation and charge balance	<i>difference</i>	equilibration atmosphere	<i>difference</i>
		input	output 1	<i>output 1 - input</i>	output 2	<i>output 2 - output 1</i>
Al <sup>+3</sup>	0.03	3E-02	3E-02	<i>1E-06</i>	3E-02	<i>no change</i>
H <sub>3</sub> AsO <sub>4</sub>	<.001	5E-04	3E-04	<i>-2E-04</i>	3E-04	<i>no change</i>
Ca <sup>+2</sup>	16.9	16.9	16.9	<i>2E-03</i>	16.9	<i>no change</i>
Cl <sup>-</sup>	3.7	3.7	3.7	<i>4E-04</i>	3.7	<i>no change</i>
F <sup>-</sup>	0.6	0.6	0.6	<i>6E-05</i>	0.6	<i>no change</i>
Fe <sup>+2</sup>	0.0109	1E-02	1E-02	<i>1E-06</i>	1E-02	<i>no change</i>
SiO <sub>2</sub>	5.1	5.1	5.1	<i>5E-04</i>	5.1	<i>no change</i>
HCO <sub>3</sub> <sup>-</sup>	46.6	46.6	46.1	<i>-5E-01</i>	45.5	<i>-0.7</i>
K <sup>+</sup>	3.7	3.7	3.7	<i>4E-04</i>	3.7	<i>no change</i>
Mg <sup>+2</sup>	2.2	2.2	2.2	<i>2E-04</i>	2.2	<i>no change</i>
Mn <sup>+2</sup>	0.0012	1E-03	1E-03	<i>1E-07</i>	1E-03	<i>no change</i>
NO <sub>3</sub> <sup>-</sup>	0.02	0.1	0.1	<i>7E-06</i>	0.1	<i>no change</i>
Na <sup>+</sup>	0.9	0.9	0.9	<i>9E-05</i>	0.9	<i>no change</i>
PO <sub>4</sub> <sup>-3</sup>	<0.01	0.005	2E-02	<i>1E-02</i>	0.0	<i>no change</i>
SO <sub>4</sub> <sup>-2</sup>	14.9	14.9	12.3	<i>-3</i>	12.3	<i>no change</i>
SeO <sub>4</sub> <sup>-2</sup>	<.005	3E-03	3E-03	<i>2E-07</i>	3E-03	<i>no change</i>
TDS	84	<i>n/a</i>	85.9	<i>n/a</i>	85.2	<i>n/a</i>
pH	7.9	7	7	<i>no change</i>	8	<i>1</i>
pe	<i>n/a</i>	10	10	<i>no change</i>	13.5	<i>3.5</i>

Table 16: Dakota Hypothetical Native Water Pre-Mixing Solutions - All units mg/L

	raw	PHREEQC	speciation and charge balance	<i>difference</i>	equilibration subsurface	<i>difference</i>
		<i>input</i>	<i>output 1</i>	<i>output 1 - input</i>	<i>output 2</i>	<i>output 2 - output 1</i>
Al <sup>+3</sup>	<.01	0.005	5E-03	5E-06	5E-03	<i>no change</i>
H <sub>3</sub> AsO <sub>4</sub>	<.001	0.0005	3E-04	-2E-04	3E-04	<i>no change</i>
Ca <sup>+2</sup>	133	133	133.2	2E-01	133.15	<i>no change</i>
Cl <sup>-</sup>	14.1	14	14.0	2E-02	14.0	<i>no change</i>
F <sup>-</sup>	0.78	0.78	0.8	9E-04	0.8	<i>no change</i>
Fe <sup>+2</sup>	0.018	0.0177	2E-02	2E-05	2E-02	<i>no change</i>
SiO <sub>2</sub>	14.3	14.3	14.3	2E-02	14.3	<i>no change</i>
HCO <sub>3</sub> <sup>-</sup>	195.8	238.8	232.3	-7	231.6	-1
K <sup>+</sup>	4.75	4.75	4.8	5E-03	4.8	<i>no change</i>
Mg <sup>+2</sup>	39.6	39.6	39.6	4E-02	39.6	<i>no change</i>
Mn <sup>+2</sup>	0.131	0.131	1E-01	1E-04	1E-01	<i>no change</i>
NO <sub>3</sub> <sup>-</sup>	<0.04	0.02	2E-02	2E-05	2E-02	-1E-03
Na <sup>+</sup>	138	138	138.2	2E-01	138.2	<i>no change</i>
PO <sub>4</sub> <sup>-3</sup>	<0.01	0.005	2E-02	1E-02	2E-02	<i>no change</i>
SO <sub>4</sub> <sup>-2</sup>	508	508	561.2	53	561.2	<i>no change</i>
SeO <sub>4</sub> <sup>-2</sup>	<.005	0.0025	3E-03	3E-06	3E-03	<i>no change</i>
TDS	1005	<i>n/a</i>	1123.2	<i>n/a</i>	1122.5	<i>n/a</i>
pH	7.1	7	7	<i>no change</i>	7.3	0.3
pe	<i>n/a</i>	4	4	<i>no change</i>	12.3	8.3

Table 17: Ingleside Hypothetical Native Water Pre-Mixing Solutions - All units mg/L

	raw	PHREEQC	speciation and charge balance	<i>difference</i>	equilibration subsurface	<i>difference</i>
		<i>input</i>	<i>output 1</i>	<i>output 1 - input</i>	<i>output 2</i>	<i>output 2 - output 1</i>
Al <sup>+3</sup>	<.01	0.005	5E-03	1E-06	5E-03	<i>no change</i>
H <sub>3</sub> AsO <sub>4</sub>	0.002	0.0016	1E-03	-6E-04	1E-03	<i>no change</i>
Ca <sup>+2</sup>	55	55.4	55.4	2E-02	55.4	<i>no change</i>
Cl <sup>-</sup>	6.6	6.6	6.6	2E-03	6.6	<i>no change</i>
F <sup>-</sup>	0.55	0.55	0.6	2E-04	0.6	<i>no change</i>
Fe <sup>+2</sup>	0.013	0.005	5E-03	2E-06	5E-03	<i>no change</i>
SiO <sub>2</sub>	15.5	15.5	15.5	5E-03	15.51	<i>no change</i>
HCO <sub>3</sub> <sup>-</sup>	181.8	181	176.5	-5	177.6	<i>1</i>
K <sup>+</sup>	1.8	1.8	1.8	6E-04	1.8	<i>no change</i>
Mg <sup>+2</sup>	18.5	18.5	18.5	6E-03	18.5	<i>no change</i>
Mn <sup>+2</sup>	0.001	0.0011	1E-03	4E-07	1E-03	<i>no change</i>
NO <sub>3</sub> <sup>-</sup>	3.63	3.36	3.4	1E-03	3.4	-3E-04
Na <sup>+</sup>	13	13	13.0	4E-03	13.0	<i>no change</i>
PO <sub>4</sub> <sup>-3</sup>	0.03	0.03	0.1	6E-02	0.1	<i>no change</i>
SO <sub>4</sub> <sup>-2</sup>	24.7	24.7	70.9	46	70.9	<i>no change</i>
SeO <sub>4</sub> <sup>-2</sup>	<.005	0.0025	3E-03	8E-07	3E-03	<i>no change</i>
TDS	295	<i>n/a</i>	342.7	<i>n/a</i>	343.8	<i>n/a</i>
pH	7.4	7.6	7.6	<i>no change</i>	7.2	-0.4
pe	<i>n/a</i>	4	4	<i>no change</i>	12.8	8.8

Table 18: Fountain Hypothetical Native Water Pre-Mixing Solutions - All units mg/L

	raw	PHREEQC	speciation and charge balance	<i>difference</i>	equilibration subsurface	<i>difference</i>
		<i>input</i>	<i>output 1</i>	<i>output 1 - input</i>	<i>output 2</i>	<i>output 2 - output 1</i>
Al <sup>+3</sup>	<.01	5E-03	5E-03	2E-06	5E-03	<i>no change</i>
H <sub>3</sub> AsO <sub>4</sub>	0.002	2E-03	1E-03	-8E-04	1E-03	<i>no change</i>
Ca <sup>+2</sup>	48	48	47.7	2E-02	47.7	<i>no change</i>
Cl <sup>-</sup>	6.4	6	6.4	3E-03	6.4	<i>no change</i>
F <sup>-</sup>	0.55	1	0.6	2E-04	0.6	<i>no change</i>
Fe <sup>+2</sup>	0.01	0	1E-02	4E-06	1E-02	<i>no change</i>
SiO <sub>2</sub>	15.3	15	15.2	6E-03	15.2	<i>no change</i>
HCO <sub>3</sub> <sup>-</sup>	201	246	242.2	-4	241.6	-0.6

$K^+$	2.22	2	2.2	$9E-04$	2.2	<i>no change</i>	
$Mg^{+2}$	16.6	17	16.6	$7E-03$	16.6	<i>no change</i>	
$Mn^{+2}$	<.001	1E-03	1E-03	$4E-07$	1E-03	<i>no change</i>	
$NO_3^-$	3	3	2.6	$1E-03$	2.6	$-1E-03$	
$Na^+$	38	38	38.4	$2E-02$	38.4	<i>no change</i>	
$PO_4^{-3}$	0.1	0	0.3	$2E-01$	0.3	<i>no change</i>	
$SO_4^{-2}$	49.8	50	50.1	$4E-01$	50.1	<i>no change</i>	
$SeO_4^{-2}$	0.007	7E-03	7E-03	$3E-06$	7E-03	<i>no change</i>	
TDS	326	<i>n/a</i>	403.6	<i>n/a</i>	403.0	<i>n/a</i>	
pH	7	7	7	<i>no change</i>	7.3	0.3	
pe	<i>n/a</i>	4	4	<i>no change</i>	12.8	8.8	

### *Single Pass Mixing Model Fluid Evolution*

Tables 19-21 show the distribution of dissolved species observed in (1) the modeled fluids after physical mixing, (2) the same physically mixed fluids after precipitation of hematite, kaolinite and quartz and (3) the difference between (1) and (2). In all three models, most dissolved species appeared to have a higher concentration in the final model step (step 7) than in the first (step 1). For all three formations, only  $SeO_4^{-2}$ ,  $Mn^{+2}$ ,  $PO_4^{-3}$  and  $SO_4^{-2}$  showed no difference between the resulting fluid derived from mixing alone and the resulting fluid derived from mixing and mineral precipitation. Similarly,  $H_3AsO_4$ ,  $Fe^{+2}$  and  $Na^+$  in the Dakota model,  $F^-$ ,  $Mg^{2+}$  and  $Ca^{2+}$ , in the Ingleside model and  $Na^+$  and  $Ca^{2+}$  in the Fountain model showed no difference between the resulting fluid derived from mixing alone and the resulting fluid derived from mixing and mineral precipitation (Tables 19-21). It should be noted that  $SeO_4^{-2}$ ,  $Mn^{+2}$  and  $PO_4^{-3}$  were mostly set to identical, low values in the model input dataset because the actual water analyses reported them as below the level of detection. Therefore, they do not show changes during mixing.

Specifically in the Dakota SPMM large overall concentration increases from the first model step to the last model step occurred in  $SO_4^{-2}$  (~138.2 mg/L),  $HCO_3^-$  (~47.4 mg/L),  $Na^+$  (~34.5 mg/L),  $Ca^{2+}$  (~29.3 mg/L) and  $Mg^{2+}$  (~9.4 mg/L). However, the modeled fluids are changing twice at each step. Once

when the fluids physically mix and then chemically when species are removed by precipitation. Table 19 includes these concentration changes with a delta ( $\Delta$ ) column at each step, and a final column that shows the overall change from the first model step to the last. In the Dakota SPMM, SiO<sub>2</sub> decreased by ~ 1.1 mg/L on the first model step and ~ 3.5 mg/L on the last model step after mineral precipitation with an average decrease of 2.3 mg/L per step. Al<sup>3+</sup> decreased by ~ 28.1  $\mu$ g/L on the first model step and ~ 22.1  $\mu$ g/L on the last model step after mineral precipitation with an average decrease of ~25  $\mu$ g/L per step. The remaining dissolved species were not involved in the modeled mineral precipitation, so changed only because of physical mixing (Table 19).

Within the Ingleside SPMM, notable overall changes in dissolved solid concentration between the first model step and the last occurred as increases in HCO<sub>3</sub><sup>-</sup> (~33.5 mg/L), SO<sub>4</sub><sup>-2</sup> (~14.8 mg/L) and Ca<sup>2+</sup> (~9.7 mg/L) (Table 20). In the Ingleside SPMM, SiO<sub>2</sub> decreased by ~ 1.1 mg/L on the first model step and ~ 3.7 mg/L on the last model step after mineral precipitation with an average decrease of 2.5 mg/L per step. Al<sup>3+</sup> decreased by ~ 28.1  $\mu$ g/L on the first model step and ~ 22.0  $\mu$ g/L on the last model step after mineral precipitation with an average decrease of ~25  $\mu$ g/L per step. The remaining dissolved species changed only as a result of physical mixing. After mineral precipitation, pH decreased from 7.8 in the first model step to 7.4 last model step (Table 20).

Lastly, in the Fountain SPMM largest change in dissolved solid concentration from the first model step to the last model step occurred as increases in HCO<sub>3</sub><sup>-</sup> (~49.7 mg/L), SO<sub>4</sub><sup>-2</sup> (~9.5 mg/L), Na<sup>+</sup> (~9.4 mg/L), Ca<sup>2+</sup> (~7.8 mg/L) and Mg<sup>2+</sup> (~3.6 mg/L) (Table 21). In the Ingleside SPMM, SiO<sub>2</sub> decreased by ~ 1.2 mg/L on the first model step and ~ 3.7 on the last model step after mineral precipitation with an average decrease of 2.5 mg/L per step. Al<sup>3+</sup> decreased by ~ 28.1  $\mu$ g/L on the first model step and ~ 22.1  $\mu$ g/L on the last model step after mineral precipitation with an average decrease of ~25  $\mu$ g/L per step. The remaining dissolved species varied very little. After mineral precipitation, pH decreased from 7.8 in the first model step to 7.5 last model step (Table 21).

Table 19: Dakota Single Pass Mixing Model Results

	units	model step 1 5% HNW/95% HIW			model step 2 5% HNW/95% fluid 1			model step 3 5% HNW/95% fluid 2			model step 4 5% HNW/95% fluid 3		
		Mix 1	fluid 1	$\Delta 1$	Mix 2	fluid 2	$\Delta 2$	Mix 3	fluid 3	$\Delta 3$	Mix 4	fluid 4	$\Delta 4$
pe		13.7	13.7		13.8	13.8		13.9	13.9		14	14	
temp	°C	15	15		15	15		15	15		15	15	
TDS	mg/L	137.4	137.5	0.1	186.9	186.9		233.8	233.9	0.1	278.4	278.5	0.1
pH		7.8	7.8		7.6	7.7	0.1	7.6	7.6		7.5	7.5	
H <sub>3</sub> AsO <sub>4</sub>	µg/L	0.3	0.3		0.3	0.3		0.3	0.3		0.3	0.3	
SeO <sub>4</sub> <sup>-2</sup>	µg/L	2.5	2.5		2.5	2.5		2.5	2.5		2.5	2.5	
Mn <sup>+2</sup>	µg/L	7.7	7.7		13.9	13.9		19.7	19.7		25.3	25.3	
Fe <sup>+2</sup>	µg/L	11.2	11.2		11.6	11.6		11.9	11.9		12.2	12.2	
PO <sub>4</sub> <sup>-3</sup>	µg/L	15.3	15.3		15.3	15.3		15.3	15.3		15.3	15.3	
Al <sup>+3</sup>	µg/L	28.7	0.6	-28.1	27.5	0.5	-27.0	26.4	0.4	-26.0	25.3	0.4	-24.9
NO <sub>3</sub> <sup>-</sup>	mg/L	0.1	0.1		0.1	0.1		0.1	0.1		0.1	0.1	
F <sup>-</sup>	mg/L	0.6	0.6		0.6	0.6		0.6	0.6		0.6	0.6	
K <sup>+</sup>	mg/L	3.8	3.8		3.8	3.8		3.9	3.9		3.9	3.9	
Mg <sup>+2</sup>	mg/L	4.1	4.1		5.9	5.9		7.5	7.5		9.1	9.1	
Cl <sup>-</sup>	mg/L	4.2	4.2		4.7	4.7		5.2	5.2		5.6	5.6	
SiO <sub>2</sub>	mg/L	5.6	4.5	-1.1	6	4.4	-1.6	6.4	4.4	-2.0	6.8	4.4	-2.4
Na <sup>+</sup>	mg/L	7.8	7.8		14.3	14.3		20.5	20.5		26.4	26.4	
Ca <sup>+2</sup>	mg/L	22.7	22.7		28.2	28.2		33.5	33.5		38.5	38.5	
SO <sub>4</sub> <sup>-2</sup>	mg/L	39.7	39.7		65.8	65.8		90.6	90.6		114.1	114.1	
HCO <sub>3</sub> <sup>-</sup>	mg/L	55.1	55.2	0.1	64.2	64.2		72.7	72.8	0.1	80.8	80.8	

$\Delta$  model step: reacted and mixed fluid - mixed fluid = delta

positive values indicate an increase and negative values indicate a decrease; blank cell behaved conservatively

Mix# - composition of modeled fluids after mixing, fluid #: composition of modeled fluids after mixing and precipitation of supersaturated minerals

Table 19 continued: Dakota Single Pass Mixing Model Results

	units	model step 5 5% HNW/95% fluid 4			model step 6 5% HNW/95% fluid 5			model step 7 5% HNW/95% fluid 6			OVERALL CHANGE*
		Mix 5	fluid 5	$\Delta 5$	Mix 6	fluid 6	$\Delta 6$	Mix 7	fluid 7	$\Delta 7$	
pe		14	14		14	14		14	14		0.3
temp	°C	15	15		15	15		15	15		
TDS	mg/L	320.7	320.8	0.1	360.9	361	0.1	399.1	399.1		261.6
pH		7.5	7.5		7.5	7.5		7.4	7.4		-0.4
H <sub>3</sub> AsO <sub>4</sub>	µg/L	0.3	0.3		0.3	0.3		0.3	0.3		
SeO <sub>4</sub> <sup>-2</sup>	µg/L	2.5	2.5		2.5	2.5		2.5	2.5		
Mn <sup>+2</sup>	µg/L	30.6	30.6		35.6	35.6		40.4	40.4		32.7
Fe <sup>+2</sup>	µg/L	12.4	12.4		12.7	12.7		13	13		1.8
PO <sub>4</sub> <sup>-3</sup>	µg/L	15.3	15.3		15.3	15.3		15.3	15.3		
Al <sup>+3</sup>	µg/L	24.3	0.3	-24.0	23.3	0.3	-23.0	22.4	0.3	-22.1	-0.3
NO <sub>3</sub> <sup>-</sup>	mg/L	0.1	0.1		0.1	0.1		0.1	0.1		0.01
F <sup>-</sup>	mg/L	0.6	0.6		0.6	0.6		0.7	0.7		0.1
K <sup>+</sup>	mg/L	3.9	3.9		4	4		4	4		0.2
Mg <sup>+2</sup>	mg/L	10.7	10.7		12.1	12.1		13.5	13.5		9.4
Cl <sup>-</sup>	mg/L	6	6		6.4	6.4		6.8	6.8		2.6
SiO <sub>2</sub>	mg/L	7.2	4.4	-2.8	7.5	4.4	-3.1	7.9	4.4	-3.5	-0.1
Na <sup>+</sup>	mg/L	31.9	31.9		37.3	37.3		42.3	42.3		34.5
Ca <sup>+2</sup>	mg/L	43.2	43.2		47.7	47.7		52	52		29.3
SO <sub>4</sub> <sup>-2</sup>	mg/L	136.5	136.5		157.7	157.7		177.9	177.9		138.2
HCO <sub>3</sub> <sup>-</sup>	mg/L	88.4	88.5	0.1	95.7	95.7		102.6	102.6		47.4

$\Delta$  model step: reacted and mixed fluid - mixed fluid = delta

positive values indicate an increase and negative values indicate a decrease; blank cell behaved conservatively

Mix# - composition of modeled fluids after mixing, fluid #: composition of modeled fluids after mixing and precipitation of supersaturated minerals \*This value is the difference between fluid 7 and fluid 1.

Table 20: Ingleside Single Pass Mixing Model Results

	units	model step 1 5% HNW/95% HIW			model step 2 5% HNW/95% fluid 1			model step 3 5% HNW/95% fluid 2			model step 4 5% HNW/95% fluid 3		
		Mix 1	fluid 1	$\Delta 1$	Mix 2	fluid 2	$\Delta 2$	Mix 3	fluid 3	$\Delta 3$	Mix 4	fluid 4	$\Delta 4$
pe		13.7	13.7		13.9	13.8	-0.1	13.9	13.9		14	14	
temp	°C	15.1	15.1		15.1	15.1		15.2	15.2		15.2	15.2	
TDS	mg/L	98.3	98.4	0.1	110.7	110.8	0.1	122.5	122.5		133.6	133.7	0.1
pH		7.8	7.8		7.6	7.6		7.5	7.6	0.1	7.5	7.5	
H <sub>3</sub> AsO <sub>4</sub>	ug/L	0.3	0.3		0.4	0.4		0.4	0.4		0.4	0.4	
SeO <sub>4</sub> <sup>-2</sup>	ug/L	2.5	2.5		2.5	2.5		2.5	2.5		2.5	2.5	
Mn <sup>+2</sup>	ug/L	1.2	1.2		1.2	1.2		1.2	1.2		1.2	1.2	
Fe <sup>+2</sup>	ug/L	10.6		-10.6	10.3		-10.3	10.1		-10.1	9.8		-9.8
PO <sub>4</sub> <sup>-3</sup>	ug/L	19.1	19.1		22.8	22.8		26.2	26.2		29.5	29.5	
Al <sup>+3</sup>	ug/L	28.70	0.60	-28.1	27.50	0.50	-27.0	26.40	0.40	-26.0	25.30	0.30	-25.0
NO <sub>3</sub> <sup>-</sup>	mg/L	0.3	0.3		0.4	0.4		0.6	0.6		0.7	0.7	
F <sup>-</sup>	mg/L	0.6	0.6		0.6	0.6		0.6	0.6		0.6	0.6	
K <sup>+</sup>	mg/L	3.6	3.6		3.5	3.5		3.4	3.4		3.3	3.3	
Mg <sup>+2</sup>	mg/L	3	3		3.8	3.8		4.5	4.5		5.2	5.2	
Cl <sup>-</sup>	mg/L	3.9	3.9		4	4		4.1	4.1		4.3	4.3	
SiO <sub>2</sub>	mg/L	5.6	4.5	-1.1	6.1	4.5	-1.6	6.6	4.5	-2.1	7	4.5	-2.5
Na <sup>+</sup>	mg/L	1.5	1.5		2.1	2.1		2.6	2.6		3.1	3.1	
Ca <sup>+2</sup>	mg/L	18.8	18.8		20.7	20.7		22.4	22.4		24	24	
SO <sub>4</sub> <sup>-2</sup>	mg/L	15.2	15.2		17.9	17.9		20.6	20.6		23.1	23.1	
HCO <sub>3</sub> <sup>-</sup>	mg/L	52.4	52.4		58.8	58.8		64.8	64.8		70.5	70.5	

$\Delta$  model step: reacted and mixed fluid - mixed fluid = delta

positive values indicate an increase and negative values indicate a decrease; blank cell behaved conservatively

Mix# - composition of modeled fluids after mixing, fluid #: composition of modeled fluids after mixing and precipitation of supersaturated minerals

Table 20 continued: Ingleside Single Pass Mixing Model Results

	units	model step 5 5% HNW/95% fluid 4			model step 6 5% HNW/95% fluid 5			model step 7 5% HNW/95% fluid 6			OVERALL CHANGE*
		Mix 5	fluid 5	$\Delta 5$	Mix 6	fluid 6	$\Delta 6$	Mix 7	fluid 7	$\Delta 7$	
pe		14	14		14	14		14	14		0.3
temp	°C	15.3	15.3		15.3	15.3		15.4	15.4		0.3
TDS	mg/L	144.2	144.2		154.2	154.3	0.1	163.7	163.8	0.1	65.4
pH		7.4	7.4		7.4	7.4		7.4	7.4		-0.4
H <sub>3</sub> AsO <sub>4</sub>	ug/L	0.4	0.4		0.5	0.5		0.5	0.5		0.2
SeO <sub>4</sub> <sup>-2</sup>	ug/L	2.5	2.5		2.5	2.5		2.5	2.5		
Mn <sup>+2</sup>	ug/L	1.2	1.2		1.2	1.2		1.2	1.2		
Fe <sup>+2</sup>	ug/L	9.6		-9.6	9.3		-9.3	9.1		-9.1	
PO <sub>4</sub> <sup>-3</sup>	ug/L	32.6	32.6		35.6	35.6		38.4	38.4		19.3
Al <sup>+3</sup>	ug/L	24.30	0.30	-24.0	23.30	0.30	-23.0	22.40	0.30	-22.1	-0.3
NO <sub>3</sub> <sup>-</sup>	mg/L	0.8	0.8		1.0	1.0		1.1	1.1		0.8
F <sup>-</sup>	mg/L	0.6	0.6		0.6	0.6		0.6	0.6		
K <sup>+</sup>	mg/L	3.3	3.3		3.2	3.2		3.1	3.1		-0.5
Mg <sup>+2</sup>	mg/L	5.9	5.9		6.5	6.5		7.1	7.1		4.1
Cl <sup>-</sup>	mg/L	4.4	4.4		4.5	4.5		4.6	4.6		0.7
SiO <sub>2</sub>	mg/L	7.5	4.5	-3.0	7.9	4.5	-3.4	8.2	4.5	-3.7	
Na <sup>+</sup>	mg/L	3.6	3.6		4.1	4.1		4.6	4.6		3.1
Ca <sup>+2</sup>	mg/L	25.6	25.6		27.1	27.1		28.5	28.5		9.7
SO <sub>4</sub> <sup>-2</sup>	mg/L	25.5	25.5		27.8	27.8		29.9	29.9		14.7
HCO <sub>3</sub> <sup>-</sup>	mg/L	75.9	76	0.1	81	81.1	0.1	85.9	86	0.1	33.6

$\Delta$  model step: reacted and mixed fluid - mixed fluid = delta

positive values indicate an increase and negative values indicate a decrease; blank cell behaved conservatively

Mix# - composition of modeled fluids after mixing, fluid #: composition of modeled fluids after mixing and precipitation of supersaturated minerals \*This value is the difference between fluid 7 and fluid 1

Table 21: Fountain Single Pass Mixing Model Results

	units	model step 1 5% HNW/95% HIW			model step 2 5% HNW/95% fluid 1			model step 3 5% HNW/95% fluid 2			model step 4 5% HNW/95% fluid 3		
		Mix 1	fluid 1	$\Delta 1$	Mix 2	fluid 2	$\Delta 2$	Mix 3	fluid 3	$\Delta 3$	Mix 4	fluid 4	$\Delta 4$
pe		13.7	13.7		13.9	13.8	-0.1	13.9	13.9		14	14	
temp	°C	15	15		14.9	14.9		14.9	14.9		14.8	14.8	
TDS	mg/L	101.3	101.4	0.1	116.5	116.6	0.1	131	131		144.6	144.7	0.1
pH		7.8	7.8		7.6	7.7	0.1	7.6	7.6		7.5	7.5	
H <sub>3</sub> AsO <sub>4</sub>	ug/L	0.3	0.3		0.4	0.4		0.4	0.4		0.5	0.5	
SeO <sub>4</sub> <sup>-2</sup>	ug/L	2.7	2.7		2.9	2.9		3.1	3.1		3.3	3.3	
Mn <sup>+2</sup>	ug/L	1.2	1.2		1.2	1.2		1.2	1.2		1.2	1.2	
Fe <sup>+2</sup>	ug/L	10.9		-10.9	10.8		-10.8	10.8		-10.8	10.7		-10.7
PO <sub>4</sub> <sup>-3</sup>	ug/L	29.8	29.8		43.7	43.7		56.8	56.8		69.3	69.3	
Al <sup>+3</sup>	ug/L	28.7	0.6	-28.1	27.5	0.5	-27.0	26.4	0.4	-26.0	25.3	0.4	-24.9
NO <sub>3</sub> <sup>-</sup>	mg/L	0.2	0.2		0.3	0.3		0.4	0.4		0.6	0.6	
F <sup>-</sup>	mg/L	0.6	0.6		0.6	0.6		0.6	0.6		0.6	0.6	
K <sup>+</sup>	mg/L	3.6	3.6		3.6	3.6		3.5	3.5		3.4	3.4	
Mg <sup>+2</sup>	mg/L	2.9	2.9		3.6	3.6		4.3	4.3		4.9	4.9	
Cl <sup>-</sup>	mg/L	3.9	3.9		4	4		4.1	4.1		4.2	4.2	
SiO <sub>2</sub>	mg/L	5.6	4.4	-1.2	6.1	4.4	-1.7	6.5	4.4	-2.1	7.0	4.4	-2.6
Na <sup>+</sup>	mg/L	2.8	2.8		4.6	4.6		6.3	6.3		7.9	7.9	
Ca <sup>+2</sup>	mg/L	18.4	18.4		19.9	19.9		21.3	21.3		22.6	22.6	
SO <sub>4</sub> <sup>-2</sup>	mg/L	14.1	14.1		15.9	15.9		17.6	17.6		19.2	19.2	
HCO <sub>3</sub> <sup>-</sup>	mg/L	55.6	55.6	0.1	65	65.1	0.1	73.9	74	0.1	82.4	82.5	0.1

 $\Delta$  model step: reacted and mixed fluid - mixed fluid = delta

positive values indicate an increase and negative values indicate a decrease; blank cell behaved conservatively

Mix# - composition of modeled fluids after mixing, fluid #: composition of modeled fluids after mixing and precipitation of supersaturated minerals

Table 21 continued: Fountain Single Pass Mixing Model Results

	units	model step 5 5% HNW/95% fluid 4			model step 6 5% HNW/95% fluid 5			model step 7 5% HNW/95% fluid 6			OVERALL CHANGE*
		Mix 5	fluid 5	$\Delta 5$	Mix 6	fluid 6	$\Delta 6$	Mix 7	fluid 7	$\Delta 7$	
pe		14	14		14	14		14	14		0.3
temp	°C	14.8	14.8		14.7	14.7		14.7	14.7		-0.3
TDS	mg/L	157.6	157.7	0.1	170	170		181.7	181.7		80.3
pH		7.5	7.5		7.5	7.5		7.4	7.5	0.1	-0.3
H <sub>3</sub> AsO <sub>4</sub>	ug/L	0.5	0.5		0.5	0.5		0.6	0.6		0.3
SeO <sub>4</sub> <sup>-2</sup>	ug/L	3.5	3.5		3.7	3.7		3.9	3.9		1.2
Mn <sup>+2</sup>	ug/L	1.2	1.2		1.1	1.1		1.1	1.1		-0.1
Fe <sup>+2</sup>	ug/L	10.7		-10.7	10.7		-10.7	10.6		-10.6	
PO <sub>4</sub> <sup>-3</sup>	ug/L	81.1	81.1		92.4	92.4		103	103		73.2
Al <sup>+3</sup>	ug/L	24.3	0.3	-24.0	23.3	0.3	-23.0	22.4	0.3	-22.1	-0.3
NO <sub>3</sub> <sup>-</sup>	mg/L	0.7	0.7		0.8	0.8		0.8	0.8		0.6
F <sup>-</sup>	mg/L	0.6	0.6		0.6	0.6		0.6	0.6		
K <sup>+</sup>	mg/L	3.4	3.4		3.3	3.3		3.2	3.2		-0.4
Mg <sup>+2</sup>	mg/L	5.5	5.5		6	6		6.5	6.5		3.6
Cl <sup>-</sup>	mg/L	4.3	4.3		4.4	4.4		4.5	4.5		0.6
SiO <sub>2</sub>	mg/L	7.4	4.4	-3.0	7.8	4.4	-3.4	8.1	4.4	-3.7	
Na <sup>+</sup>	mg/L	9.4	9.4		10.8	10.8		12.2	12.2		9.4
Ca <sup>+2</sup>	mg/L	23.9	23.9		25.1	25.1		26.2	26.2		7.8
SO <sub>4</sub> <sup>-2</sup>	mg/L	20.8	20.8		22.3	22.3		23.6	23.6		9.5
HCO <sub>3</sub> <sup>-</sup>	mg/L	90.4	90.5	0.1	98.1	98.1		105.3	105.3		49.7

$\Delta$  model step: reacted and mixed fluid - mixed fluid = delta

positive values indicate an increase and negative values indicate a decrease; blank cell behaved conservatively

Mix# - composition of modeled fluids after mixing, fluid #: composition of modeled fluids after mixing and precipitation of supersaturated minerals \*This value is the difference between fluid 7 and fluid 1

Figure 20 is a set of Stiff diagrams illustrating the evolution of the fluid mixtures as they pass, conceptually, through unreactive rock chambers. Stiff diagrams characterize water visually by plotting major cations and anions in a way that creates a distinctive shape correlating with the distinctive fluid composition (Hem, 1985). A first-order observation of these diagrams is that when comparing model step 1 (HIW to HNW ratio 95/5) to the HIW, a nearly identical shape can be seen. As the model progresses and continues to mix additional HNW, the result is a shape that resembles a more dilute version of the initial HNW shape.

Figure 21 is a piper diagram depicting the chemical/concentration evolution of the modeled fluid mixtures. A piper diagram characterizes water into types by plotting them graphically on trilinear plots, according to major cations and anions (Hem, 1985). The water type classification used here is based on Kumar (2013). Initially, the raw Dakota water sample plotted as a calcium-magnesium-chloride water type, while both the Ingleside and Fountain sample averages were calcium-bicarbonate water type (Fig. 10). The final fluids remain plotted in the same water type categories. A pattern of model step 1 result fluid plotting near the composition of the HIW water then plotting progressively closer to the HNW composition is observed here. This pattern is similar to the one seen in the Stiff diagrams.

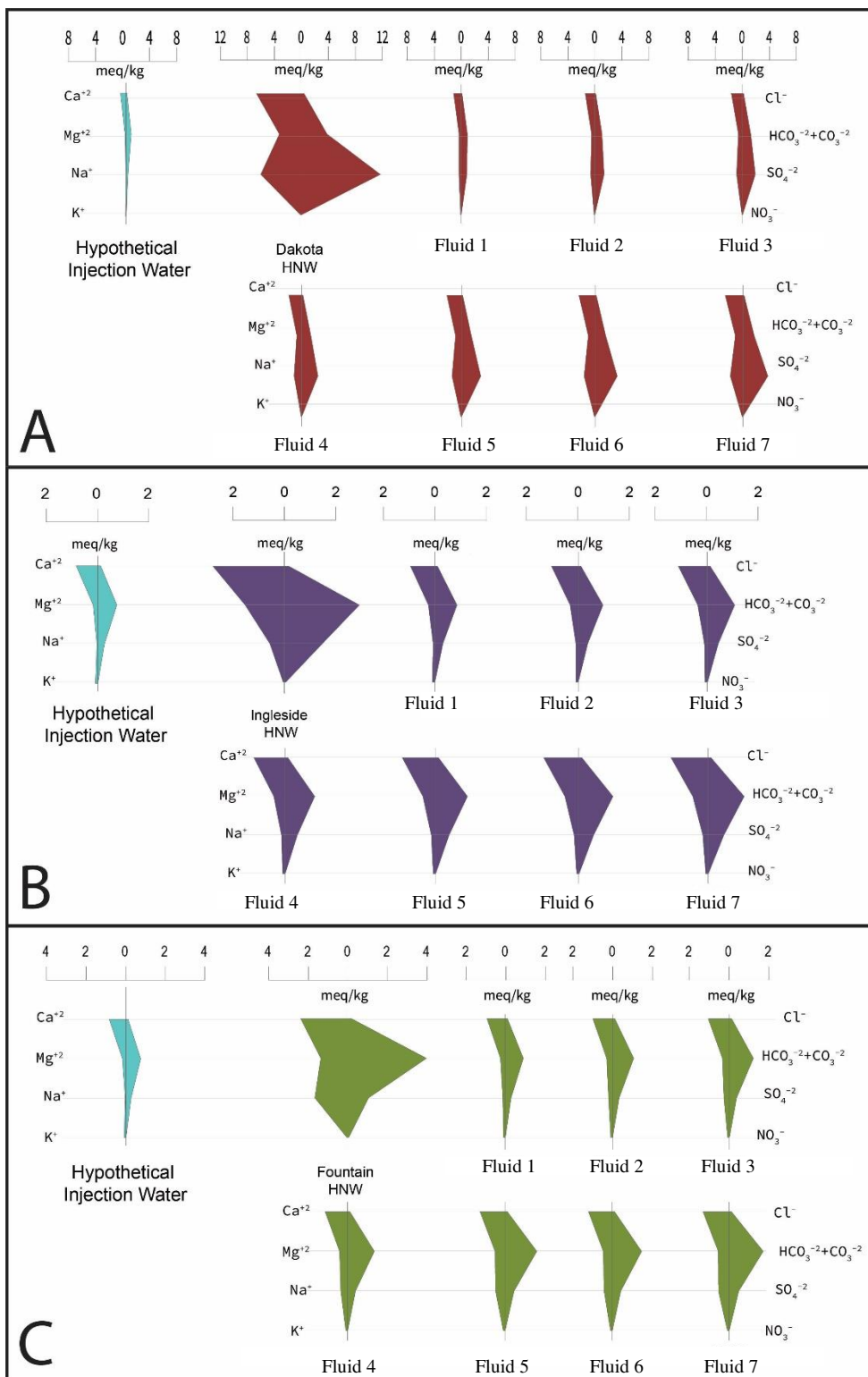


Figure 20: Stiff diagrams representing the resulting fluids of the Dakota (A), Ingleside (B), and Fountain (C) formations, derived using a Single Pass Mixing Model

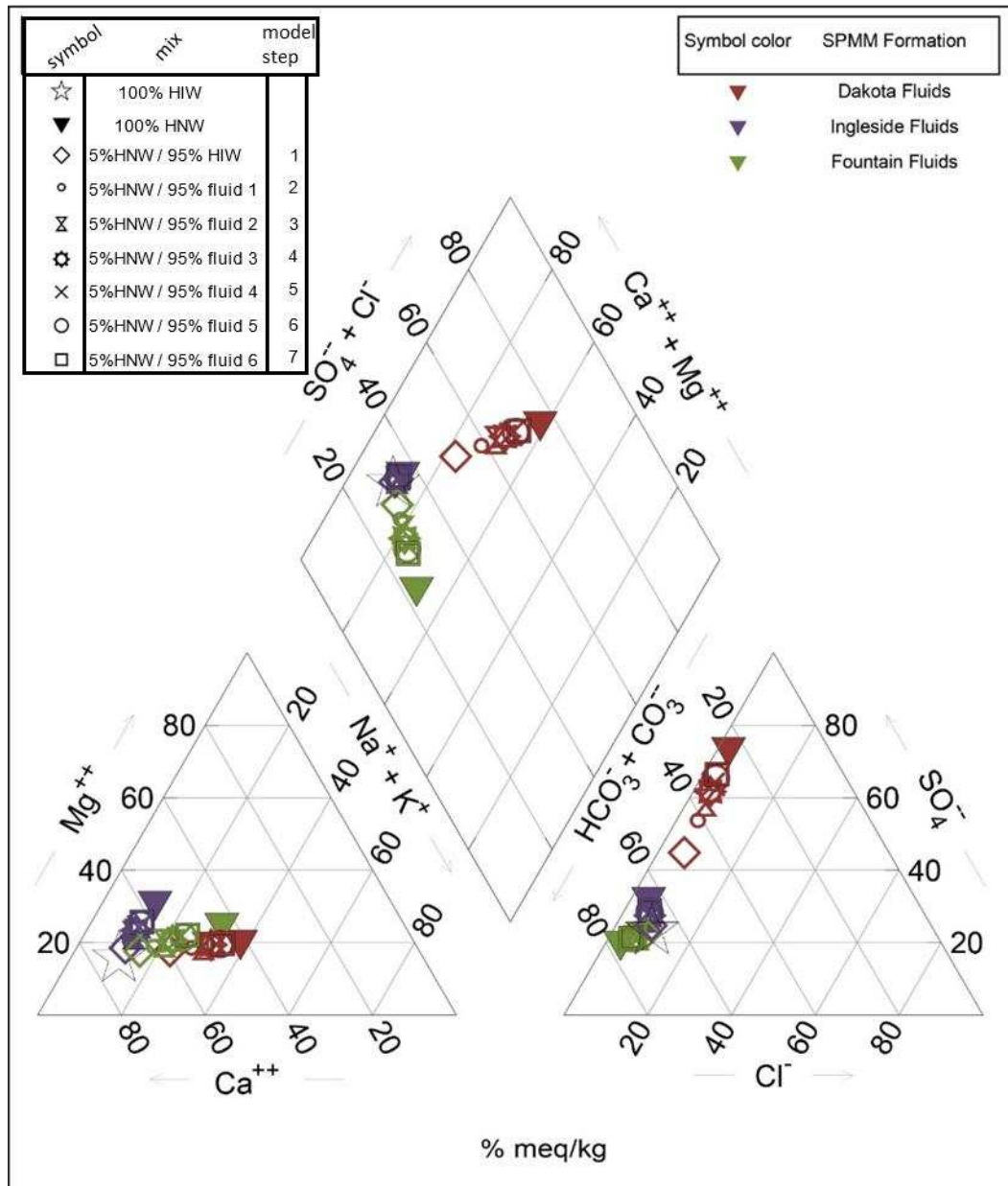


Figure 21: Piper diagram showing fluid composition results from each model step for all three formation Single Pass Mixing Models. Classification types based on (Sajil Kumar, 2013)

#### 4.4.2 Mineral Precipitation

The Dakota water SPMM predicts precipitation of quartz and kaolinite. Unlike the other two models, hematite was not included in the input file; therefore it was not allowed to precipitate. Before the physical mixing step, saturation index (S.I.) values of quartz and kaolinite (with respect to the HIW and HNW) are supersaturated. S.I. values for quartz are 0.1 with respect to the HIW and 0.5 with respect to the Dakota HNW. S.I. values for kaolinite are 3 with respect to the HIW and 3.7 with respect to the Dakota HNW. The model forces S.I. values for both quartz and kaolinite to 0, or in equilibrium with model fluids in steps 1 - 7. During model step 1, ~ 1.1 mg/kg of quartz and ~ 0.13 mg/kg of kaolinite (Table 22) are predicted to precipitate, removing ~ 28 µg/L Al<sup>3+</sup> and 1.1 mg/L SiO<sub>2</sub> from solution (Table 19). As the model progresses, the modeled fluids are predicted to precipitate larger amounts of quartz with each model step while precipitating smaller amounts of kaolinite. The amount of kaolinite precipitation per model step decreases from ~ 0.13 mg/kg (step 2) to ~ 0.11 mg/kg (step 7), while the amount of quartz per precipitation per model step increases from ~ 1.0 mg/kg (step 2) to ~ 3.4 mg/kg (step 7) (Fig. 22). S.I. values for several other minerals are included in Table 22. These minerals were either supersaturated or undersaturated with respect to all modeled fluids. Notably, siderite S.I. values ranged from -9 to -12 and goethite S.I. values were ~7 for all fluids.

### Mineral Precipitation vs Aqueous Species Removal – Dakota SPMM

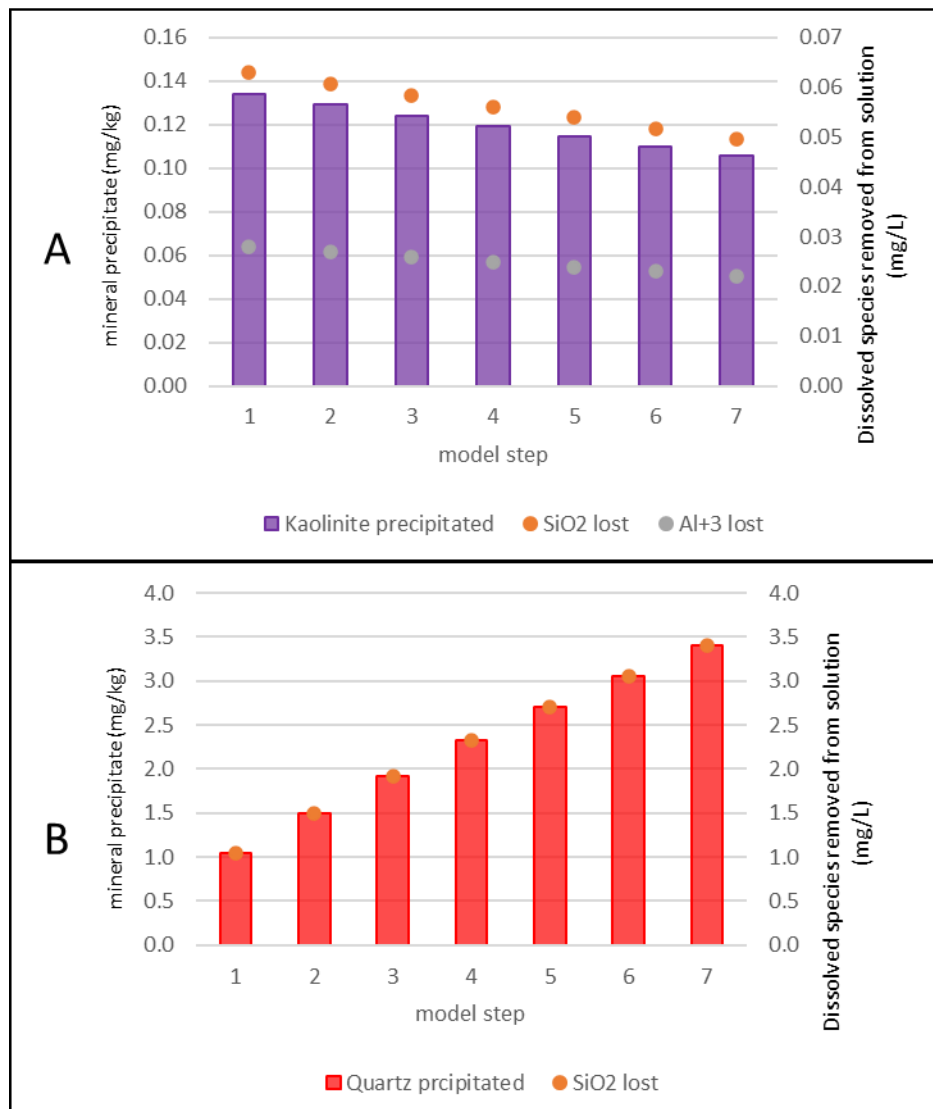


Figure 22: Tabulated results of the Dakota SPMM. Mineral precipitation is shown as bar graph. The concentration of aqueous species removed from the mixed fluids to form the minerals are plotted as points. A - kaolinite precipitation with Al<sup>3+</sup> and aqueous SiO<sub>2</sub> removal. B - quartz precipitation with aqueous SiO<sub>2</sub> removal.

Table 22: Dakota SPMM Saturation Indices

	HIW	HNW	step 1	step 2	step 3	step 4	step 5	step 6	step 7
K-feldspar	-0.9	-0.3	-2.8	-2.9	-2.9	-3.0	-3.0	-3.1	-3.1
Albite	-4	-1.3	-4.9	-4.8	-4.7	-4.6	-4.6	-4.6	-4.5
Anhydrite	-3.1	-1.1	-2.6	-2.3	-2.1	-2.0	-1.9	-1.8	-1.7
Calcite	-0.6	0	-0.7	-0.6	-0.6	-0.6	-0.5	-0.5	-0.5
Gibbsite	1.1	1	-0.4	-0.4	-0.4	-0.4	-0.4	-0.4	-0.4
Goethite	7	7.1	7	7.0	7.0	7.0	7.0	7.0	7
Gypsum	-2.9	-0.8	-2.3	-2.0	-1.9	-1.7	-1.6	-1.5	-1.5
Hematite	16	16.1	16	16.0	16.0	16.0	16.0	16.0	16
Illite	0.6	1.4	-3.2	-3.3	-3.3	-3.4	-3.4	-3.4	-3.4
Siderite	-12.6	-9.2	-12.3	-12.1	-12.0	-11.9	-11.8	-11.7	-11.7
Talc	-3.2	-2.8	-4.1	-4.5	-4.7	-4.8	-4.8	-4.9	-4.9
Dolomite	-1.9	-0.4	-1.8	-1.8	-1.7	-1.6	-1.5	-1.4	-1.3
Muscovite	6.8	7.1	2	1.9	1.8	1.8	1.7	1.7	1.7
<b>Kaolinite</b>	<b>3</b>	<b>3.7</b>	<b>0</b>	0.0	0.0	0.0	0.0	0.0	<b>0</b>
kaolinite precipitated (mg/kg)				0.13	0.13	0.12	0.12	0.11	0.11
<b>Quartz</b>	<b>0.1</b>	<b>0.5</b>	<b>0</b>	0.0	0.0	0.0	0.0	0.0	<b>0</b>
quartz precipitated (mg/kg)				1.0	1.5	1.9	2.3	2.7	3.1
									3.4

The Ingleside average water SPMM resulted in precipitation of quartz, hematite and kaolinite, with supersaturated conditions in the first fluid, created during step 1. Before step 1, saturation index values of quartz, kaolinite and hematite with respect to the HNW are 0.5, 3.8 and 14.9 respectively. During step 1, ~ 1.0 mg/kg of quartz, ~ 0.13 mg/kg of kaolinite and ~ 0.02 mg/kg of hematite precipitate, and ~ 0.03 mg/L of Al<sup>3+</sup>, ~ 0.01 mg/L of Fe<sup>2+</sup> and ~ 1.2 mg/L of SiO<sub>2</sub> are removed from solution to precipitate these three minerals (Tables 20 and 23). As the model progresses, the modeled fluids continue to precipitate these three minerals. The mass of kaolinite and hematite precipitate decreases with each model step, while the mass of quartz precipitate increases (Fig. 23). Model step 7 produces ~0.11 mg/kg, ~3.7 mg/kg, ~0.01 mg/kg of kaolinite, quartz and hematite respectively. S.I. values for several other minerals are included in Table 23. These minerals were either supersaturated or undersaturated with respect to all modeled fluids. Notably, siderite S.I. values ranged from -12 to -19 and talc S.I. values range from -3.2 to -5.7 with respect to modeled fluids.

### Mineral Precipitation vs Aqueous Species Removal – Ingleside SPMM

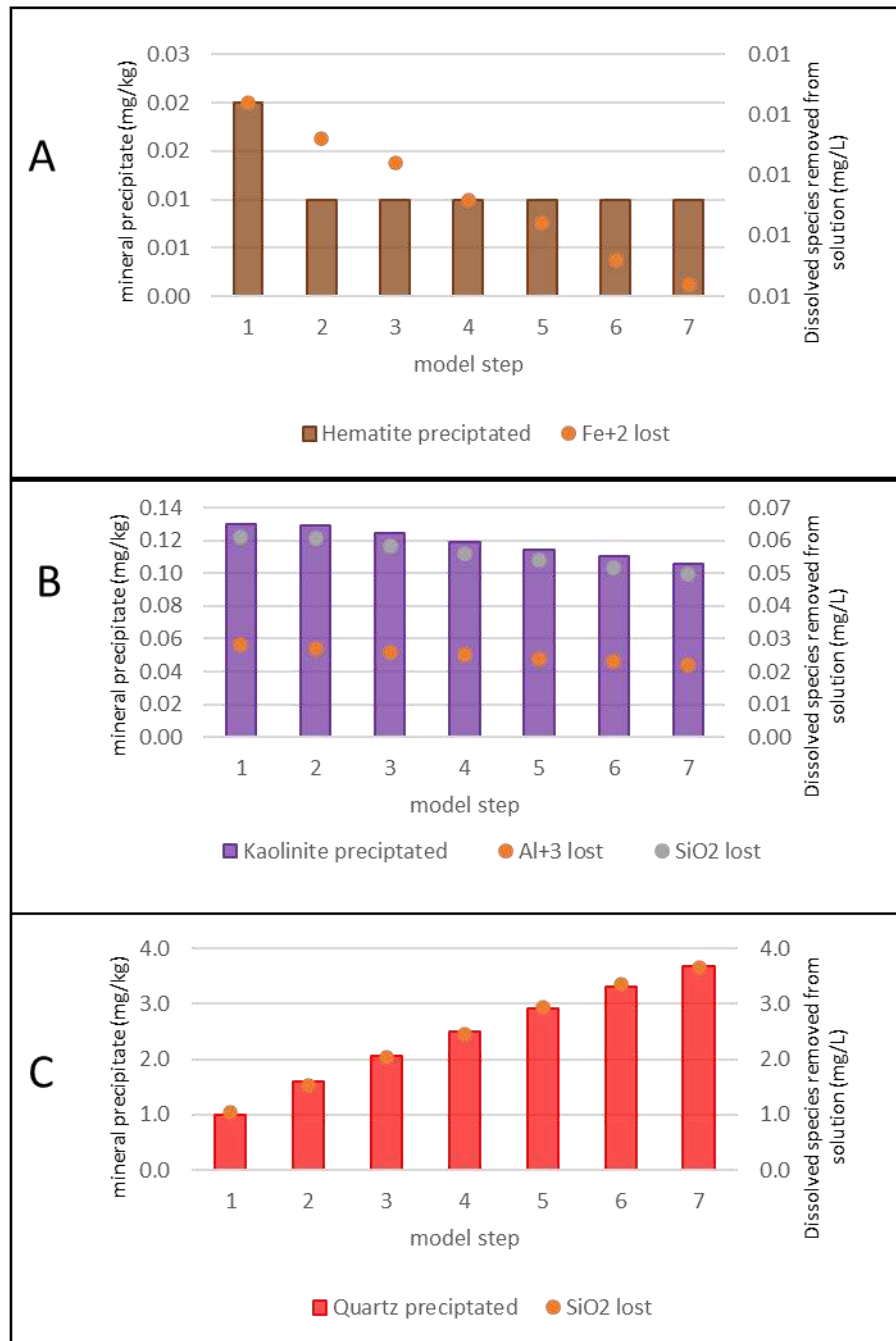


Figure 23: Tabulated results of the Ingleside SPMM. Mineral precipitation is shown as bar graph. The concentration of aqueous species removed from the mixed fluids to form the minerals are plotted as lines. A - hematite precipitation with Fe<sup>2+</sup> removal. B - kaolinite precipitation with Al<sup>3+</sup> and aqueous SiO<sub>2</sub> removal. C - quartz precipitation with aqueous SiO<sub>2</sub> removal.

Table 23: Ingleside SPMM Saturation Indices

	HIW	HNW	step 1	step 2	step 3	step 4	step 5	step 6	step 7
K-feldspar	-0.9	-0.7	-2.8	-2.9	-3.0	-3.1	-3.1	-3.2	-3.2
Albite	-4	-2.3	-5.6	-5.6	-5.6	-5.6	-5.6	-5.5	-5.5
Anhydrite	-3.1	-2.1	-3	-2.9	-2.8	-2.8	-2.7	-2.6	-2.6
Calcite	-0.6	-0.4	-0.7	-0.8	-0.8	-0.8	-0.8	-0.8	-0.8
Gibbsite	1.1	1	-0.4	-0.4	-0.4	-0.4	-0.4	-0.4	-0.4
Goethite	7	6.5	-1	-1.0	-1.0	-1.0	-1.0	-1.0	-1
Gypsum	-2.9	-1.8	-2.8	-2.7	-2.6	-2.5	-2.4	-2.4	-2.3
Illite	0.6	1.2	-3.2	-3.3	-3.4	-3.5	-3.5	-3.6	-3.6
Siderite	-12.6	-10.3	-20.3	-20.1	-20.0	-19.9	-19.8	-19.7	-19.7
Talc	-3.2	-3.5	-4.5	-5.0	-5.3	-5.5	-5.6	-5.6	-5.7
Dolomite	-1.9	-1	-2.1	-2.1	-2.1	-2.1	-2.0	-2.0	-1.9
Muscovite	6.8	6.8	2	1.9	1.8	1.7	1.6	1.6	1.6
<b>Hematite</b>	<b>16</b>	<b>14.9</b>	<b>0</b>	0.0	0.0	0.0	0.0	0.0	<b>0</b>
hematite precipitated (mg/kg)			0.02	0.01	0.01	0.01	0.01	0.01	0.01
<b>Kaolinite</b>	<b>3</b>	<b>3.8</b>	<b>0</b>	0.0	0.0	0.0	0.0	0.0	<b>0</b>
kaolinite precipitated (mg/kg)			0.13	0.13	0.12	0.12	0.11	0.11	0.11
<b>Quartz</b>	<b>0.1</b>	<b>0.5</b>	<b>0</b>	0.0	0.0	0.0	0.0	0.0	<b>0</b>
quartz precipitated (mg/kg)			1.0	1.6	2.1	2.5	2.9	3.3	3.7

The Fountain average water solution SPMM resulted in precipitation of quartz, hematite and kaolinite. Before mixing, the saturation index values of quartz and kaolinite with respect to the HIW are the same as the other models. Additionally, the S.I. value of hematite with respect to the HIW is 16, and also is supersaturated. S.I. values for quartz, hematite and kaolinite with respect to the HNW are 0.6, 15.7 and 3.9 respectively. The model forces S.I. values for both quartz and kaolinite to 0, or in equilibrium with model fluids in steps 1 - 7. During model step 1, ~ 1.0 mg/kg of quartz, ~ 0.13 mg/kg of kaolinite and ~ 0.02 mg/kg of hematite precipitate. As a result, ~ 0.03 mg/L of  $\text{Al}^{3+}$ , ~ 0.01 mg/L of  $\text{Fe}^{2+}$  and ~ 1.2 mg/L of  $\text{SiO}_2$  are removed from solution during step 1 (Tables 21 and 24). As the model progresses, these three minerals continue to precipitate at each model step. The mass of kaolinite and hematite precipitated at each model step changes very little compared to the mass of quartz (Fig. 24). Model step 7 produces ~0.11 mg/kg, ~3.7 mg/kg, ~0.02 mg/kg of kaolinite, quartz and hematite respectively. Saturation index

values for several other minerals were either supersaturated or undersaturated with respect to the modeled fluids but did not precipitate or dissolve (Table 24). Notably, with respect to the resulting fluid from model step 1, siderite has an S.I. of -20.3.

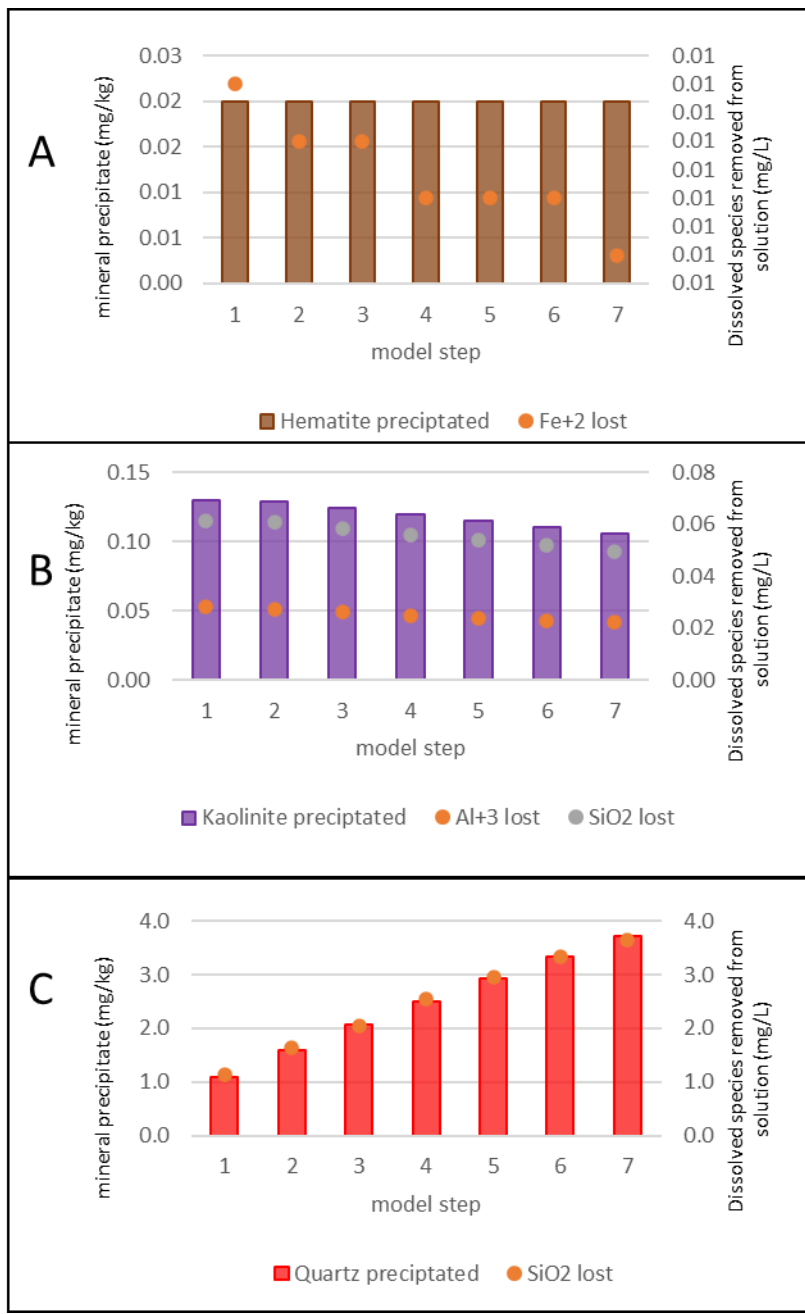


Figure 24: Tabulated results of the Fountain SPMM. Mineral precipitation is shown as bar graph. The concentration of aqueous species removed from the mixed fluids to form the minerals are plotted as lines. A - hematite precipitation with Fe<sup>2+</sup> removal. B - kaolinite precipitation with Al<sup>3+</sup> and aqueous SiO<sub>2</sub> removal. C - quartz precipitation with aqueous SiO<sub>2</sub> removal.

Table 24: Fountain SPMM Saturation Indices

	HIW	HNW	step 1	step 2	step 3	step 4	step 5	step 6	step 7
K-feldspar	-0.9	-0.4	-2.8	-2.9	-3.0	-3.0	-3.1	-3.1	-3.1
Albite	-4	-1.7	-5.3	-5.3	-5.2	-5.1	-5.1	-5.1	-5
Anhydrite	-3.1	-2.3	-3	-3.0	-2.9	-2.9	-2.8	-2.8	-2.7
Calcite	-0.6	-0.2	-0.7	-0.7	-0.7	-0.7	-0.7	-0.7	-0.7
Gibbsite	1.1	1	-0.4	-0.4	-0.4	-0.4	-0.4	-0.4	-0.4
Goethite	7	6.9	-1	-1.0	-1.0	-1.0	-1.0	-1.0	-1
Gypsum	-2.9	-2	-2.8	-2.7	-2.7	-2.6	-2.6	-2.5	-2.5
Illite	0.6	1.4	-3.2	-3.3	-3.4	-3.5	-3.5	-3.5	-3.5
Siderite	-12.6	-9.9	-20.3	-20.1	-20.0	-19.9	-19.8	-19.7	-19.7
Talc	-3.2	-3.2	-4.5	-5.0	-5.2	-5.4	-5.5	-5.5	-5.5
Dolomite	-1.9	-0.8	-2	-2.0	-2.0	-1.9	-1.8	-1.8	-1.7
Muscovite	6.8	7.1	2	1.9	1.8	1.7	1.7	1.7	1.6
<b>Hematite</b>	<b>16</b>	<b>15.7</b>	<b>0</b>	0.0	0.0	0.0	0.0	0.0	<b>0</b>
hematite precipitated (mg/kg)				0.02	0.02	0.02	0.02	0.02	0.02
<b>Kaolinite</b>	<b>3</b>	<b>3.9</b>	<b>0</b>	0.0	0.0	0.0	0.0	0.0	<b>0</b>
kaolinite precipitated (mg/kg)				0.13	0.13	0.12	0.12	0.11	0.11
<b>Quartz</b>	<b>0.1</b>	<b>0.6</b>	<b>0</b>	0.0	0.0	0.0	0.0	0.0	<b>0</b>
quartz precipitated (mg/kg)				1.1	1.6	2.1	2.5	2.9	3.3
									3.7

## Chapter 5 - Discussion

### 5.1 Formation Aquifer Compositional Characterization

This study attempted to characterize the subsurface mineralogy and bulk chemical composition of rock and native water of three formations within the vicinity of a potential ASR location using well water samples and surface rock samples. Far fewer samples were collected and analyzed than would be needed to completely characterize the composition of these heterogeneous formations. Among only three samples each for the Fountain and Ingleside formations, significant variation in both composition and porosity was identified and suggests equally significant heterogeneity throughout the formations. Previous work presented in Chapter 2 agrees with the assumption that there is significant heterogeneity within these formations.

I did not attempt to address compositional heterogeneity throughout the formations within the model. Instead, compositional data obtained from the surface samples from chemical and petrographic analyses provided only a baseline for the geochemical models. Without proper representation of the heterogeneity within the formations, the model is a simplification of the geochemical environment and should be treated as a pilot study to be refined with further investigations.

### 5.2 Bulk Chemical Composition Approximated from Point Count Analyses Results

Bulk rock geochemical analysis of sandstones does not give definitive information about specific mineral phases, which is why the point counting data were compared to analysis results. The mineral recalculation of the bulk rock chemical analysis served as an additional check, but the results of the recalculation did not match the point counted modal abundances well in many cases.

Discrepancies between the two analyses are due in large part to the natural variability of composition even within a grapefruit sized sample. It is unlikely that a thin section would adequately capture the variability that a larger rock sample would exhibit. In addition, some of the error is likely due to misidentification of matrix forming minerals and opaque phases as they can be difficult to identify during petrographic analysis. Solid solutions or elemental replacements within minerals could have also affected the results as end-member mineral formulas were used for recalculation. However, the bulk rock and petrographic analysis results were never intended to precisely match, they were instead done as a hybrid process of identifying a baseline description of the aquifer material.

### 5.3 Water Chemistry and Characterization

Potential issues with aquifer water characterization include failure to collect redox sensitive parameters such as oxidation-reduction potential. During water quality sampling, the probe used to measure temperature, pH, specific conductivity and dissolved oxygen was giving inconsistent and unrealistic readings and so the specific conductivity and dissolved oxygen measurements were deemed unreliable and not used as model input. Dissolved oxygen (D.O.) in particular would have been useful in determining a redox environment for the model, however, given that the water samples were collected by filling a 5-gallon bucket from a garden spigot the potential for the sample to be aerated was essentially inevitable. Therefore, the dissolved oxygen measurement that would have been recorded had the probe been functioning properly likely would not have been a realistic measure of the subsurface.

### 5.4 Leaching Experiments

Initially the benchtop experiments were meant to serve as a comparison to the computer simulations. However, it is difficult to compare the benchtop experiment results with the model results given the dissimilarity between the processes simulated within the model and those carried out in the

experiment. For example, the experiment was essentially a one-step process of one fluid reacting with one set of rock material in a closed system. The model was a multi-step process that simulated introduction of an evolving solution to several “fresh” batches of rock material. In addition, the rock samples used in the benchtop experiment were surface rock samples that showed evidence of surface weathering including oxidized iron phases, and possible alteration of feldspar to kaolinite. Although every attempt was made to collect samples with as little surface weathering as possible, it is almost certain that the composition of the surface samples would differ from the same sample in the subsurface. The water used in the experiments was tap water that was hypothetically similar to treated surface water composition used in the models, but not necessarily the same. In addition, the benchtop experiment does not include the mixing of native water with the hypothetical injection solution. The benchtop experiment is therefore not analogous to the computer simulation because it has no way to account for the effect of introducing native water to the system.

However, aside from the anomalously high arsenic concentration (discussed below), results of the benchtop leaching experiment were interesting because the resulting leachate was highly concentrated in TDS and in nitrate in both samples E-F2 and E-D2 most notably. High nitrate and sulfate values here could suggest surface contamination as both are common ingredients in fertilizers and are common anthropogenic contaminants. In addition, high TDS and specifically high levels of chloride and magnesium also suggest contamination due to incorporation of road salt (USGS, 2018).

#### 5.4.1 Repeat Experiment Explanation

The initial experiment returned an anomalously high value for arsenic of 3.39 mg/L from the leached solution I3 that made that result suspect. The bulk geochemical analysis of the same rock sample yielded a result for arsenic below the detection limit of 0.5ppm. Given the rock sample contained an arsenic value below the detection limit, the highest concentration of arsenic could have only been a value below 0.5ppm. Given the amount of sample in the experiment (150g) and the volume of leachate (300ml),

and assuming all 0.5 ppm that could exist dissolved into the leachate, it is possible for a maximum of 0.25mg/L arsenic to be leached into solution. In addition, minerals likely to contain arsenic, for example pyrite and iron-hydroxides, were not seen petrographically. Given this reasoning, it is unlikely that the rock sub-sample I3 actually leached the large arsenic value into the tap water during the experiment. The sample could have picked up some contaminated material during the sample preparation process.

However, to confirm that the arsenic did not come from the sub-sample I3 the experiment was repeated with a similar sub-sample for a shorter duration of one month instead of six.

This second water quality analysis, conducted by a different lab, yielded a result for arsenic right at the detection limit of 0.04mg/L. This discrepancy suggested that the sample used in the initial experiment was likely contaminated. Possible sources of contamination include residue on the rock saw or crushing plate used to prepare the rock samples. However, the exact cause of the high levels of arsenic could not conclusively be determined.

In addition, the results of both analyses showed that several parameters were significantly different. Notably, nitrate, sulfate, and TDS were elevated in the second experiment compared to the initial experiment and exceeded Primary and Secondary EPA regulations. The first experiment ran for six months while the duration of the repeat run was only one month. Differences in initial composition of the rock sample likely play an important role. The higher values of calcium and sulfate specifically may indicate that the sub-sample used in the second experimental run had a greater concentration of anhydrite than the first run. Anhydrite was found to be 7.1% of sample I3 when the data was normalized without pore space, but it was mostly a cement, which was not evenly distributed throughout the thin section.

## 5.5 Interpretation of Geochemical Modeling Results

### 5.5.1 Implications of Model Input and Parameter Selection

Speciation calculations corrected charge imbalances within the raw water chemistry datasets to provide input for the SPMMs that is as close to charge neutral as possible. The speciation-premixing step modified the raw data slightly in most cases and did not drastically change the dataset, except with regard to sulfate concentration. During the speciation calculation, the concentration of sulfate increased by 53 mg/L in the Dakota SPMM and by 46 mg/L in the Ingleside SPMM. The selection of sulfate as the charge balance species resulted in the relatively large changes in concentration. Aqueous solutions are charge neutral but can show apparent charge imbalance in chemical analyses. Reasons for the apparent imbalance can include inaccurate analyses or failure to analyze for some ions, but for groundwater samples the most important cause of analyses that do not appear charge-balanced is usually related to exposure to atmospheric CO<sub>2</sub>. Hence, bicarbonate is typically adjusted to achieve a charge-balanced data set (Parkhurst and Appelo, 2013). Here, however, sulfate was used and the large percentage change in sulfate concentrations suggests that this was not the optimal choice. The charge balance species, specified in the input file, increases or decreases in order achieve equal proportions of cations and anions within a solution (Hem, 1985). PHREEQC coding does not allow the use of alkalinity or pH as a charge balance species if alkalinity is fixed, which it is here. The choice to make alkalinity a fixed value was initially based on an attempt to keep the PHREEQC input dataset as close to the raw analysis as possible but allowing alkalinity to be used for charge balance is likely a more realistic approach to achieving a realistic dataset for groundwater samples that have been exposed to the atmosphere.

Another way that the models here are impacted by choices made during initial setup is the arbitrary selection of pe values for all hypothetical input waters. Data on dissolved oxygen levels within the aquifers sampled for this study was unavailable due to equipment malfunction. So, instead of measured values, pe was estimated from a generalization of aqueous environments taken from Garrels and Christ (1965) (Fig. 25). Electron potential or pe is value that estimates the concentration of hydrated

electrons in an aqueous solution and provides information about the redox conditions of a solution (Zhu and Anderson, 2002). Since pH and water type are generally known, it is reasonable to use this estimation, however, real *pe* values may have been quite different from those used in the model and thus yielded different results. Changes in dissolved oxygen levels within an aquifer are critically important because they will directly affect redox sensitive elements such as iron. When an aqueous solution containing dissolved iron as  $\text{Fe}^{2+}$  is exposed to oxygen, it is oxidized to  $\text{Fe}^{3+}$ . Hematite ( $\text{Fe}_2\text{O}_3$ ) and goethite ( $\text{FeOOH}$ ) are common sedimentary minerals that form in oxidizing environments often as ferric hydroxide first before crystal systems are fully developed (Hem, 1985).

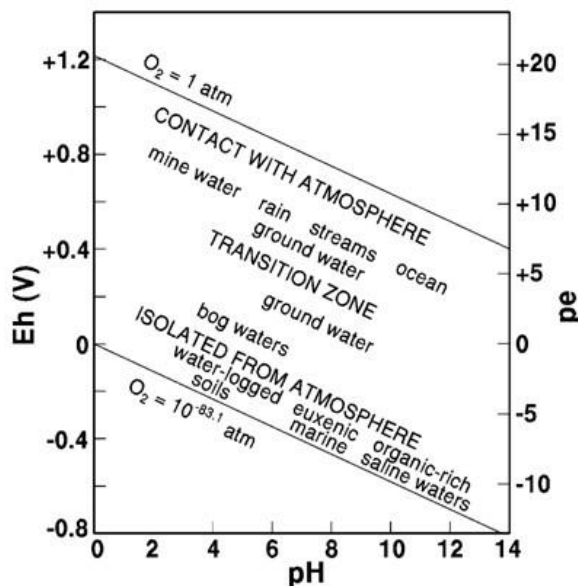


Figure 25: Eh/pH Diagram after Garrels and Christ (1965)

The effect and implications of modifying the redox environment is especially important in the case of ASR because introducing dissolved oxygen while injecting surface water is inevitable. Thus, the purpose of incorporating the second premixing process, or  $\text{O}_2$  or  $\text{CO}_2$  equilibration step, was to create an acidic and oxidizing environment. Introducing free oxygen causes *pe* or redox potential to increase in every model. Fluid from the first model step mixture was charged by oxygen and carbon dioxide making it a favorable environment for hematite formation. In the case of both the Ingleside and Fountain SPMMS

and would have precipitated in the Dakota model if hematite was included in the input file. Concentration changes in nitrate are likely due to *pe* changes as it is a redox sensitive species. In addition, bicarbonate concentrations decrease slightly in all models except the Ingleside SPMM where it increases slightly. Although redox conditions are impacted during the step of forcing equilibrium with O<sub>2</sub> and CO<sub>2</sub>, none of the dissolved concentration changes were > 1 mg/L and these results suggest that this step had a larger impact on mineral precipitation than aqueous species distribution.

The modeled fluids do not deviate significantly from the composition of the initial HIW and HNW fluids. The piper and stiff diagrams show this very clearly. This result indicates that the composition of the modeled fluids is strongly influenced by the successive pulses of HNW at each model step and they are not changed significantly by removal of ions during precipitation. If the models allowed mineral phases to dissolve, as well as precipitate within the model it is likely that 1) several minerals would have dissolved and 2) the fluid compositions would have changed more. Minerals common to all three models that were undersaturated with respect to initial fluids include: albite, anhydrite, adularia, calcite and dolomite (Tables 22-24). This is due to the model setup and specifically which minerals were included in the generalized mineral suites. Evidence for this comes from comparing the behavior of hematite in the Dakota SPMM vs its behavior in both the other models. Hematite is supersaturated with respect to the HNWs and the HIW in all three models, however it is only included in the generalized mineral suite within the Ingleside and Fountain input files, and not the Dakota. Therefore, the code simply does not allow hematite to precipitate in the Dakota model even though S.I. values have an average of 16 from model step 1 to 7 and strongly predict it to do so. Although, not every mineral that is supersaturated with respect to a fluid will precipitate and not all minerals that are undersaturated with respect to a fluid will dissolve, minerals such as anhydrite, calcite and dolomite are expected to dissolve readily in normal to acidic groundwater Robb (2005).

### 5.5.2 Fluid Evolution, Mineral Solubility and Mineral Precipitation

All three SPMMs predict precipitation of quartz and kaolinite, and both the Ingleside and Fountain models predict precipitation of hematite. All three minerals could precipitate in a sedimentary environment; however, in a natural environment kaolinite and hematite may be more likely than quartz to do so. In addition, because the models described here did not allow for mineral dissolution, only precipitation, the model did not capture all possible mineral modifications or variation in fluid composition. Lastly, there is not enough information provided here to assess the potential of formation/aquifer damage or well screen destruction due to mineral precipitation that was predicted in the SPMMs.

Hematite precipitation was expected in these models due to surface water injection, but also because the iron containing mineral is found abundantly in the Fountain and Ingleside formations and is responsible for the characteristic red coloration of the sandstones (Hogan, 2013; Hogan and Sutton, 2014; Adam, 2017; Collazo, 2018; Issa, 2018; Nair, 2018). The implications of hematite precipitation for ASR involve the possibility of oxide scale coating the well screen and reducing recovery efficiency (Pyne, 2005). Therefore, scaling due to precipitation of hematite could damage the well itself or reduce permeability into the aquifer. However, of the three minerals predicted to precipitate within the models of this study, hematite was never predicted to produce more than 0.02 mg/kg which was the smallest amount of the three mineral solids predicted to precipitate.

A maximum mass of 0.13 mg/kg per model step of kaolinite is also predicted to precipitate in all three models. Kaolinite can precipitate in sedimentary environments and requires both aluminum and silica in solution to form (Table 25). All groundwater samples analyzed in this study show aluminum below the detection limit of 0.01 mg/L. This means that dissolved aluminum in these formations is somewhere between 0 and 0.01 mg/L. Consequently, for purposes of modeling aluminum concentrations for the groundwater samples have been arbitrarily set to 0.005 mg/L, half the detection limit. In contrast, the sample of treated city water modeled as the injection water had modest, but detectable,  $\text{Al}^{3+}$  at 0.03

mg/l. Kaolinite can be a byproduct of weathering or alteration of aluminosilicates, but it can also precipitate from a supersaturated aqueous solution and because the models did not allow for dissolution of minerals, precipitation is the only process of interest here. The implications of kaolinite precipitation have more to do with clogging of pore spaces within the formation than with they do with damage to the well screen, but again ultimately decreases recovery efficiency for the ASR system. However, given that the presence of aluminum is mostly speculative in these models, as it was reported to be below detection, and that the predicted precipitated mass based on the arbitrarily assumed Al concentration is so small that kaolinite precipitation impacting ASR viability is likely not a concern here.

When compared to hematite and kaolinite a relatively large amount (max - ~3.7 mg/kg) of quartz was predicted to precipitate in all three models, which assumed thermodynamic equilibrium would control precipitation. It is not likely, however, that quartz would precipitate in this environment naturally. Silica is present in solution as  $H_4SiO_4$ , and quartz is supersaturated in some natural waters. However, quartz does not always precipitate in sedimentary environments because of kinetic controls (Zhu and Anderson, 2002). Although, quartz is kinetically inhibited at the given temperatures and pressures, the model input selected specified quartz and not amorphous silica as the phase available to precipitate. The model was constrained to allow only the minerals that were present in the generalized formation suite to precipitate. A better approach could have been to allow amorphous silica or quartz to precipitate.

Mineral precipitation of any kind is concerning for an ASR operation mainly due to reduction of permeability and decreased recovery efficiency, but also due to damage of the well screen due to mineral scaling. The amount of mineral precipitation that can occur without causing adverse effects during ASR depends on several factors including: the rate of infiltration of injection water, rate of precipitation, and available pore space in order to determine if the mass of mineral precipitate would be detrimental to the formation or the well, none of which were considered in this study. Because the models here are based on equilibrium thermodynamics, they assume instantaneous mineral precipitation at each step. In reality, it is known that mineral reactions are not always instantaneous and are sometimes reversible, meaning that

precipitation can take place very slowly or that once precipitated minerals in a system can dissolve again (Zhu and Anderson, 2002). Therefore, when evaluating the implications of the mineral volumes predicted to precipitate here it is important to remember that some minerals, like quartz, may precipitate over a longer period of time. In addition, minerals with slower rates of reaction may not ever end up precipitating in the long term because the formation water may also change over time decreasing or increasing saturation index values with respect to them. Furthermore, given that quartz would likely be kinetically inhibited and both hematite and kaolinite are predicted to precipitate in such small amounts <1 mg/kg water in all cases, it is reasonable to assume that they would likely not be an issue in a real-world ASR implementation in the rocks considered here.

Table 25:WATQ4F Database Thermodynamic Data - Model Input

phase	Reaction	log_k [equilibrium constant for the reaction]	delta_h (kcal) [enthalpy of reaction]
Albite	$\text{NaAlSi}_3\text{O}_8 + 8\text{H}_2\text{O} = \text{Na}^+ + \text{Al(OH)}_4^- + 3\text{H}_4\text{SiO}_4$	-18.002	25.896
Anhydrite*	$\text{CaSO}_4 = \text{Ca}^{+2} + \text{SO}_4^{-2}$	-4.36	-1.71
Calcite*	$\text{CaCO}_3 = \text{Ca}^{+2} + \text{CO}_3^{-2}$	-8.48	-2.297
Dolomite	$\text{CaMg}(\text{CO}_3)_2 = \text{Ca}^{+2} + \text{Mg}^{+2} + 2\text{CO}_3^{-2}$	-16.54	-11.09
Hematite	$\text{Fe}_2\text{O}_3 + 6\text{H}^+ = 2\text{Fe}^{+3} + 3\text{H}_2\text{O}$	-4.008	-30.845
Illite	$\text{K}_{0.6}\text{Mg}_{0.25}\text{Al}_{2.3}\text{Si}_{3.5}\text{O}_{10}(\text{OH})_2 + 11.2\text{H}_2\text{O} = 0.6\text{K}^+ + 0.25\text{Mg}^{+2} + 2.3\text{Al(OH)}_4^- + 3.5\text{H}_4\text{SiO}_4 + 1.2\text{H}^+$	-40.267	54.684
Kaolinite	$\text{Al}_2\text{Si}_2\text{O}_5(\text{OH})_4 + 6\text{H}^+ = 2\text{Al}^{+3} + 2\text{H}_4\text{SiO}_4 + \text{H}_2\text{O}$	7.435	-35.3
Adularia	$\text{KAlSi}_3\text{O}_8 + 8\text{H}_2\text{O} = \text{K}^+ + \text{Al(OH)}_4^- + 3\text{H}_4\text{SiO}_4$	-20.573	30.82
Kmica	$\text{KAl}_3\text{Si}_3\text{O}_{10}(\text{OH})_2 + 10\text{H}^+ = \text{K}^+ + 3\text{Al}^{+3} + 3\text{H}_4\text{SiO}_4$	12.703	-59.376
Quartz*	$\text{SiO}_2 + 2\text{H}_2\text{O} = \text{H}_4\text{SiO}_4$	-3.98	5.99
Goethite	$\text{FeOOH} + 3\text{H}^+ = \text{Fe}^{+3} + 2\text{H}_2\text{O}$	-1.0	-14.48
Gibbsite	$\text{Al}(\text{OH})_3 + 3\text{H}^+ = \text{Al}^{+3} + 3\text{H}_2\text{O}$	8.11	-22.8

\*log\_Kr  
[analytical]

Calcite = -171.9065-0.077993T+2839.319/T+71.595Log10T

Anhydrite = 197.52T-8669.8/T-69.835Log10T

Quartz = 0.41-1309/T

Data taken from Ball and Nordstrom (1991) “Table 2 Thermodynamic Data”

### 5.5.3 Model Limitations

As is the case with all models, geochemical modeling is limited in its ability to simulate the natural world (Merkel and Planer-Friedrich, 2002; Parkhurst and Appelo, 2013; Zhu and Anderson, 2002). Human error is an important limitation of any model. One possible source of error in these models are the values used to reference species behavior within the chosen databases. PHREEQC comes with several thermodynamic databases for use in modeling (Merkel and Planer-Friedrich, 2002; Parkhurst and Appelo, 2013; Zhu and Anderson, 2002). Thermodynamic databases are empirical and experimental data and may contain errors, which then propagate throughout a model. In this study the database Wateq4f.dat (Ball and Nordstrom, 1991) was used because of the presence of arsenic and selenium data (Parkhurst and Appelo, 2013). A second limitation of a geochemical model is a lack of necessary data to properly describe a geochemical environment. For instance, in the wells sampled for this study, the redox potential was unknown for the subsurface environment due to insufficient data relating to ORP (oxidation reduction potential), redox couples, or dissolved oxygen.

The SPMM built for this study gives an estimate of theoretical mixing of treated surface water and in situ formation water coupled with estimates of mineral precipitation in the presence of those calculated solutions. The model does not, however, permit mineral dissolution, a process that could impact water quality and aquifer permeability during an actual ASR operation. Assumptions about the chemistry of the waters, particularly the Al concentration and the pe values, limit the predictive value of the model for actual ASR operations. In addition, there is no actual spatial or time component to the model. As the conceptual model depicts (Fig. 8), the injected solution evolves through the cellblocks, but the cellblocks don't have dimensions and therefore the solution does not travel a specified distance in any direction in reality. Specifically, this means that the model does not consider the geometry of the formation, contacts in the subsurface or even the complex heterogeneity that absolutely exists in the subsurface as well. The model also does not consider residence time of the injection bubble within the

subsurface or injection rate. These hydrologic components are important to consider for an ASR system and would have an impact on the geochemical processes taking place within the injection bubble.

## Chapter 6 - Conclusions and Recommendations

### 6.1 Conclusions

This study used compositional data from surface rocks, domestic water wells, and treated surface water along with thermodynamic equilibrium geochemical modeling to:

1. Determine a generalized mineral and chemical composition of selected samples of the Fountain and Ingleside Formations, and the Dakota Group sandstones.
2. Characterize and assess the quality of treated city water and native groundwater in the above-mentioned potential host aquifers.
3. Model mixing between formation water and treated surface water and their combined interaction with host aquifers and mineral precipitation.

A complete characterization of the chemical composition of the formations of interest was not achieved. However, from the data gathered it was determined that the Dakota Group and the Ingleside and Fountain formations contain sandstones with high percentages of silicates. With the exception of TDS in the Dakota formation water sample, water in all sampled wells complied with EPA quality standards for all three formations and was potable. Mixing HNW from the formations of interest with dilute treated water (HIW) did not significantly change their water type. In a real-life scenario there may be precipitation of kaolinite, hematite and some form of silica, however, further modeling is needed to verify this conclusion. Furthermore, the modeling presented here does not permit evaluation of the water quality or permeability impacts of possible dissolution of minerals. Given the previous conclusions, the Dakota sandstones, Ingleside and Fountain Formations are recommended for further site-specific study.

## 6.2 Future Recommendations

As a master's thesis, this study was intentionally broad and serves as a pilot study to guide future investigations. In the future, a similar study with a goal if assessing suitability of ASR would benefit from the following:

1. Better defined and smaller study area
2. many more rock samples - preferably subsurface
3. many more water samples with measurements that characterize redox environment
4. a model that involved both dissolution and precipitation reactions
5. investigations into mineral cation exchange capacities

To be confident about the feasibility of implementing an ASR program it would be necessary to install a test well to get an accurate illustration of what is happening geochemically in the aquifer. Not only would it be better to analyze rock material from sidewall core (or wireline coring) and water directly from the subsurface of the location in question, but it would also be possible to record the changes in the geochemical environment in real time by running multiple ASR cycles and measuring water quality.

Geochemical modeling can then be executed from a pilot operation that will include accurate well capacities and recovery efficiencies and site-specific water quality and composition. The best way to do this is to not only install one test well, but also 1-3 monitoring wells to record the distance the water is traveling after injection and the evolution of its quality. In addition, including kinetic, biologically mediated reactions, as well as reactive transport modeling would enhance the investigation if a subsequent study were done.

## References Cited

- Adam, A., 2017, Hydrologic characterization of upper permian-cenozoic sedimentary strata of larimer county: Prospective aquifer storage and recovery targets [Master of Science thesis]: Colorado State University, 178 p.
- Antoniou, E. A., Hartog, N., van Breukelen, B. M., *et al.*, 2014, Aquifer pre-oxidation using permanganate to mitigate water quality deterioration during aquifer storage and recovery: Applied Geochemistry, v. 50, p. 25-36, 10.1016/j.apgeochem.2014.08.006.
- Antoniou, E. A., Stuyfzand, P. J., and van Breukelen, B. M., 2013, Reactive transport modeling of an aquifer storage and recovery (asr) pilot to assess long-term water quality improvements and potential solutions: Applied Geochemistry, v. 35, p. 173-186, 10.1016/j.apgeochem.2013.04.009.
- Antoniou, E. A., van Breukelen, B. M., Putters, B., *et al.*, 2012, Hydrogeochemical patterns, processes and mass transfers during aquifer storage and recovery (asr) in an anoxic sandy aquifer: Applied Geochemistry, v. 27, no. 12, p. 2435-2452, 10.1016/j.apgeochem.2012.09.006.
- Antoniou, E. A., van Breukelen, B. M., and Stuyfzand, P. J., 2015, Optimizing aquifer storage and recovery performance through reactive transport modeling: Applied Geochemistry, v. 61, p. 29-40, 10.1016/j.apgeochem.2015.05.009.
- Appelo, C., and Postma, D., 2005, Geochemistry, groundwater and pollution, Leiden, The Netherlands A.A. Balkema Publishers, 647 p.
- Azobu, J. O., 2013, Using geochemical modeling (phreeqc) to determine edwards volume fraction in mixed groundwaters from the edwards and carrizo aquifers at saws aquifer storage and recovery (asr) site, bexar county texas [Master of Science in Geology thesis]: The University of Texas at San Antonio, 82 p.
- Ball, J. W., and Nordstrom, D. K., 1991, User's manual for wateq4f, with revised thermodynamic data base and text cases for calculating speciation of major, trace, and redox elements in natural waters: Open-File Report 91-183, p. 193, doi:10.3133/ofr91183
- Blakey, R. C., 2008, Pennsylvanian-jurassic sedimentary basins of the colorado plateau and southern rocky mountains, The sedimentary basins of the united states and canada, p. 245-296, 10.1016/s1874-5997(08)00007-5.
- Braddock, W. A., 1988, Geologic map of the laporte quadrangle, larimer county, colorado: Geologic Quadrangle 1621, United States Geological Survey, 10.3133/gq1621
- Braddock, W. A., Calvert, R. H., O'Connor, J. T., *et al.*, 1989, Geologic map of the horsetooth reservoir quadrangle, larimer county, colorado, 10.3133/gq1625.

- Camprovin, P., Hernández, M., Fernández, S., *et al.*, 2017, Evaluation of clogging during sand-filtered surface water injection for aquifer storage and recovery (asr): Pilot experiment in the llobregat delta (barcelona, spain): Water, v. 9, no. 4, 10.3390/w9040263.
- Collazo, D., 2018, Hydrogeologic characterization of the fountain formation: Prospective aquifer storage and recovery targets in front range colorado [Master of Science: Colorado State University, 127 p.
- Gaus, Williams, and Shand, 2000, Physical and geochemical modelling (swift-phreeqc) of british aquifers for aquifer storage and recovery purposes part 1: Physical modelling and geochemical model calibration: British Geological Survey Natural Environment Research Council, no. Report WD/00/08.
- Gaus, I., Shand, P., Williams, A., *et al.*, 2002, Geochemical modelling of fluoride concentration changes during aquifer storage and recovery (asr) in the chalk aquifer in wessex, england: Quarterly Journal of Engineering Geology and Hydrogeology, p. 6.
- Glynn, P. D., and Plummer, L. N., 2005, Geochemistry and the understanding of ground-water systems: Hydrogeology Journal, v. 13, no. 1, p. 263-287, 10.1007/s10040-004-0429-y.
- Hem, J. D., 1985, Study and interpretation of the chemical characteristics of natural water, United States Geological Survey, U.S geological survey water-supply paper, 263 p.
- Hogan, I. M., and Sutton, S. J., 2014, The role of mudstone baffles in controlling fluid pathways in a fluvial sandstone: A study in the pennsylvanian-permian fountain formation, northern colorado, u.S.A: Journal of Sedimentary Research, v. 84, no. 11, p. 1064-1078, 10.2110/jsr.2014.81.
- Holbrook, J., and Ethridge, F. G., 1996, Sequence stratigraphy of the dakota group and equivalents from north-central colorado to northeastern new mexico: Down-dip variations in sequence anatomy: A field trip guide for the 1996 gsa annual meeting, p. 43.
- Jones, G., and Pichler, T., 2007, Relationship between pyrite stability and arsenic mobility during aquifer storage and recovery in southwest central florida: Environmental Science and Technology, v. 41, no. 3, p. 723–730.
- Merkel, B. J., and Planer-Friedrich, B., 2002, Groundwater geochemistry a practical guide to modeling of natural and contaminated aquatic systems, Berlin Heidelberg New York, Springer, 207 p.
- Mirecki, J. E., Bennett, M. W., and Lopez-Balaez, M. C., 2013, Arsenic control during aquifer storage recovery cycle tests in the floridan aquifer: Ground Water, v. 51, no. 4, p. 539-549, 10.1111/j.1745-6584.2012.01001.x.
- Nair, K., 2018, Facies reconstruction and detrital zircon geochronology of the ingleside/casper formation [Master of Science thesis]: Colorado State University, 117 p.

Ni, P., Guo, H., Yuan, R., *et al.*, 2017, Arsenic migration and transformation in aquifer sediments under successive redox oscillations: Procedia Earth and Planetary Science, v. 17, p. 384-387, 10.1016/j.proeps.2016.12.097.

Parkhurst, D. L., and Appelo, C. A. J., 2013, Description of input and examples for phreeqc version 3—a computer program for speciation, batch-reaction, one-dimensional transport, and inverse geochemical calculations, U.S. Geological survey techniques and methods, U.S. Department of the Interior U.S. Geological Survey, p. 497.

Pyne, R. D. G., 2005, Aquifer storage recovery : A guide to groundwater recharge through wells, Gainesville, Florida, ASR Systems.

Rinck-Pfeiffer, S., Ragusa, S., Sztajnbok, P., *et al.*, 2000, Interrelationships between biological, chemical, and physical processes as an analog to clogging in aquifer storage and recovery (asr) wells: Water Resources, v. 34, no. 7, p. 9.

Ringleb, J., Sallwey, J., and Stefan, C., 2016, Assessment of managed aquifer recharge through modeling—a review: Water, v. 8, no. 12, 10.3390/w8120579.

Robb, L. J., 2005, Introduction to ore-forming processes, 350 Main Street, Malden, MA 02148-5020, USA, Blackwell Publishing, 373 p.

Robson, S., 1987, Bedrock aquifers in the denver basin, colorado a quantitative water-resources appraisal: U.S. Geological Survey Professional Paper, no. 1257, p. 80.

Sajil Kumar, P. J., 2013, Interpretation of groundwater chemistry using piper and chadha's diagrams: A comparative study from perambalur taluk: Elixir Geoscience, v. 54, p. 12208-12211.

Waagé, K. M., 1955, Dakota group in northern front range foothills, colorado : A revised subdivision and terminology for the dakota group and local details of its stratigraphy, Washington, United States Government Printing Office, Geological survey professional paper ; 274-b.

Zhu, C., and Anderson, G., 2002, Environmental applications of geochemical modeling, Cambridge University Press, 299 p, 10.1017/CBO9780511606274.

## Appendix

## A.1 Injection Solution

Treated Water Composition, provided by Fort Collins Water Treatment Plant

### Fort Collins Treated Water Data - = Sample Station 2, Official Distribution System Entry Point

TEST TYPE	SS#2 (HSPS)	TEST TYPE	SS#2 (HSPS)
<b>BACTERIOLOGY</b>		<b>METALS (ug/L) by ICP-MS</b>	
Free Chlorine Residual mg/L	0.83	Aluminum	29.9
Temperature degrees C	7.4	Antimony	<1.0
Quanti-tray, Total Coliform CFU/100ml	0	Arsenic	<1.0
Quanti-Tray, E. Coli CFU/100ml	0	Barium	18.3
Fecal Strep CFU/100ml	0	Beryllium	<1.0
Heterotrophic Plate Count / 1.0 ml	0	Cadmium	<1.0
<b>CHEMISTRY</b>		Chromium	<1.0
Alkalinity as CaCO3 mg/L	38.2	Copper	0.4
Ammonia as N mg/L	<0.02	Iron	10.9
Calcium as CaCO3 mg/L	42.1	Lead	<1.0
Calcium mg/L	16.84	Manganese	1.2
Color Color Units	0.7	Mercury by CVA	<0.2
Hardness, Lachat as CaCO3 mg/L	53.9	Molybdenum	<1.0
Langlier Larson Saturation Index	-1.28	Nickel	<1.0
ortho-Phosphate mg/L	0.005	Selenium	<5.0
pH S.U.	7.91	Silver	<1.0
Silica mg/L	5.1	Thallium	<1.0
Specific Conductance umhos/cm	126	Zinc	<1.0
Total Dissolved Solids mg/L	84	<b>METALS (mg/L) by ICP-MS</b>	
Turbidity NTU	0.1	Calcium	16.9
<b>ION CHROMATOGRAPHY (mg/L)</b>		Magnesium	2.2
IC_Chlorate	0.04	Potassium	3.7
IC_Chloride	3.72	Sodium	0.9
IC_Chlorite	0.23	<b>NUTRIENTS (mg/L)</b>	
IC_Fluoride	0.6	Total Kjeldahl Nitrogen as N	
IC_Nitrate	0.07	Total Phosphorus	<0.01
IC_Nitrite	<0.04	<b>TOTAL ORGANIC CARBON (mg/L)</b>	
IC_Sulfate	14.9	TOC - Sievers	1.78
<b>VOLATILE ORGANIC COMPOUNDS(ug/L)</b>		<b>UV (ug/L)</b>	
Total Trihalomethane	15.3	Chlorophyl a	-

## A.2 Full Results of Water Chemistry Analysis for Experiment

### A.2.1 First Leaching Experiment

Full Results of Water Chemistry Analysis for First Experiment - Round 1

Parameter (mg/L)	DL	E-F1	E-F2	E-F3	E-I1	E-I2	E-I3	E-D1	E-D2	T.W.C.
Alkalinity	2	80	172	86.2	79.6	67.4	82	43.2	68	37.6
Ammonia	0.01	0.03	2.28	1.1	0.05	0.03	0.09	0.82	3.13	0.03
ortho-P	0.005	0.032	0.027	0.046	0.016	<DL	0.358	0.065	0.098	<DL
Silica	2	11	17.5	9.9	10.6	6.8	10.1	9.8	19.8	5.5
Chloride	1	5.1	135.2	36.0	26.7	4.2	5.0	4.2	37.4	3.9
Fluoride	0.04	0.45	0.48	0.68	0.69	0.57	0.58	0.60	0.57	0.63
Nitrate	0.04	1.81	34.3	3.19	2.13	0.08	0.13	0.63	173	0.06
Sulfate	5	14.1	244.6	14.6	17.5	13.6	14.3	14.2	104	12.9
Aluminum	0.01	<DL	<DL	0.038	0.012	0.012	0.012	0.011	<DL	<DL
Arsenic	0.001	0.022	0.008	0.008	0.006	0.001	3.390	0.004	0.006	<DL
Calcium	0.2	34.2	187.8	34.4	34	22.7	13.5	18.5	154	17
Copper	0.001	0.075	0.089	0.099	0.042	0.039	0.070	0.057	0.251	0.172
Iron	0.01	<DL								
Potassium	0.1	3.8	8.7	4.1	2.3	0.9	3.4	1.4	90	0.8
Magnesium	0.1	1.7	37.8	8	5.6	6	14.8	2.4	76.2	2
Manganese	0.001	<DL	0.003	0.002	<DL	0.002	0.006	0.003	0.051	<DL
Sodium	0.2	3.9	58.7	18.1	16.7	4.4	4.6	4.5	13.6	3.9
Selenium	0.005	<DL	0.022	<DL						
Total Phos	0.01	0.04	0.04	0.05	0.02	<DL	0.5	0.08	0.13	<DL
TOC	0.5	4.3	24.3	3.59	4.74	2.66	3.22	3.6	52	1.84
TDS	10	104	1042	158	144	72	102	86	1432	38

### A.2.2 Second Leaching Experiment

Full Results of Water Chemistry Analysis for Second Experiment - Round 2

LABID	CLIENTID	DEPTNAME	ANALYTE	RESULT	UNIT S	MDL	PQL	METHOD
L48818-01	BS-I-1	Metals Analysis	Aluminum, dissolved		mg/L	0.03	0.2	M200.7 ICP
L48818-01	BS-I-1	Metals Analysis	Arsenic, dissolved		mg/L	0.04	0.2	M200.7 ICP
L48818-01	BS-I-1	Metals Analysis	Calcium, dissolved	330	mg/L	0.1	0.5	M200.7 ICP
L48818-01	BS-I-1	Metals Analysis	Copper, dissolved	0.02	mg/L	0.01	0.05	M200.7 ICP
L48818-01	BS-I-1	Metals Analysis	Iron, dissolved		mg/L	0.02	0.05	M200.7 ICP
L48818-01	BS-I-1	Metals Analysis	Magnesium, dissolved	74.7	mg/L	0.2	1	M200.7 ICP
L48818-01	BS-I-1	Metals Analysis	Manganese, dissolved	0.009	mg/L	0.005	0.03	M200.7 ICP
L48818-01	BS-I-1	Metals Analysis	Potassium, dissolved	21.2	mg/L	0.2	1	M200.7 ICP
L48818-01	BS-I-1	Metals Analysis	Selenium, dissolved	0.09	mg/L	0.05	0.3	M200.7 ICP
L48818-01	BS-I-1	Metals Analysis	Silica, dissolved	16.7	mg/L	0.2	1	M200.7 ICP
L48818-01	BS-I-1	Metals Analysis	Sodium, dissolved	11.3	mg/L	0.2	1	M200.7 ICP
L48818-01	BS-I-1	Wet Chemistry	Bicarbonate as CaCO <sub>3</sub>	206	mg/L	2	20	SM2320B - Titration
L48818-01	BS-I-1	Wet Chemistry	Carbon, total organic (TOC)	32.7	mg/L	5	25	SM5310B
L48818-01	BS-I-1	Wet Chemistry	Carbonate as CaCO <sub>3</sub>		mg/L	2	20	SM2320B - Titration
L48818-01	BS-I-1	Wet Chemistry	Cation-Anion Balance	2.1	%			Calculation
L48818-01	BS-I-1	Wet Chemistry	Chloride	31	mg/L	0.5	2	SM4500Cl-E
L48818-01	BS-I-1	Wet Chemistry	Fluoride	0.3	mg/L	0.1	0.5	SM4500F-C
L48818-01	BS-I-1	Wet Chemistry	Hydroxide as CaCO <sub>3</sub>		mg/L	2	20	SM2320B - Titration
L48818-01	BS-I-1	Wet Chemistry	Nitrate as N, dissolved	118	mg/L	2	10	Calculation: NO <sub>3</sub> NO <sub>2</sub>

L48818-01	BS-I-1	Wet Chemistry	Nitrate/Nitrite as N, dissolved	122	mg/L	2	10	M353.2 - Automated C
L48818-01	BS-I-1	Wet Chemistry	Nitrite as N, dissolved	4.5	mg/L	0.5	3	M353.2 - Automated C
L48818-01	BS-I-1	Wet Chemistry	Nitrogen, ammonia	5.36	mg/L	0.05	0.2	M350.1 Auto Salicyla
L48818-01	BS-I-1	Wet Chemistry	Phosphate, total		mg/L	3	9	Calculation based on
L48818-01	BS-I-1	Wet Chemistry	Phosphorus, total		mg/L	1	3	M365.1 - Auto Ascorb
L48818-01	BS-I-1	Wet Chemistry	Residue, Filterable (TDS) @180C	1570	mg/L	50	100	SM2540C
L48818-01	BS-I-1	Wet Chemistry	Sulfate	454	mg/L	30	150	D516-07 - Turbidimet
L48818-01	BS-I-1	Wet Chemistry	Sum of Anions	23	meq/L			Calculation
L48818-01	BS-I-1	Wet Chemistry	Sum of Cations	24	meq/L			Calculation
L48818-01	BS-I-1	Wet Chemistry	TDS (calculated)	1620	mg/L			Calculation
L48818-01	BS-I-1	Wet Chemistry	TDS (ratio - measured/calculated)	0.97				Calculation
L48818-01	BS-I-1	Wet Chemistry	Total Alkalinity	206	mg/L	2	20	SM2320B - Titration
L48818-02	FILTER BLANK	Metals Analysis	Aluminum, dissolved		mg/L	0.03	0.2	M200.7 ICP
L48818-02	FILTER BLANK	Metals Analysis	Arsenic, dissolved		mg/L	0.04	0.2	M200.7 ICP
L48818-02	FILTER BLANK	Metals Analysis	Calcium, dissolved	16.3	mg/L	0.1	0.5	M200.7 ICP
L48818-02	FILTER BLANK	Metals Analysis	Copper, dissolved	0.05	mg/L	0.01	0.05	M200.7 ICP
L48818-02	FILTER BLANK	Metals Analysis	Iron, dissolved		mg/L	0.02	0.05	M200.7 ICP
L48818-02	FILTER BLANK	Metals Analysis	Magnesium, dissolved	1.6	mg/L	0.2	1	M200.7 ICP
L48818-02	FILTER BLANK	Metals Analysis	Manganese, dissolved		mg/L	0.005	0.03	M200.7 ICP
L48818-02	FILTER BLANK	Metals Analysis	Potassium, dissolved	0.8	mg/L	0.2	1	M200.7 ICP

L48818-02	FILTER BLANK	Metals Analysis	Selenium, dissolved		mg/L	0.05	0.3	M200.7 ICP
L48818-02	FILTER BLANK	Metals Analysis	Silica, dissolved	5.7	mg/L	0.2	1	M200.7 ICP
L48818-02	FILTER BLANK	Metals Analysis	Sodium, dissolved	2.9	mg/L	0.2	1	M200.7 ICP
L48818-02	FILTER BLANK	Wet Chemistry	Bicarbonate as CaCO <sub>3</sub>	40.1	mg/L	2	20	SM2320B - Titration
L48818-02	FILTER BLANK	Wet Chemistry	Carbon, total organic (TOC)	1.4	mg/L	1	5	SM5310B
L48818-02	FILTER BLANK	Wet Chemistry	Carbonate as CaCO <sub>3</sub>		mg/L	2	20	SM2320B - Titration
L48818-02	FILTER BLANK	Wet Chemistry	Cation-Anion Balance	-8.3	%			Calculation
L48818-02	FILTER BLANK	Wet Chemistry	Chloride	3.9	mg/L	0.5	2	SM4500Cl-E
L48818-02	FILTER BLANK	Wet Chemistry	Fluoride	0.7	mg/L	0.05	0.3	SM4500F-C
L48818-02	FILTER BLANK	Wet Chemistry	Hydroxide as CaCO <sub>3</sub>		mg/L	2	20	SM2320B - Titration
L48818-02	FILTER BLANK	Wet Chemistry	Nitrate as N, dissolved	0.09	mg/L	0.02	0.1	Calculation: NO <sub>3</sub> NO <sub>2</sub>
L48818-02	FILTER BLANK	Wet Chemistry	Nitrate/Nitrite as N, dissolved	0.09	mg/L	0.02	0.1	M353.2 - Automated C
L48818-02	FILTER BLANK	Wet Chemistry	Nitrite as N, dissolved		mg/L	0.01	0.05	M353.2 - Automated C
L48818-02	FILTER BLANK	Wet Chemistry	Nitrogen, ammonia		mg/L	0.05	0.2	M350.1 Auto Salicyla
L48818-02	FILTER BLANK	Wet Chemistry	Phosphate, total		mg/L	0.2	0.3	Calculation based on
L48818-02	FILTER BLANK	Wet Chemistry	Phosphorus, total		mg/L	0.05	0.1	M365.1 - Auto Ascorb
L48818-02	FILTER BLANK	Wet Chemistry	Residue, Filterable (TDS) @180C	74	mg/L	10	20	SM2540C
L48818-02	FILTER BLANK	Wet Chemistry	Sulfate	16.1	mg/L	1	5	D516-07 - Turbidimet
L48818-02	FILTER BLANK	Wet Chemistry	Sum of Anions	1.3	meq/L			Calculation
L48818-02	FILTER BLANK	Wet Chemistry	Sum of Cations	1.1	meq/L			Calculation
L48818-02	FILTER BLANK	Wet Chemistry	TDS (calculated)	74.4	mg/L			Calculation

L48818-02	FILTER BLANK	Wet Chemistry	TDS (ratio - measured/calculated)	0.99			Calculation
L48818-02	FILTER BLANK	Wet Chemistry	Total Alkalinity	40.1	mg/L	2	20

### A.3 PHREEQC Model Input

### A.3.1 Input parameters common to all three Single Pass Mixing Models

```
TITLE - Formation - water samples - rock

#REFERENCES
#Ball, J. W., Nordstrom, D. K. (1991) User's manual for WATEQ4F, with revised
#thermodynamic data base and test cases for calculating speciation of major,
#trace, and redox elements in natural waters. U.S. Geological Survey Open-
File
#Report, 91-183.

SOLUTION_MASTER_SPECIES #wateq4f database
As      H3AsO4      -1.0      74.9216      74.9216
SOLUTION_SPECIES #wateq4f database
H3AsO4 = H3AsO4
    log_k      0
SOLUTION_MASTER_SPECIES #wateq4f database
Se      SeO4-2      0.0      78.96      78.96
SOLUTION_SPECIES #wateq4f database
SeO4-2 = SeO4-2
    log_k      0
    delta_h 0      kcal
    -gamma   4.0  0.0

SOLUTION 1 (SS2) Injection Water - Fort Collin Water Treatment Facility
temp      15
pH        7
pe        10
redox     pe
units     mg/l
density   1
Al        0.0299
Alkalinity 46.604 gfw 61 #HCO3
As        0.0005 as H3AsO3 #below Detection Limit of 0.001 mg/L
Ca        16.9
Cl        3.72
F         0.6
Fe        0.0109
K          3.7
Mg        2.2
Mn        0.0012
N(5)      0.07
Na        0.9
P          0.005 #below Detection Limit of 0.01 mg/L
S(6)      14.9 charge
Se        0.0025 #below Detection Limit of 0.005 mg/L
Si        5.1
-water    1 # kg

EQUILIBRIUM_PHASES 3 #equilibrate with atmosphere
CO2(g)    -3.4 10
O2(g)    -0.67 10
SAVE Solution 1
END

SOLUTION 2 # [Formation] Water
```

```

temp          #
pH           #
pe           #
redox         pe
units         mg/l
density       1
Al            #
Alkalinity    #
As            #
Ca            #
Cl            #
F             #
Fe            #
K             #
Mg            #
Mn            #
N(5)          #
Na            #
P             #
S(6)          # charge
Se            #
Si            #
-water        1 # kg

EQUILIBRIUM_PHASES 2 # equilibrated to sub-surface conditions
CO2(g)      -2 10
SAVE solution 2
END

EQUILIBRIUM_PHASES 1 #representative [Formation] minerals
Mineral_1    0 0
Mineral_2    0 0
SAVE EQUILIBRIUM_PHASES 1
END

USE EQUILIBRIUM_PHASES 1 #95% injection water/ 5% native water
MIX 1
1     0.95
2     0.05
SAVE solution 3
END

USE EQUILIBRIUM_PHASES 1 #95% fluid 1/ 5% native water
MIX 2
3 .95
2 .05
SAVE SOLUTION 4
END

USE EQUILIBRIUM_PHASES 1 #95% fluid 2/ 5% native water
MIX 3
4 .95
2 .05
SAVE SOLUTION 5
END

```

```

USE EQUILIBRIUM_PHASES 1 #95% fluid 3/ 5% native water
MIX 4
5 .95
2 .05
SAVE SOLUTION 6
END

USE EQUILIBRIUM_PHASES 1 #95% fluid 4/ 5% native water
MIX 5
6 .95
2 .05
SAVE SOLUTION 7
END

USE EQUILIBRIUM_PHASES 1 #95% fluid 5/ 5% native water
MIX 6
7 .95
2 .05
SAVE SOLUTION 8
END

USE EQUILIBRIUM_PHASES 1 #95% fluid 6/ 5% native water
MIX 7
8 .95
2 .05
SAVE SOLUTION 9
END

```

### A.3.2 Dakota

TITLE Dakota Single Pass Mixing Model - site C - Dakota Minerals - Samples D1, D2

```

SOLUTION 2 # Dakota Water
    temp      14.95
    pH        7
    pe        4
    redox     pe
    units     mg/l
    density   1
    Al        0.005 #below Detection Limit of 0.01 mg/L
    Alkalinity 238.8 gfw 61
    As        0.0005 as H3AsO3 #below Detection Limit of 0.001 mg/L
    Ca        133
    Cl        14
    F         0.78
    Fe        0.0177
    K         4.75
    Mg        39.6
    Mn        0.131
    N(5)      0.02 #below Detection Limit of 0.04 mg/L
    Na        138
    P         0.005 #below Detection Limit of 0.01 mg/L

```

```

S(6)      508 charge
Se       0.0025 #below Detection Limit of 0.005 mg/L
Si       14.3
-water   1 # kg

EQUILIBRIUM_PHASES 1 #representative Dakota minerals
Quartz   0 0
Kaolinite 0 0
Adularia  0 0
Calcite   0 0
SAVE EQUILIBRIUM_PHASES 1
END

```

### A.3.3 Ingleside

TITLE Ingleside Single Pass Mixing Model - Ingleside Minerals - Samples I1, I3, I4 Ingleside Solution Average - A and F

```

SOLUTION 2 Ingleside Average
temp      16.26
pH        7.62
pe        4
redox     pe
units     mg/l
density   1
Al        0.005 #below Detection Limit of 0.01 mg/L
Alkalinity 181 gfw 61 #HCO3
As        0.0016 as H3AsO3
Ca        55.4
Cl        6.6
F         0.55
Fe        0.005 #below Detection Limit of 0.01 mg/L
K         1.8
Mg        18.5
Mn        0.0011
N(5)      3.36
Na        13
P         0.03
S(6)      24.7 charge
Se        0.0025 #below Detection Limit of 0.005 mg/L
Si        15.5 # gram formula weight = 60.0843
-water   1 # kg

```

```

EQUILIBRIUM_PHASES 1 #representative Ingleside minerals
Albite    0 0
Anhydrite 0 0
Calcite   0 0
Dolomite  0 0
Hematite  0 0
Kaolinite 0 0
Quartz   0 0
adularia  0 0
kmica    0 0 Dissolve only

```

```
SAVE EQUILIBRIUM_PHASES 1
END
```

### A.3.4 Fountain

```
TITLE - Fountain Single Pass Leaching Model - Average of Solutions: 3,5,9,10
- Fountain Samples: F1, F2, F3
```

```
SOLUTION 2 Native Fnt water / Fnt Ave Waters
    temp   14
    pH     7
    pe     4
    redox pe
    units mg/l
    density 1
    Al      0.005 #below Detection Limit of 0.01 mg/L
    Alkalinity 246 gfw 61 #HCO3
    As      0.002 as H3AsO3
    Ca      47.7
    Cl      6.4
    F       0.55
    Fe      0.01
    K       2.2
    Mg      16.6
    Mn      0.001 #below Detection Limit of 0.001 mg/L
    N(5)   2.6
    Na      38.4
    P       0.1
    S(6)   49.7 charge
    Se      0.007
    Si      15.2 # gram formula weight = 60.0843
    -water   1 # kg
```

```
EQUILIBRIUM_PHASES 1 #representative Fountain minerals
    Albite   0 0
    Anhydrite 0 0
    Calcite   0 0
    Dolomite  0 0
    Hematite  0 0
    Illite    0 0
    Adularia  0 0
    Kmica    0 0 Dissolve only
    Kaolinite 0 0
    Quartz    0 0
SAVE EQUILIBRIUM_PHASES 1
END
```